ISSN 2056-5135

JOHNSON MATTHEY
TECHNOLOGY REVIEW

Johnson Matthey's international journal of research
exploring science and technology in industrial applications

Volume 61, Issue 1, January 2017

Published by Johnson Matthey

www.technology.matthey.com

Johnson Matthey Technology Review is published by Johnson Matthey Plc.

JOHNSON MATTHEY
TECHNOLOGY REVIEW

www.technology.matthey.com

Johnson Matthey's international journal of research exploring science and technology in industrial applications

Contents

Volume 61, Issue 1, January 2017

JOHNSON MATTHEY
TECHNOLOGY REVIEW
www.technology.matthey.com

Guest Editorial

The Business of Sustainability

Johnson Matthey Plc, along with many similar companies and institutions, have found that sustainability can and should form the basis for their business of the future. These companies are setting aggressive targets for reducing the resources consumed in producing a unit of product, and finding these targets achievable when the whole workforce is engaged in addressing the issues.

It starts with simple resource efficiency: turning items off when not in use, conserving energy and heat, and reducing waste to landfill. Then it moves into designing new products that perform just as well as (or indeed better than) the ones they replace, but need less resources to produce: production efficiency. Waste products from a particular process become the raw materials for another process. The near term target is not zero consumption, but experience shows us that it can be much nearer to zero than anyone contemplated (1).

The pure business motivation for a sustainability effort is therefore cost control. Using less resource to make the same product saves money. But experience tells us that this is not the biggest benefit to a sustainability initiative. The biggest benefit is that sustainability has the potential to engage and motivate every employee, to harvest ideas and changing behaviours, and to give employees another reason to value their work for the company. Everyone agrees that this activity is helping the planet and is what the responsible company should be doing, and success makes employees proud of the company they work for.

Fundamental Role of Science

Science, of course, has a fundamental role in this process. It is scientists that can find the solutions to the big questions by using innovation to redesign existing products and processes, as well as bringing to market novel solutions that utilise resources in a much more efficient manner. But science needs funding and direction, and this is where business can be motivated to step in. Good businesses know that they want to be first to market with these solutions. The funding required will not be insignificant, but the business drivers are in place and the benefits to the successful company will be substantial. The early engagement of customers is an essential, but sometimes overlooked, step in this process. A good business puts its scientists close to its customers and provides the resources and direction for the science.

When employees and customers are all engaged in sustainability at work, a partnership between business and government can then deliver the necessary fiscal or regulatory action to drive the process further.

Feeding 9 billion people (2) whilst reducing dependence on non-renewable resources sounds an impossible task. But I believe that science, and in particular chemistry, has the potential to achieve such a feat. I believe that we do have time, as long as we get on with addressing the problems and start to take meaningful action now. Think of what we have achieved in our lifetimes, and how much more can be achieved in the next ten or twenty years dedicated to the task.

It starts with business and sustainability is good business.

NEIL CARSON, OBE

Honorary President, SCI, London, UK

References

1. “2016 Annual Report & Accounts: Sustainable Technologies for Today and for the Future”, Johnson Matthey Plc, London, UK, 2016, p. 25
2. UN News Centre, ‘World Population Projected to Reach 9.6 Billion by 2050 – UN Report’, 13th June, 2013: http://www.un.org/apps/news/story.asp?NewsID=45165#.WBdbrRvcuUl (Accessed on 31st October 2016)

http://dx.doi.org/10.1595/205651317X694317 *Johnson Matthey Technol. Rev.*, 2017, **61**, (1), 3–4

JOHNSON MATTHEY
TECHNOLOGY REVIEW
www.technology.matthey.com

Guest Editorial

Health Technologies at Johnson Matthey

In celebration of the 2017 year of "Sustainability" we here present the first of a series of Themed issues, this one focusing on the role of products and services, including many supplied by Johnson Matthey Plc, on human health.

Innovation and Long Term Value in Healthcare

With life expectancy on the rise and rapid urbanisation taking place in the developing world the prevalence of chronic, non-communicable disease (NCD) such as cardiovascular disease and diabetes has grown as a major societal cost. Once thought to be a malady primarily of the industrialised world, changing diets and lifestyles have led to a disproportionate increase in NCD prevalence in developing economies.

As costs rise, provider systems are looking to the benefits of delivering therapy with the help of single use devices that often have greater one-time payments, but are able to reduce the overall price of treating a chronic disease. In a surprising twist, many of the medical devices being developed to treat NCD in the most cost-effective manner have incorporated platinum and platinum group metals (pgm) selected over alternate lower-cost materials because of their unique combination of chemical, physical and mechanical properties. Another surprising material is the alloy known as Nitinol, a nickel titanium alloy with shape memory properties that make it uniquely suitable for medical applications.

Stroke is the world's second leading cause of death behind heart disease, and is the leading preventable cause of disability. Platinum is at the heart of devices that are being used by neurovascular surgeons to radically improve outcomes for patients either through the revascularisation of a diseased vessel (ischemic stroke) or by preventing the rupture of weakened blood vessels (haemorrhagic stroke).

A second area where pgms are performing a critical role is within devices used to treat the cardiovascular condition of atrial fibrillation (AF) where disordered electrical signals in the heart lead to poor blood flow. These radiofrequency ablation catheters take advantage of the electrical, biocompatible and radiopaque features unique to platinum alloys to improve patient quality of life, without the need for long term pharmaceutical use.

One of the most exciting emergent uses of pgms in medical devices is their application in neurostimulation devices. Many systems within the human body, including the central and peripheral nervous systems, are regulated *via* the transmission of electrical signals through and between the brain and the rest of the body. Innovative neurostimulation devices take advantage of pgm-based electrode arrays to make the critical connection between implantable pulse generators and parts of the body including the deep brain and the spinal cord.

Peripheral arterial disease is a growing problem in which normal blood flow is impaired due to narrowing of the artery. It often affects the lower limbs and is associated with the growth in incidence of diabetes, high blood pressure and obesity worldwide. Endovascular treatment for this condition *via* stenting restores blood flow through the affected artery. Due to its flexibility and crush resistance, Nitinol is used to make self-expanding stents for such applications.

As society is looking towards exerting greater control over rising health costs, while at the same time delivering high quality care, a shift towards the use of medical devices for the treatment of NCD is gaining favour. Because of the unique properties of materials like pgm and Nitinol, they have become central components in many of the devices being introduced to treat these diseases in a cost effective, sustainable way.

Johnson Matthey's Pharmaceutical Products and Services

Johnson Matthey has a long history with the pharmaceutical industry, and many readers of this journal are likely to be familiar with our background in platinum-based active pharmaceutical ingredients (APIs) such as cisplatin and carboplatin which are used in cancer therapies (and can be read about in this issue of the journal). However the scope and scale of our current pharmaceutical activities now reaches far beyond these specialised precious metal based drugs.

Johnson Matthey now has a wide range of products and services applied across the pharmaceutical industry. We partner with companies which are investigating and developing novel therapies that will address significant unmet medical needs of patients with debilitating and degenerative diseases.

We also have significant activity in the supply of products which are no longer under patent protection, the so-called generics industry. These generic APIs are extensively used to provide cost effective medical care all over the world.

In addition to pharmaceutical actives, we are also a major supplier of catalysts to the pharma industry.

Our offerings that support the pharmaceutical industry can be summarised as follows:

- **Custom Manufacturing**: This is a service offering to innovative pharmaceutical companies developing novel drugs. Many of these customers do not have their own manufacturing facilities and they typically partner with Johnson Matthey to take advantage of our chemistry expertise and manufacturing assets to help develop and commercialise their products.
- **Controlled Substances**: A specific class of APIs that are used, for example, in pain management, psychiatric disorders and other disease management. Because of their nature and potential for illicit use, they are subject to stringent government controls which restrict their manufacture and distribution. This requires additional expertise and capabilities for manufacture and supply.
- **Other APIs**: This is Johnson Matthey's wider product offering of APIs (that are not controlled substances). We identify new products that we can competitively make, manufacture and supply to the pharmaceutical industry. We supply products used in a wide range of therapies including cancer, Parkinson's disease and glaucoma.
- **Catalysts**: A cornerstone of Johnson Matthey's reputation in the pharmaceutical industry is our ability to develop and supply highly effective and efficient chemical process catalysts. As well as conventional pgm-based catalysts, we have invested in a range of novel technologies such as biocatalysts (see previous issues of this journal).

These products and services are underpinned by core Johnson Matthey capabilities and technologies. For example, utilising our expertise in materials science we carefully control the physical form and morphology of APIs to enhance their performance. We employ large scale advanced chromatographic techniques such as supercritical fluid chromatography (SFC) and preparative high-pressure liquid chromatography (HPLC) to purify highly complex materials.

So from origins based around our heritage skills in pgms, Johnson Matthey has significantly expanded its reach within the health industries. Using our core scientific capabilities, manufacturing excellence and focus on sustainability we now help support the development of novel products and the cost effective provision of healthcare.

JOHN F. X. MORLEY

Global Commercial Manager - Medical Components, Johnson Matthey Inc., West Whiteland, USA

Email: john.morley@jmusa.com

NICHOLAS JOHNSON

Strategic Marketing Director, Johnson Matthey Fine Chemicals, Edinburgh, UK

Email: nicholas.johnson@matthey.com

http://dx.doi.org/10.1595/205651317X693516 Johnson Matthey Technol. Rev., 2017, 61, (1), 5–15

JOHNSON MATTHEY
TECHNOLOGY REVIEW
www.technology.matthey.com

Molybdenum/Bismuth Based Mixed Metal Oxide Catalysts for Selective Propylene Oxidation and Zeolite Membrane Protected Palladium/Alumina Catalysts for Selective Carbon Monoxide Oxidation and Application in a Process Loop Using a Propane Feed

By Maria Rivas Velazco, William McDonnell* and Andrew W. J. Smith
Johnson Matthey Technology Centre, Blount's Court, Sonning Common, Reading, RG4 9NH, UK

***Email:** william.mcdonnell@matthey.com

As part of a process loop to make acrylic acid from propane, catalysts for two reactions have been investigated. Mo/Bi based mixed metal oxides for selective oxidation of propylene in a propane feed have been prepared by a sol-gel method which increased activity over the standard catalyst. Modifications of the molecular formula led to an increase in selectivity towards acrolein whilst maintaining the improved conversion. X-ray diffraction (XRD) analysis showed the sol-gel method helped incorporate the various mixed metal oxides and prevented segregation during reaction conditions. A Pd-loaded 4A zeolite membrane catalyst was developed on the surface of 1 mm beads γ-Al_2O_3 support. The membrane was employed in the selective oxidation of CO in a propane-rich mixture. The zeolite coating was developed by using a new modification of the hydrothermal synthesis (dilution method). Catalytic test results confirmed that the selective oxidation of CO in the presence of propane is possible by using a 4A zeolite membrane coated on a Pd based catalyst. Temperature and time during zeolite preparation are key parameters in the stability and reproducibility of the zeolite membrane. The seeding method improves the growth of the zeolite on the catalyst surface and does not affect the stability and reproducibility of catalyst. By using this catalyst it is possible to get a temperature window for the selective oxidation of CO (65ºC).

Introduction

CARENA (CAtalytic membrane REactors based on New mAterials for C1-C4 valorization) was a four-year Seventh Framework Programme (FP7) funded EU project carried out between 2011 and 2015 with a consortium consisting of 18 members. The partners were a mix of universities, research centres and industrial companies. The purpose of the project was to investigate several areas of industrial interest where current technology prevents commercialisation and to couple new catalysts with new membranes with the aim of improving the state of the art for these processes. Each partner would bring their own area

of expertise, i.e. catalysis, membrane development, modelling, reactor design, and characterisation.

The project was split into six main Work Packages. There were three reaction based Work Packages which aimed to develop and improve specific reactions:

- WP1 investigated methane activation. More specifically steam methane reforming (SMR), oxidative coupling of methane (OCM), and direct methane to methanol (MTM)
- WP2 developed a new process loop for the production of acrylic acid from propane. This included propane dehydrogenation (PDH), selective oxidation of propylene and selective oxidation of CO
- WP3 investigated the potential use of CO_2 as a reactant. The two reactions researched were CO_2 + H_2 to methanol, and CO_2 + methanol to dimethyl carbonate.

There were also three transversal Work Packages. These aimed to investigate more general research and methodologies that could be applied to all three of the reaction Work Packages:

- WP4 was the membrane toolbox. This investigated new high risk membranes which could be applicable in WP1–3 and also new ways to characterise membranes
- WP5 was the catalyst toolbox. The work in this WP concerned new catalyst designs, kinetic studies, mechanistic studies and characterisation
- WP6 was the modelling toolbox. The work here pertained to reactor modelling and the integration of membranes with catalysts.

One of the primary obstacles the project had to overcome was the disparity between catalyst and membrane operating conditions that often existed. As such there was a special focus within the project to develop new materials that were active at new temperatures to accommodate integrated catalytic membrane reactors for the processes investigated.

The focus of this paper is Work Package 2 and the work carried out by Johnson Matthey within it. WP2 investigated a new process loop for propane to acrylic acid (**Figure 1**) (1). Traditionally after propane dehydrogenation the resulting propane/propylene mixture has to be separated and the propylene then diluted in N_2 down to ~8%. This is then selectively oxidised to acrolein and then acrylic acid. Within CARENA the aim was to remove the separation and dilution steps and retain propane as the carrier gas for propylene during the selective oxidation steps. After removal of acrylic acid the propane can then be recycled.

The use of propane has the added benefit that the amount of propylene in the feed can be doubled to ~15%. This is because propane has a higher heat capacity and the exothermicity can be more easily controlled. A selective CO oxidation unit has been included as a buildup of CO in the loop could poison the propylene oxidation catalysts.

Johnson Matthey had two main roles within this Work Package. The first was to develop and test novel catalysts for the selective oxidation of propylene into acrolein. During this period Johnson Matthey Technology Centre, Sonning Common, UK, supplied catalysts developed on site. New synthesis methods were investigated for catalyst preparation and a new test rig was constructed so testing could be achieved in the correct gas composition. The second part of Johnson Matthey's input was working on a novel membrane catalyst for selective CO oxidation in a propane feed. Here the goal was to combine the catalyst and membrane into a single piece which could distinguish the CO from the propane and hence only combust the CO into CO_2 without converting the remaining propylene and propane. The membrane catalyst preparation was based on previous work (2–4). However the original preparation method was not reproducible and work concentrated on modifying the reaction conditions to produce a stable reproducible catalyst which gave a good separation and excellent selectivity. The material may also have other applications for gas separation and catalysis in mixed gas streams. The objective was to scale-up the membrane catalyst for testing in a demonstrator unit.

Propylene oxidation was to be carried out with pure oxygen on a pilot scale unit (at a scale of about 1–3 kg h^{-1}) where the catalyst arrangements are designed to operate at a conversion above 95% and at an acrylic acid yield above 85%. The reaction should benefit from other positive effects of the alkane rich ballast gas, which has a much higher specific heat capacity. This allows a higher heat transfer to the gas phase, a better control of the reactor temperature and thus a higher productivity, or a higher selectivity. This reduces either capital expenditure or operating cost.

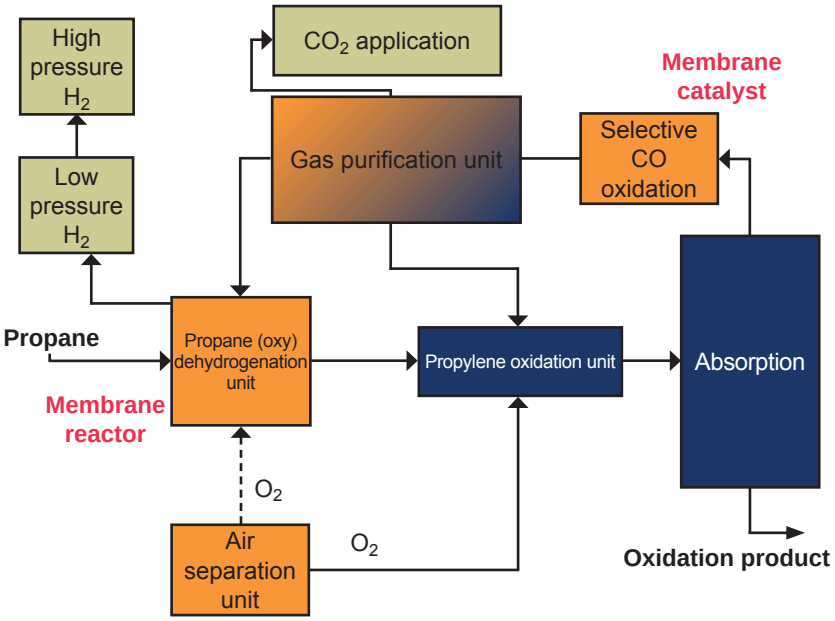

Fig. 1. Proposed process scheme for propane to acrylic acid (1)

Experimental

Propane to Acrolein: Synthesis, Characterisation and Testing

Catalysts were prepared using either slurry or a sol-gel preparation method. The slurry method reported previously was used to prepare the standard catalyst for testing (5). The sol-gel method entailed dissolving ethylene glycol and citric acid in water and heating at 60ºC until a gel was formed. The nitrates were dissolved in water. The bismuth nitrate required some extra nitric acid to dissolve fully. The ammonium molybdate and tin chloride were dissolved separately in water. The nitrates were added to the gel first followed by the chloride and then the molybdate which initiates precipitation of the product. Tungsten oxide powder was then added to the mixture. The temperature was maintained at 60ºC for several days until the majority of water had been evaporated. The resulting paste or gel was dried at 140ºC for 12 h and calcined at 500ºC for 6 h.

The catalysts were characterised by their catalytic properties as well as by XRD and temperature-programmed reduction (TPR). XRD data were collected in reflection geometry over at least the 10º < 2θ <100º range, on a Bruker AXS D8 ADVANCE fitted with a Göbel mirror using Cu Kα (λ = 1.5406 + 1.54439 Å). The diffraction patterns were fitted in TOPAS with instrumental peak profiles determined experimentally using data collected from a NIST LaB_6 standard. TPR was performed on a Micromeritics AutoChem II 2920 chemisorption analyser using 5% H_2/N_2 at 30 ml min^{-1} up to 900ºC with a ramp of 10ºC min^{-1}.

Catalytic testing was performed in a continuous flow fixed bed reactor working at atmospheric pressure. 200 mg of catalyst, pelleted to 255–350 µm size fraction, was held in a quartz reactor (internal diameter 4 mm) by quartz wool plugs. A gas mixture of $C_3H_8/C_3H_6/O_2/H_2O/N_2$ = 23/7/10/6/4 at a flow rate of 50 ml min^{-1} was passed over the catalyst and the temperature was raised to 320ºC. The reaction products were analysed online on a Varian gas chromatograph fitted with a 1.5 M 1/8 2 mm 13X 80/100 molecular sieve, an Agilent J&W PoraPLOT for separation and two thermal conductivity detectors and a flame ionisation detector for measurement.

Selective Carbon Monoxide Oxidation: Synthesis, Characterisation and Testing

A series of catalysts with different platinum group metal (pgm) loading was made by incipient wetness, using γ-Al_2O_3, 1 mm beads as supports. The alumina beads were coated with a zeolite 4A, as this zeolite has the correct pore size (~0.4 nm) to distinguish

CO and propane. The zeolite coating was developed by using a variation of a hydrothermal synthesis (2–4). The synthesis was modified (temperature, time and dilution) in order to improve the uniformity of the zeolite coating, thus increasing the operating window and making the zeolite synthesis more applicable in terms of scale up. The effect of seeding on the zeolite growth was also investigated. Seeding has been reported before to promote the uniformity of the zeolite layer (6). The solution was prepared using a commercial LTA nanozeolite with 100 nm particle size (4). The nanozeolite was dispersed in water in order to produce a very dilute solution. The final mixture was stirred at 40ºC for 30 min. Subsequently the Pd/γ-Al_2O_3 catalyst was dipped into the zeolite solution for different times (the seeding time was optimised by varying the time from 1 s to 5 min). Finally the seeded catalyst was dried at 140ºC overnight. For the hydrothermal synthesis, the catalyst beads were added to a zeolite gel which was prepared by rapidly adding a solution of sodium aluminate to a solution of sodium metasilicate. The catalyst containing gel was stirred at room temperature for 30 min and then hydrothermally crystallised at 60ºC. The Pd/γ-Al_2O_3 zeolite coated beads were separated from the crystallisation solution and washed with demineralised water, dried overnight, and then calcined at 500ºC.

A combination of catalytic tests, scanning electron microscopy (SEM) and XRD was used to complete understanding of the performance level and the characteristics of the coating on the catalyst. XRD of the bulk material gives a general idea of the extent of crystallisation which might be extrapolated into defining the crystallinity of the thin zeolite film. By SEM it is possible to have more information about the coating uniformity. XRD data were collected in reflection geometry over at least the 10º < 2θ < 100º range, on a Bruker AXS D8 fitted with a Göbel mirror using Cu Kα (λ = 1.5406 + 1.54439 Å). The diffraction patterns were fitted in TOPAS with instrumental peak profiles determined experimentally using data collected from a NIST LaB_6 standard. SEM analyses were conducted using a Zeiss ULTRA 55 Field Emission Scanning Electron Microscope. The sample powder was placed directly on SEM stubs. The samples were carbon coated prior to analysis to provide a conductive layer for charge dissipation.

A catalytic test was the primary method used to distinguish the best performing catalysts from the rest. The 4 Å kinetic window of the zeolite was expected to selectively allow molecules of lesser dimension access to the active metal centres inside the macropores. Testing was conducted over uncoated and coated pgm catalysts. Catalytic evaluation was performed in a continuous flow fixed-bed catalytic reactor working at atmospheric pressure. 400 mg of catalyst were placed between quartz wool plugs in the centre of a cylindrical tube reactor (7 mm internal diameter). Internal and external temperatures of the catalyst reactor were measured by nickel-chromium thermocouples. The reaction was carried out by feeding a mixture of carbon monoxide/propane/oxygen = 0.5/25/1.0 and nitrogen as a diluent, at a total flow of 200 ml min^{-1}, gas hourly space velocity (GHSV) = 12000 h^{-1} and scanning reaction temperatures from room temperature to 300ºC. The reaction products CO and CO_2 were analysed online by a multi gas analyser from Sigma Instrumental provided with an infrared detector for CO and CO_2. Additional catalytic tests were carried out in order to evaluate the stability of the membrane catalysts at a set temperature (250ºC) for 5 hours.

Results and Discussion: Propylene to Acrolein

All the acrolein catalysts have been compared to the standard sent by Arkema (Mo/Bi/Fe/Co/Ni/Sn/W/Si/K) from Example 1 of the patent (5), labelled as AC. Initially the work focused on reproducing the Arkema standard. Several preparation methods were used, i.e. co-precipitation, evaporation and sol-gel. However, conversion was improved from 50% to 73% by the use of the sol-gel method. Selectivity was also improved, but only slightly, up from 79% to 84%.

A series of catalysts breaking down the Arkema composition to understand the relative importance and effect of various components was prepared by sol-gel and tested. **Figure 2(a)** shows the composition has a large influence on the conversion. The presence of nickel seems imperative for high conversions. Other elements as tungsten and tin also have a large positive effect. The effect of silicon is unclear and in certain cases even seems to reduce the conversion. Additionally, the effect of pgms on the catalytic performance was investigated. It was found that impregnating Pd onto the full composition had little effect on the conversion whereas rhodium actually had a negative effect.

Figure 2(b) shows the selectivities for the Arkema type catalysts. Again the Ni is necessary to achieve high selectivities and W also has a large positive effect

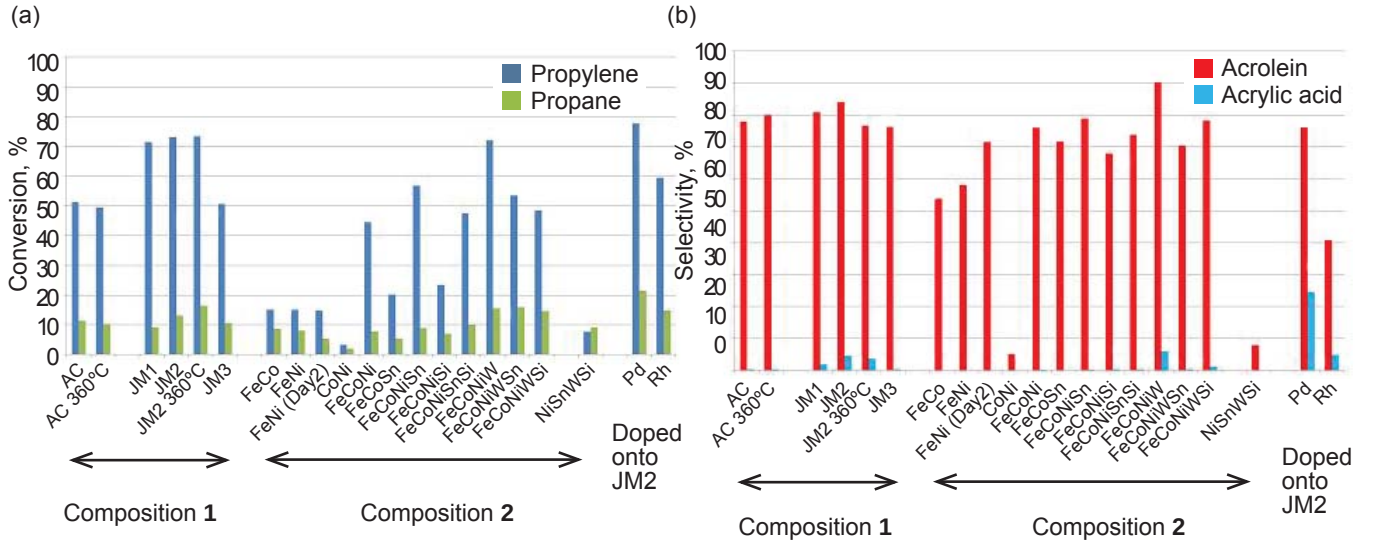

Fig. 2. Bismuth molybdate based mixed oxides for propylene to acrolein: (a) conversions of propane and propylene for Arkema type catalysts at 320ºC (unless stated); and (b) selectivities to acrolein for Arkema type catalysts at 320ºC (unless stated). Composition **1**: $BiMo_{12}Fe_{3.7}Ni_{2.6}Co_{4.7}Sn_{0.5}W_{0.5}K_{0.08}SiO_x$; Composition **2**: All contain $Mo_{12}BiK_{0.08}O_x$, other elements have molar quantities as in the Arkema composition if present

on the selectivities, whereas Sn has a small positive effect. Adding pgms (**Figure 3**) to the full composition has a negative effect on the selectivity to acrolein but in the case of Pd the amount of acrylic acid produced becomes significant (>20%). Over time the selectivity reduced at the expense of CO and CO_2 as coking of the catalyst increased.

Work was performed investigating new compositions of catalyst. This included many variations and new active sites were investigated as well as new configurations of dopants for oxygen mobility. Of particular note were the catalysts with cerium, ceria and ceria/zirconia (**Figure 4**) added to the standard composition. The promoters were incorporated into the catalyst composition mixture by different methods. Introduction of nitrate precursors into the sol-gel mixture resulted in complete deactivation in some cases. However, incorporation of the Ce by addition

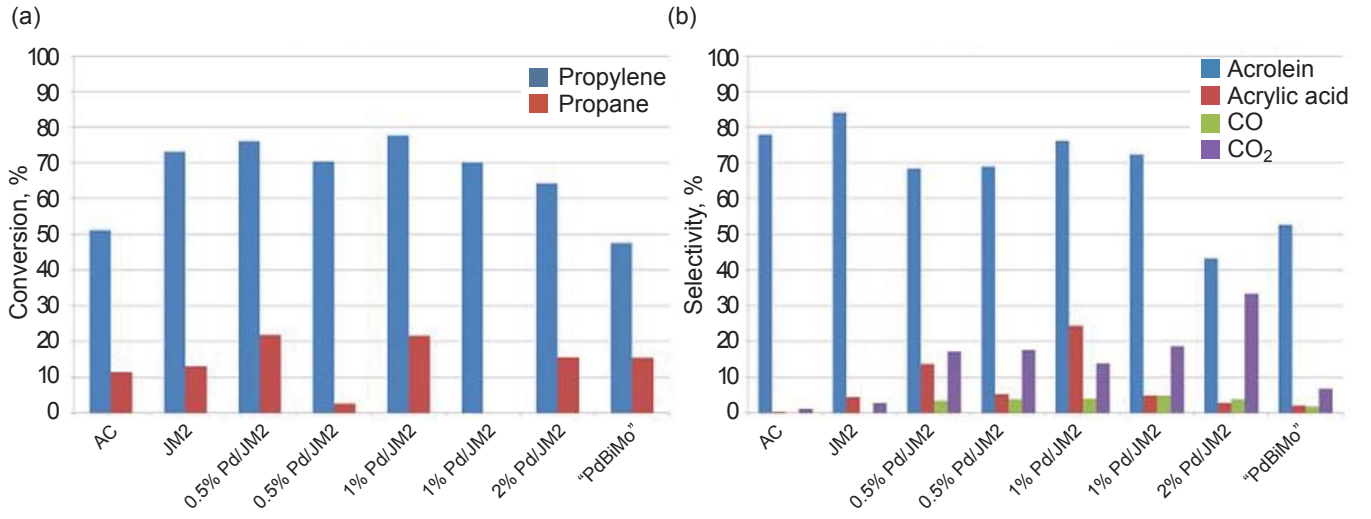

Fig. 3. (a) Conversion of propylene and propane samples based on the standard catalyst doped with Pd; (b) selectivity to acrolein and acrylic acid of samples based on the standard catalyst doped with Pd.
"PdBiMo" = $Pd_{0.205}BiMo_{12}Fe_{3.7}Ni_{2.6}Co_{4.7}Sn_{0.5}W_{0.5}K_{0.08}SiO_x$

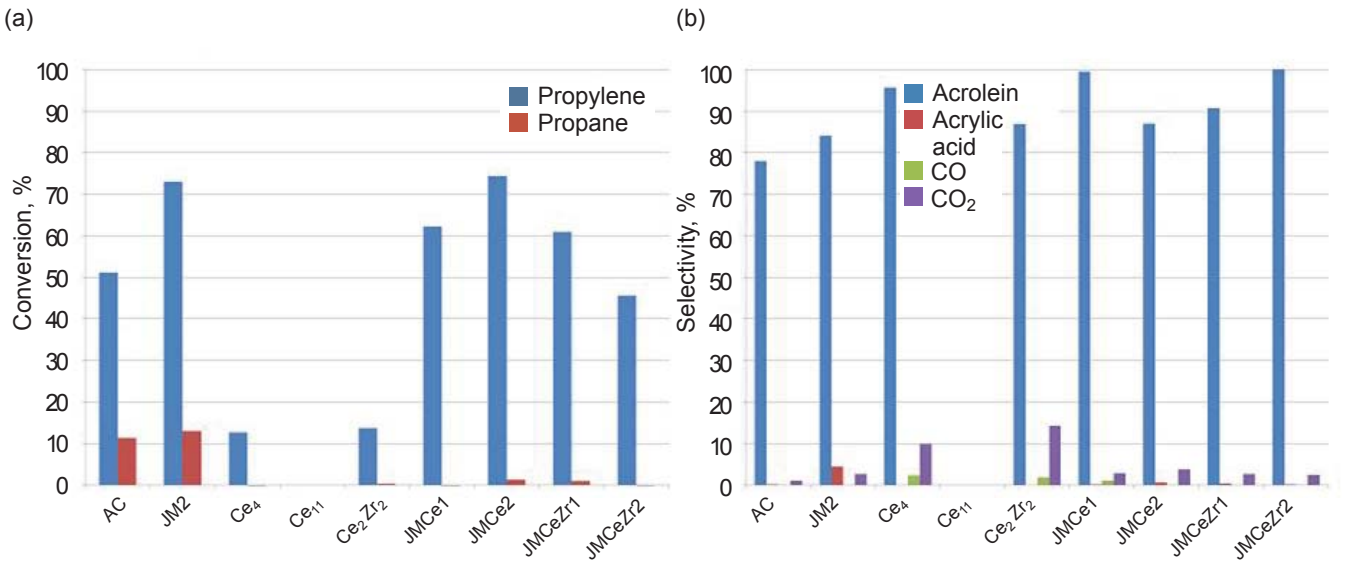

Fig. 4. Conversions and selectivities of samples incorporating Ce and CeZr: (a) conversion of propylene and propane of samples based on the standard catalyst with Ce or CeZr added; (b) selectivity to acrolein and acrylic acid of samples based on the standard catalyst with Ce or CeZr added

of preformed ceria resulted in an excellent catalyst (JMCe1) which displayed a conversion of 62% and very high selectivity >95% (**Figure 4**).

Work was also carried out on novel compositions based on molybdenum/bismuth/vanadium/cerium. A large series of catalysts was produced and tested. Mo/V ratio, Bi content and Ce content were all investigated; as was the effect of other dopants into the catalyst composition and preparation method. In general these catalysts were less active than the standard composition type catalysts and required elevated temperatures of 380ºC. The best catalyst showed a high selectivity of 90% but the conversion was only 30% even at 380ºC. Some catalysts in this series showed conversions above 40% but these had much lower selectivities.

The catalysts were then characterised to increase understanding of their behaviour. XRD characterisation of the best catalyst based on the Arkema composition (JM2) did not show the MoO_3 phase within the structure (**Figure 5**). AC on the other hand had a considerable amount of MoO_3 present. MoO_3 is known to be inactive in this reaction and its presence means not all of the Mo is being used to generate active sites. Additionally, XRD results after reaction of the AC showed a large proportion of the Bi_2Mo_x phase. This suggests bismuth molybdate is segregating out of the catalyst structure. Although bismuth molybdate is the active site, if it becomes segregated then it cannot be replenished with oxygen and the catalyst will deactivate. JM2 prepared by the sol-gel method shows a much smaller peak which means the bismuth molybdate is remaining fully integrated in the catalyst structure. **Figure 6** shows clear CeO_2 peaks in the XRD of JMCe1 meaning the ceria does not incorporate into the bulk structure but probably aids transmission of oxygen from the gas phase into the bulk catalyst. The TPR shows an extra, large peak for the AC catalyst believed to be MO_3 which is not visible in the other samples.

Selective Oxidation of CO in Propane

The zeolite made by the modified hydrothermal synthesis was characterised with the aim of understanding the characteristics of the material. **Figure 7** shows the XRD results confirming the formation of a zeolite 4A-crystalline structure.

To begin the evaluation of the membrane catalyst, the first step was to test a Pd/γ-alumina uncoated catalyst in order to establish the CO and propane oxidation temperatures under reaction conditions. Catalytic performance shows that CO oxidation is complete by ~180ºC and propane oxidation is complete by ~130ºC (**Figure 8**) under these test conditions. This result confirms that there is an overlap in the CO and propane oxidation temperatures, and therefore the need for a membrane layer on the catalyst.

The next step was to test the catalysts coated by the zeolite prepared by the modified hydrothermal method (6), with the aim to fully investigate the separation properties of the zeolite membrane. For this, effects

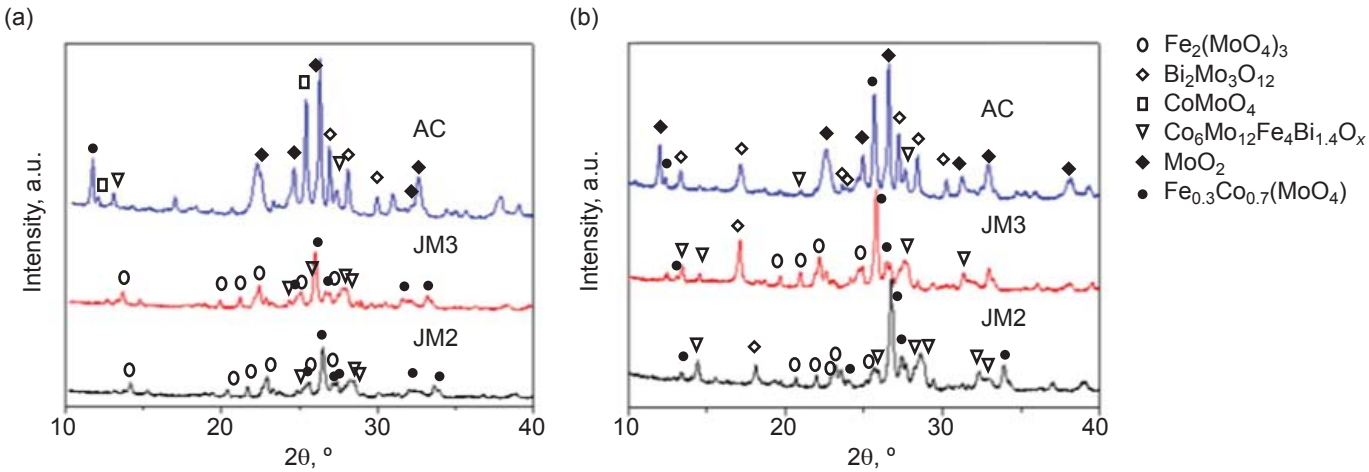

Fig. 5. XRD of standard composition catalysts prepared *via* different routes: (a) before reaction; (b) after reaction. AC is Arkema catalyst, JM3 is slurry method and JM2 is sol-gel method

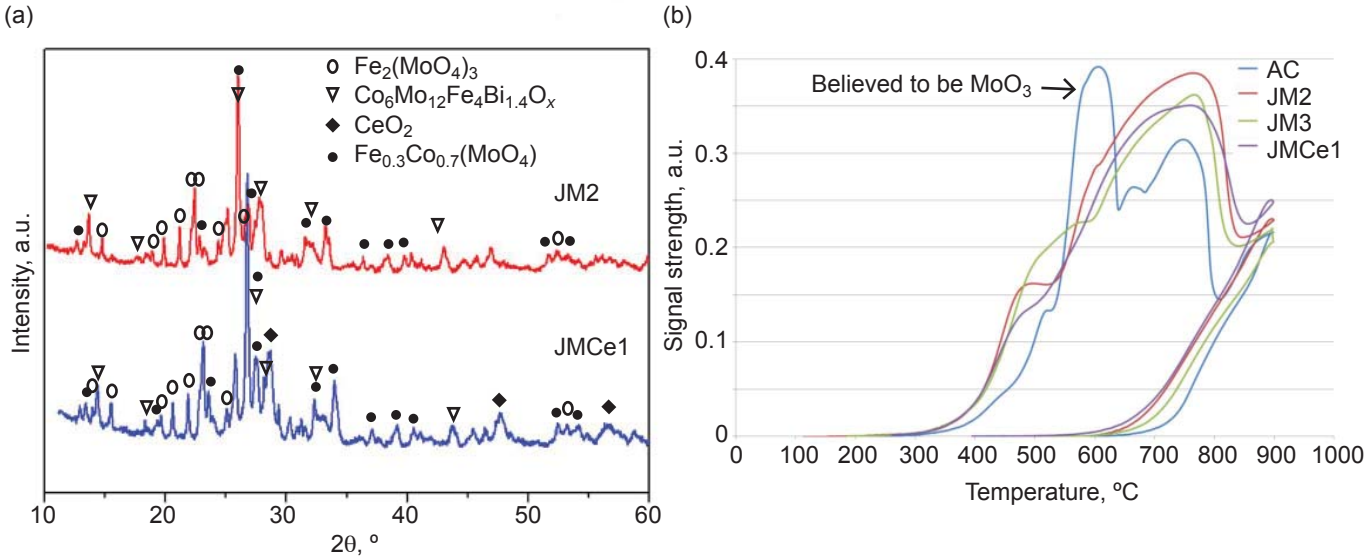

Fig. 6. (a) XRD comparison of standard composition and with ceria added; (b) TPR of different catalysts ramped to 900°C at a rate of 10 °C min^{-1} under 5% H_2 in N_2

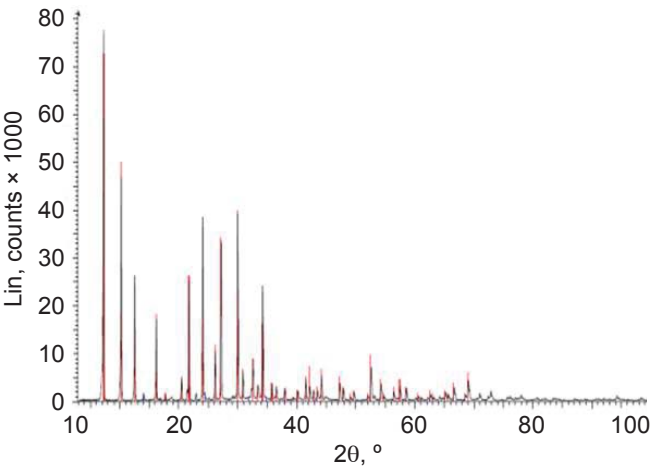

Fig. 7. XRD diffractogram of the zeolite 4A synthesised hydrothermally. The result confirms the formation of 4A crystalline structure

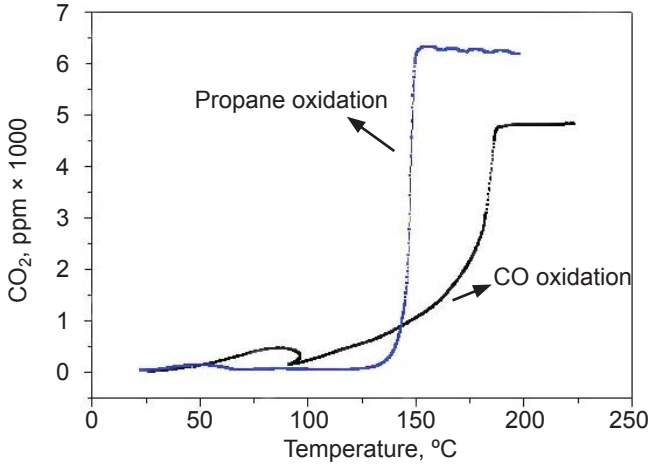

Fig. 8. Selective CO oxidation in propane *vs*. temperature (pgm uncoated catalyst) $CO/C_3H_8/O_2/N_2$ = 0.5/25/1.0/balance, total flow of 200 ml min^{-1}, GHSV = 12,000 h^{-1}, T = 25–300°C

of time and temperature on the zeolite structure were investigated. SEM results of the zeolite membrane catalyst prepared under different conditions (**Figure 9**) show a clear effect of temperature and time on the zeolite crystallinity. 3 h was not enough time for zeolite crystallisation at 60ºC. Material prepared under these conditions showed a spherical structure (**Figure 9(a)**). By increasing the synthesis time from 3 h to 6 h, a good cubic crystalline structure can be observed (**Figure 9(b)**). The degree of crystallinity of the zeolite could be improved by conducting the synthesis at 80ºC for 3 h. However, a longer synthesis time at 80ºC (6 h) led to a modification of the crystalline structure leading to a needle structure. This structure is not selective between CO and propane. Catalytic tests for selective CO oxidation in propane confirm these results (**Figure 10**). The zeolite membrane catalyst prepared at 60ºC for 6 h provided a higher operating window as shown later in the present article.

The effect of seeding on the zeolite coating was also investigated. SEM characterisation results of the membrane catalyst prepared by using the seeding step show a uniform layer of zeolite 4A formed over the catalyst (**Figure 11**). The images confirm the formation of a membrane catalyst where the active phase (PdO), γ-Al_2O_3 support, and a uniform zeolite structure can be differentiated.

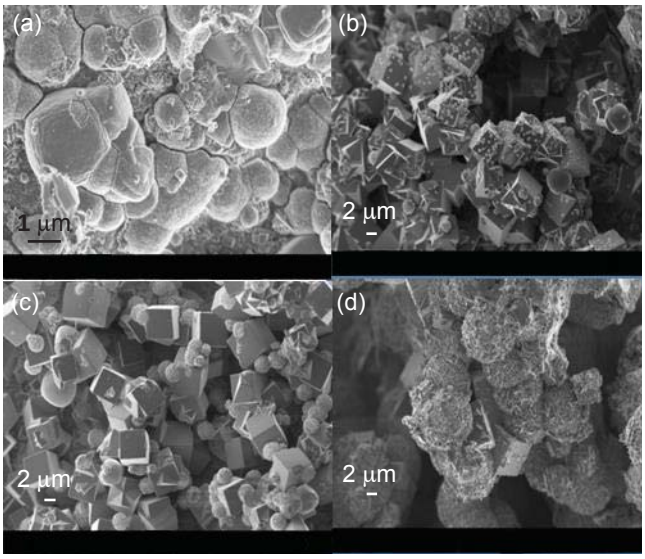

Fig. 9. SEM results of the zeolite membrane catalysts synthesised hydrothermally at different conditions (time, temperature): (a) 60ºC, 3 h; (b) 60ºC, 6 h; (c) 80ºC, 3 h; (d) 80ºC, 6 h

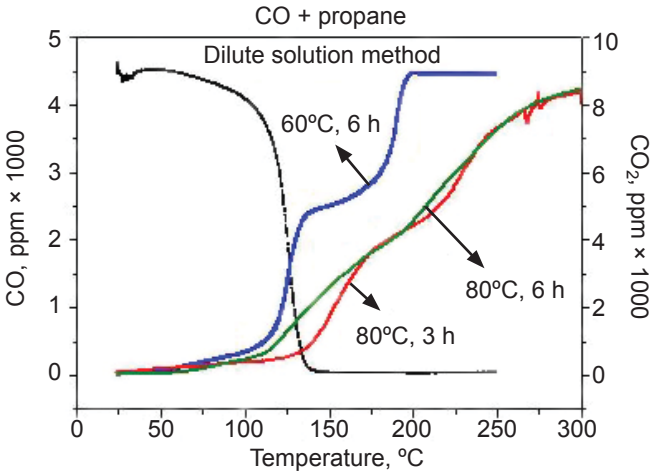

Fig. 10. Effect of temperature and time on the selective CO oxidation in propane. $CO/C_3H_8/O_2/N_2$ = 0.5/25/1.0/balance, total flow of 200 ml min^{-1}, GHSV = 12,000 h^{-1}, T= 25–300ºC

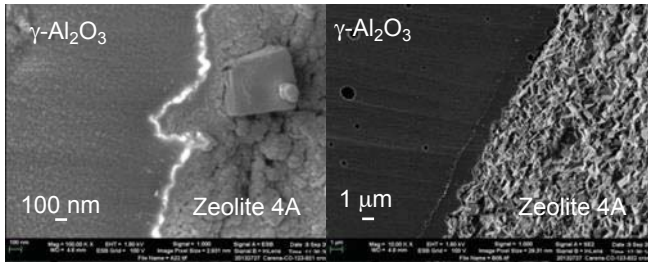

Fig. 11. Cross-section of the zeolite membrane catalyst synthesised hydrothermally

Characterisation results are in line with the catalytic behaviour where the seeded catalyst showed the best performance (7). The seeded membrane catalyst showed higher separation of CO from propane (50ºC *vs.* 60ºC). The performance was further improved after being fired at 500ºC for 2 h reaching an operation window (CO/propane separation) at 80ºC (**Figure 12**). The thermal process seems to improve the interaction between the zeolite coating and the supported catalyst, therefore improving the gas separation (8).

The stability of the zeolite membrane catalyst and the effect of propylene on the catalytic performance were also evaluated. At 230ºC for 5 h the catalyst showed only full CO conversion (no propane conversion). It is important to note that no deactivation was observed during this period of time (**Figure 13**). The results confirm that the membrane catalyst fulfils the requirements within the process loop. This process

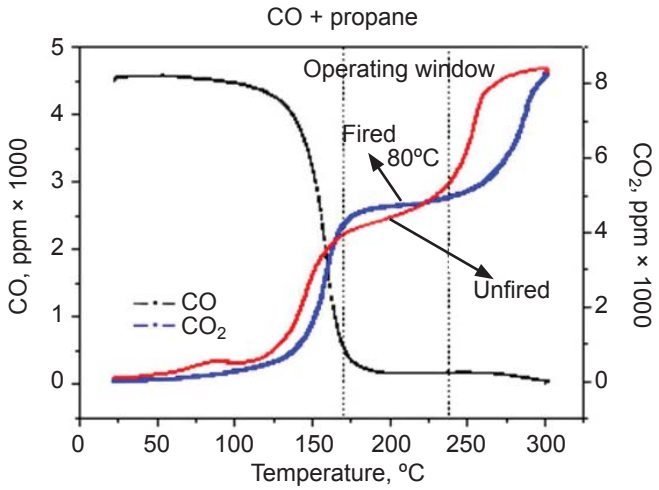

Fig. 12. Effect of seeding and calcination on the selective CO oxidation in propane. $CO/C_3H_8/O_2/N_2$ = 0.5/25/1.0/balance, total flow of 200 ml min^{-1}, GHSV = 12,000 h^{-1}, T= 25–300ºC

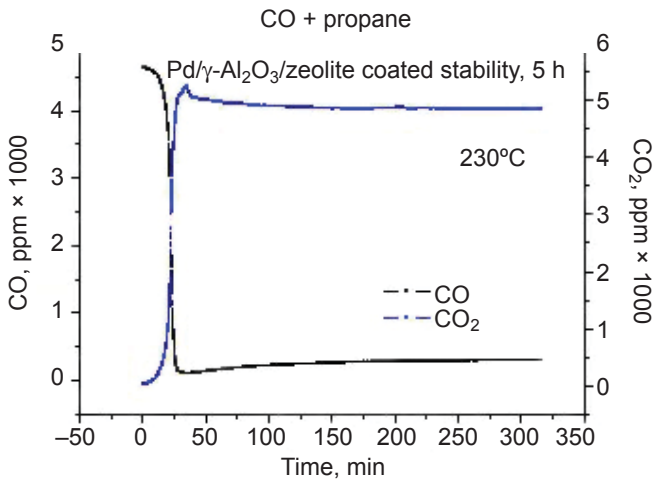

Fig. 13. Stability of the membrane catalyst for selective CO oxidation in propane. $CO/C_3H_8/O_2/N_2$ = 0.5/25/1.0/balance, total flow of 200 ml min^{-1}, GHSV = 12,000 h^{-1}, T= 230ºC

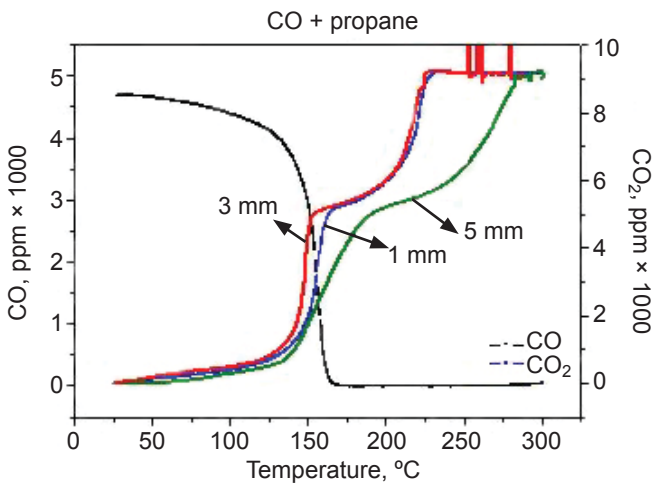

Fig. 14. Effect of the support size. $CO/C_3H_8/O_2/N_2$ = 0.5/25/1.0/balance, total flow of 200 ml min^{-1}, GHSV = 12,000 h^{-1}, T= 25–300ºC

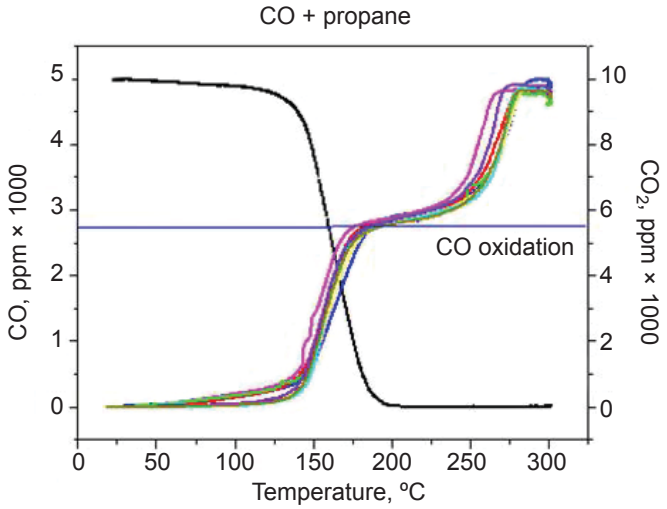

Fig. 15. Reproducibility of the zeolite coated catalyst

involves a partial oxidation of propane in propene at 250ºC.

For the scale-up process different size beads (1 mm, 3 mm and 5 mm) were coated and evaluated in the reaction. The zeolite coated catalysts showed some differences. The 1 mm and 3 mm coated beads (**Figure 14**) showed a similar catalytic behaviour, with a good separation between CO and propane. The 5 mm beads showed a more gradual oxidation over the temperature range, but still differentiated between the two gases (CO/propane). Since the catalytic performance of the zeolite membrane catalyst synthesised by using the 5 mm beads was good in terms of separation, stability and reproducibility, the last step was to scale up the catalyst for the demonstrator unit. A batch of 0.5 kg of Pd/γ-Al_2O_3 (5 mm) beads zeolite membrane catalyst was successfully scaled up. This sample was sent to Arkema for evaluation in the pilot plant.

Conclusions

The use of new preparation methods and understanding of the properties of a complex catalyst has led to a new generation catalyst that has very high selectivity and competitive conversion over the state of the art

for the propylene to acrolein catalyst. The sol-gel preparation method gives a much improved catalyst which XRD showed is due to better incorporation of Mo in the catalyst structure creating more active sites for propylene oxidation. The incorporation of CeO_2 aided the reaction as CeO_2 is a known oxygen transport compound and oxygen availability at the active site is crucial for good catalytic activity. The manner in which the CeO_2 was introduced during the preparation method was also shown to be highly important.

Novel formulations were also investigated and although less active than the current state of the art catalysts their simple formulations would allow for greater research possibilities in the future.

Selective CO oxidation in the presence of propane is possible by using a 4A zeolite membrane coated on a Pd-based catalyst. The zeolite coating was developed by a modification of an existing hydrothermal method. Temperature and time are key parameters in the stability and reproducibility of the membrane catalyst. The best synthesis conditions are 60ºC for 6 h. It was also found that the seeding method improves the growth of the zeolite on the catalyst surface over previous methods. With these conditions an operation window of 80ºC between CO and propane was achieved. Stability and reproducibility of the membrane catalyst was not affected by the dilution method. The scale-up of the membrane catalyst to several hundred grams was successful. It was possible to achieve a good separation with a good reproducibility of the material. Further work however would be required to consider this process for full scale-up to kilo or tonnage scale. Several key points would need to be addressed including moving from hydrothermal to thermal conditions.

Acknowledgements

The authors gratefully acknowledge the funding of the European Union Seventh Framework Programme (FP7/2007–2013) within the project CARENA. The authors also would like to thank: Chandresh Malde, Paul Collier and Kerry Simmance for their support in zeolite synthesis, Steve Poulston and Andrew Steele for their support in catalytic evaluation, and all the Analytical Department at Johnson Matthey Technology Centre, Sonning Common, UK.

References

1. CARENA – Project: http://www.carenafp7.eu/index.php/Project/Project.html (Accessed on 14th June 2016)
2. K. E. Goodman, J. W. Hayes, C. N. Malde and M. I. Petch, Johnson Matthey Plc, 'Method of Coating Materials with a Zeolite-Type Substance', *European Patent* 0,878,233; 1998
3. P. J. Collier and S. E. Golunski, Johnson Matthey Plc, 'Selective Oxidation', *European Patent* 1,434,833; 2007
4. P. Collier, S. Golunski, C. Malde, J. Breen and R. Burch, *J. Am. Chem. Soc*., 2003, **125**, (41), 12414
5. G. Hecquet, J.-P. Schirmann, M. Simon, G. Descat and E. Etienne, Atochem Elf SA, 'Process for the Manufacture of Acrolein from Propylene by a Redox Reaction and Use of a Solid Mixed Oxide Composition as Redox System in the Said Reaction', *US Appl*. 6,080,893; 2000
6. X. Xu, W. Yang, J. Liu and L. Lin, *Micropor. Mesopor. Mater*., 2001, **43**, (3), 299
7. Y. Liu, Z. Yang, C. Yu, X. Gu and N. Xu, *Micropor. Mesopor. Mater*., 2011, **143**, (2–3), 348
8. Y. J. Zhong, X. H. Xu, L. Chen, M. F. Luo, Y. L. Xie, C. A. Ma and W. D. Zhu, 'Reactant-Selective Oxidation Over Composite Zeolite-4A Coated Pt/γ-Al_2O_3 Particles', in "From Zeolites to Porous MOF Materials – the 40th Anniversary of International Zeolite Conference", eds. R. Xu, J. Chen, Z. Gao and W. Yan, Proceedings of the 15th International Zeolite Conference, Beijing, China, 12th–17th August, 2007, Studies in Surface Science and Catalysis, vol. 170A, Elsevier Science, Amsterdam, The Netherlands, 2007, p. 1313

The Authors

Maria Elena Rivas obtained a BSc in Chemistry from the Central University of Venezuela, and a PhD in Chemistry (Heterogeneous Catalysis) from the University Complutense of Madrid, Spain. She joined Johnson Matthey in 2012, working in a European Union-funded project (CAtalytic membrane REactors based on New mAterials for C1–C4 valorisation (CARENA)) about catalyst development for membrane reactors. Currently she is working as a Core Scientist in the New Applications group.

William McDonnell is a Research Scientist in New Applications at the Johnson Matthey Technology Centre, Sonning Common. He worked on the project CARENA.

Andrew W. J. Smith is a Senior Principal Scientist in the Gas Phase Catalysis Group at the Johnson Matthey Technology Centre. He is a synthetic inorganic chemist with experience of materials and catalyst preparation. He is interested in developing new materials and their applications in heterogeneous catalysis.

http://dx.doi.org/10.1595/205651317X693606 *Johnson Matthey Technol. Rev.*, 2017, **61**, (1), 16–28

JOHNSON MATTHEY
TECHNOLOGY REVIEW

www.technology.matthey.com

Iridium Coating: Processes, Properties and Application. Part I

Processes for protection in high-temperature environments against oxidation and corrosion

Wang-ping Wu*
School of Mechanical Engineering, Institute of Energy Chemical Equipment and Jiangsu Key Laboratory of Materials Surface Science and Technology, Changzhou University, Changzhou 213164, P.R. China

Zhao-feng Chen
International Laboratory for Insulation and Energy Efficiency materials, College of Material Science and Technology, Nanjing University of Aeronautics and Astronautics, Nanjing 210016, P.R. China

***Email:** wwp3.14@163.com

The successful use in rocket engines of iridium as a barrier coating is an important area of high-temperature application. The Ir coating must be continuous and dense in order to protect the underlying material from corrosion and oxidation. The microstructure and morphology of the coating can be effectively controlled by varying the deposition conditions. The microstructure has an important influence on the physical and mechanical properties of the coating. A number of deposition processes, which have different conditions and requirements, have been employed to produce Ir coatings on various substrate materials. Part I of this paper presents the introduction and reviews the different deposition processes, while Part II will deal with texture and structure evolution, mechanical properties, growth mechanisms and applications of Ir coatings. The mechanisms of micropore formation after high-temperature treatment will also be investigated in some detail.

1. Introduction

Platinum group metals (pgm) have attracted increasing attention due to their high melting points, excellent catalytic activity and superior resistance to corrosion (1). Both Pt and Ir can be used as protective coatings in extreme environments due to their high resistance to corrosion (2). Ir exhibits the highest resistance to corrosion in molten oxides among metals. Owing to its high cost, low catalytic activity above 800ºC and low hardness, the use of pure Pt in high temperature applications is limited. Small amounts of Ir and ruthenium are commonly added to Pt to obtain a harder and stronger alloy that retains the advantages of pure Pt. Due to the high cost of the bulk metals, Pt and Ir are often replaced with thin metal layers deposited onto cheaper supports. Depositions of noble metal thin films are of particular interest because of their unique physical and chemical properties. Ir is a promising candidate for a wide range of applications due to its

high melting point, low oxygen permeability, high chemical stability and superior oxidation resistance.

1.1 Properties and Behaviour of Iridium

Ir is the sole metal that can be used as a container material at ≥1800ºC, although its resistance to oxidation in oxygen environments is poor at these temperatures. Therefore, Ir crucibles are only exploited in inert environments (3, 4). Meanwhile, an Ir film can act as an effective barrier to carbon diffusion (5–7). Carbon contamination of Ir is undesirable as it makes it practically undeformable due to brittle intercrystalline fracture (8). The deformation behaviour of Ir is sensitive to oxygen at elevated temperatures, however Ir is the only metal to have superior high-temperature mechanical properties including creep properties in an inert environment (9, 10). Ir displays poor workability even at elevated temperatures and this substantially limits its industrial applications.

Ir has a face-centred cubic (fcc) structure and behaves like a fcc metal under high temperatures in comparison with such refractory body-centred cubic (bcc) metals as tungsten, niobium and tantalum (11). Bulk Ir shows a ductile-to-brittle transition and exhibits cleavage fracture under tensile conditions (5, 12, 13), although the type of cleavage depends on the impurity content. Carbon- and oxygen-free metal always shows transgranular cleavage despite considerable plasticity, while contaminated Ir is undeformable and its fracture mode is intergranular cleavage or brittle intercrystalline fracture (14). Monocrystalline Ir exhibits high plasticity, but cleaves under tension at room temperature, while polycrystalline Ir displays brittle fracture over a wide range of temperatures (15–21). The brittle nature of Ir remains a puzzle. Some physical properties and their general agreement with empirical cleavage criteria permit a qualitative indication that brittle fracture is an intrinsic property of fcc Ir. These physical properties are elastic moduli, which are unique for a fcc metal (22). Their formal substitution into empirical cleavage criteria including the Rice-Thomson (R-T) criterion leads to the conclusion that Ir is an intrinsically brittle fcc metal despite its high plasticity (23). However, no detailed mechanism has been proposed.

The plasticity of carbon- and oxygen-contaminated polycrystalline Ir is close to zero and does not depend on grain size. The brittle intergranular fracture encountered in polycrystalline Ir was believed to be caused by impurities (16–30). However, Panfilov (20), and Hecker, Rohr and Stein (31) suggest that it is intrinsic to high purity Ir. Lynch (32) discussed possible reasons for the anomalous cleavage fracture in fcc Ir and suggested that cleavage occurs by an alternate-slip or nanovoid coalescence process. The anomalous fracture behaviour is probably associated with unusual crack-tip surface structure and bonding characteristics rather than with some unusual bulk property. The occurrence of brittle fracture in Ir is thought to be related to the energetics of the dislocation core, in particular the extremely high unstable stacking energy (33–35). Cawkwell *et al.* (36) studied the origin of brittle cleavage in Ir by atomistic simulation using a quantum mechanically derived bond order potential and suggested two core structures for the screw dislocation, a glissile planar core and a metastable non-planar core. Transformation between the two core structures was athermal and led to exceptionally high rates of cross slip during plastic deformation. Associated with this athermal cross slip was an exponential increase in the dislocation density and strong work hardening from which brittle cleavage was a natural consequence. A polycrystalline Ir coating prepared by double glow plasma (DGP) fails predominantly by grain boundary brittle fracture at room temperature. This intergranular fracture in polycrystalline Ir coating may arise from low cohesive strength of the grain boundaries (12). Doping with thorium, cerium and W increases the ductility of Ir and its alloys and suppresses grain boundary fracture, which can be used in some high-temperature structural applications (37–42).

According to the empirical rule for a metal, $T_{re} = ½\ T_{mel}$ (where T_{re} is the recrystallisation temperature and T_{mel} is the melting point), T_{re} for Ir should be about 1200ºC. 950ºC is the lowest temperature for recrystallisation reported from experiments with highly pure polycrystalline Ir (43). At low temperatures in air, Ir oxide (IrO_2) film is formed, but at temperatures above 1100ºC, the Ir oxides decompose and the surface remains bare (44). Volatile IrO_3 is formed at 1100ºC. The oxidation rate of Ir at 1800ºC in still air at one standard atmospheric pressure is ~1 μm h^{-1}; when the temperature is increased to 2200ºC the oxidation rate is increased ten times (45). The reactions of Ir with oxygen are thought to proceed as in Equations (i) to (vi) (6, 46, 47):

$$Ir\ (s) + O_2\ (g) \rightarrow IrO_2\ (s) \quad (i)$$

$$4Ir\ (s) + 3O_2\ (g) \rightarrow 2Ir_2O_3\ (s) \quad (ii)$$

$$2IrO_2\ (s) + O_2\ (g) \rightarrow 2IrO_3\ (g) \quad (iii)$$

$$2Ir\ (s) + 3O_2\ (g) \rightarrow 2IrO_3\ (g) \quad (iv)$$

$$2Ir_2O_3\ (s) \rightarrow Ir\ (s) + 3IrO_2\ (s) \quad (v)$$

$$IrO_2\ (s) \rightarrow Ir\ (s) + O_2\ (g) \quad (vi)$$

$$Ir\ (s) \rightarrow Ir\ (g) \quad (vii)$$

Table I summarises the properties of Ir.

1.2 Applications of Iridium Coatings

The pgms are potential diffusion barriers. Pt, Ru, Ir, rhodium, osmium and rhenium have been investigated as potential diffusion barriers for carbon (55). Despite the disparity in solubility, there is significant evidence that carbon diffuses rapidly in Pt precluding its application as a discrete diffusion barrier. Re does not form carbides and has low carbon solubility. Rh and Ru display slightly lower carbon solubility, with Ir having the lowest carbon solubility. Os can perform as an environmental barrier similarly to Re and Ir. Pt, Ir and Os have served as oxidation resistant surface coatings, which can be applied as interdiffusion barriers for coatings and composites in high-temperature material systems.

Owing to its unique physical and chemical properties, Ir has been evaluated for applications in a wide range of fields, including as a barrier layer on structural carbon materials (56, 57), Ir crucibles (58), Re-Ir rocket thrusters (59), heavy metal ion sensors (60), precision glass moulding components (61, 62), patterned thin film microelectrodes (63), spark plug electrodes (64), microelectronics (65) and optical industries (66, 67). Some other applications include as a barrier material in microelectronic devices, protective coatings for some electrode materials and moulds (62), as well as the removal of carbon monoxide contaminants from hydrogen in automotive pollution control (68). Ir and its alloys can be used as anti-stick coatings for glass moulding processes (62, 69–73). An amorphous alloy of Re-Ir-Nb prepared by a sputtering method has been used as a release film for a moulding die (74). Epitaxially grown Ir films on α-alumina were successfully utilised as intermediate electrodes for epitaxial growth of aluminium nitride (AlN) films for electronic device applications (75). Ir coatings have been used as electrical contacts in oxide high-temperature superconductors and as anti-corrosive coatings for anodes in the electrolysis of seawater (76, 77).

Due to its high catalytic activity, Ir is also used as a component of binary and ternary alloy anodes for the direct oxidation of methanol, ammonia and acetic acid synthesis. Furthermore, Ir can be used in rocket combustion chambers, fuel containers for nuclear power in space, radiation sources for medical treatment and engine ignition devices. One of its more exotic uses

Table I Properties of Iridium

Property	Value	Ref.
Melting point	2447ºC	(5)
Oxygen permeability	$<10^{-14}$ g cm^{-1}s^{-1} (2200ºC)	(48)
Oxidation rate[a]	~1 μm h^{-1} (1800ºC)	(45)
	~10 μm h^{-1} (2200ºC)	(45)
Density	22.562 kg m^{-3}	(49)
Vickers hardness	3.2 GPa	(50)
Thermal expansion coefficient	~6.2 × 10^{-6} ºC^{-1}	(51)
Thermal conductivity (0–100ºC)	1.48 J cm^{-1} s^{-1} ºC^{-1}	(52)
Specific heat (0–100ºC)	0.134 J g^{-1} ºC^{-1}	(52)
Electrical resistivity	5.1 μΩ cm	(53)
Young's modulus	520 GPa	(54)
Tensile strength (annealed), 20ºC	490–740 MPa	(52)
Poisson ratio	0.26	(52)

[a]Coating, in still air at 1 atm

is as a container for the plutonium oxide fuel cladding material in radioisotope thermoelectric generators – the major source of onboard electric power in spacecraft sent to explore the outer planets (21). The Ir-Re rocket chamber is also a successful application, allowing an increase in satellite life from 12 to 15 years and gaining US$30–60 million in added revenue per satellite (78).

1.3 Failure Modes and Protection of Iridium Coatings

Ir coatings tend to fail at high temperatures through an oxide sublimation mechanism. Above 1100ºC, formation of gaseous IrO_3 results in active surface oxidation in air. **Figure 1** shows the oxidation behaviour of a DGP Ir coating debonded from a graphite substrate heated in air. An endothermic reaction was observed at 1074ºC as shown in **Figure 1(a)**, consistent with the formation of IrO_3 at 1100ºC. The weight changes are shown in the thermogravimetry (TG) curve (**Figure 1(b)**). A mass gain was observed above 800ºC followed by a significant mass loss above 1227ºC. The mass gain and loss were due to the formation of solid IrO_2 and gaseous IrO_3, respectively. The mass changes corresponded to Ir oxides formation.

Typically, alloying additions (73, 79) or oxide overcoats (80, 81) are used to mitigate sublimation losses. Sublimation losses may not be a real concern in the inert gas coolant chosen for a space reactor. Composite coatings may however endure higher service temperature and could ensure longer service life for the Ir coating, providing better protection for the substrate from oxidation at high temperature. Refractory oxide coatings such as zirconium dioxide (ZrO_2), hafnium(IV) oxide (HfO_2) and Al_2O_3 have been produced on an Ir coating surface to inhibit the evaporation and oxidation of Ir and seal the micropores in the coating (78, 82). An Al_2O_3 layer was formed on the surface of a magnetron sputtered Ir-Al composite coating after oxidation, which could improve the oxidation resistance of the coating (83). Ir-Al forms an Al_2O_3 layer, effectively suppressing excessive surface oxidation. An Ir aluminide alloy or Ir with a surface aluminide seems favourable as an oxidation and diffusion resistant coating. At present, Ir-based alloys, Ir-M (M = Ti, Nb, Hf, Zr, Ta and V), have gained attention as new high-temperature materials due to their high melting points and superior oxidation resistances (84). Ir-based alloy coatings such as Ir-Al (82), Ir-Ta (85), Ir-Pt (86), Ir-Ni (87) and Re-Ir-based alloy coatings (74) have also been investigated as high-temperature oxidation coatings. There is much interest in Ir as a barrier coating in advanced materials for high technology applications.

2. Processes of Iridium Coating

For the coating to adhere well to the substrate, the coating should have a similar coefficient of thermal expansion to that of the substrate, or form a strong chemical or metallurgical bond with the substrate at the interface (88). A dense layer is required for

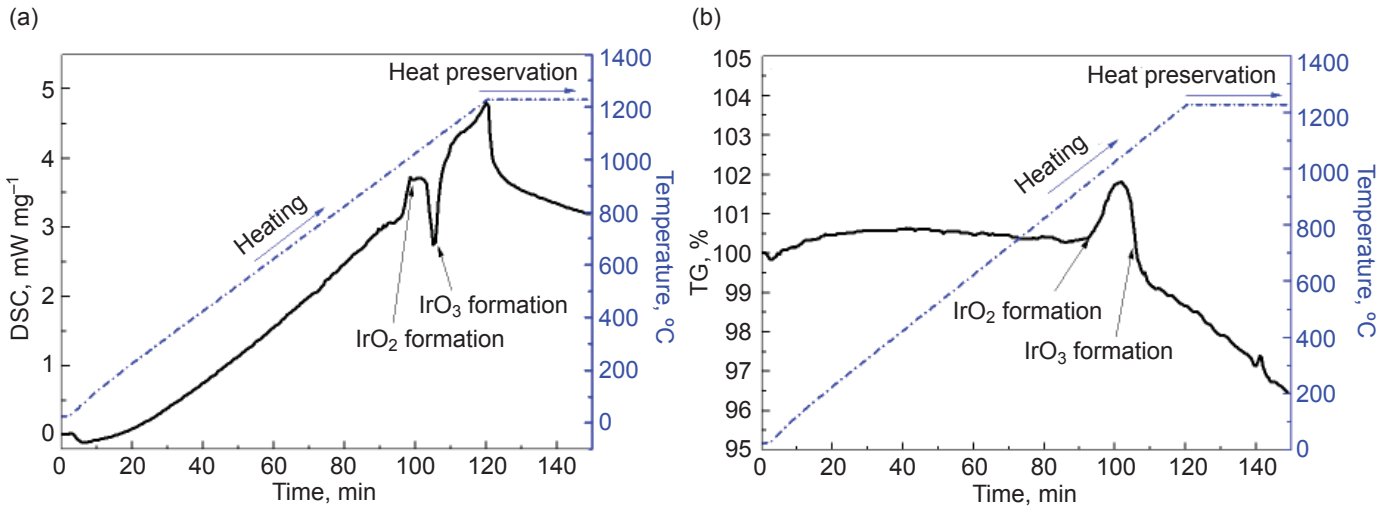

Fig. 1. (a) Differential scanning calorimetry (DSC); (b) TG lines of Ir coating (Reproduced with permission of Elsevier (6))

high-temperature environments, while a nanoporous Ir film can be used in catalytic applications due to its high specific surface area. The structure of an Ir coating is determined by the deposition processes. These include magnetron sputtering (both direct current magnetron sputtering (DCMS) and radio frequency magnetron sputtering (RFMS)) (89–91), chemical vapour deposition (CVD) (92), metal-organic CVD (MOCVD) (93, 94), atomic layer deposition (ALD) (95), physical vapour deposition (PVD), laser-induced chemical vapour deposition (LCVD) (7), electrodeposition (96–99), pulsed laser deposition (PLD) (100) and DGP (51, 101). Many processes can produce Ir coatings on various substrates, and the quality of the as-deposited coating varies. **Table II** shows the quality of Ir coatings produced by different deposition processes.

2.1 Slurry Dip

Slurry dip is a conventional process to prepare coatings. A single dipping operation produces a coating and the coated specimens are heated in an argon atmosphere. The upper temperature is limited by the melting point of the coating material and this is also the limit for high-temperature applications. A strongly adherent Ir coating on graphite was obtained by fused Ir powder (111). After oxidation at 2050ºC, some pores were present on the coating surface. A combination of slurry dipping and sintering, vapour-plating and electrodeposition processes could produce a dense Ir coating which could protect graphite from oxidation at 2100ºC (111, 112). The slurry was made from xylene and milled Ir powder. After heat treatment, the film of Ir powder was adherent to the substrate. The adherence of the sintered Ir coating depends critically on the formation of a eutectic melt at the interface between Ir and carbon.

2.2 Metal-Organic Chemical Vapour Deposition

MOCVD is an advanced method of coating preparation which relies on chemical reactions of a vapour at a

Table II Quality of Iridium Coating by Different Deposition Processes

Method	Coating thickness, μm	Deposition rate, μm s^{-1}	Deposition temperature, ºC	Coating quality	Ref.
LCVD	100	–	300~400	Microcracks and non-uniform thickness	(7)
DCMS	4	0.02×10^{-3}	25	Pores and rough surface	(55)
RFMS	4.5	1×10^{-3}	25~800	Fine, dense, uniform and thorough coverage	(55)
Electrodeposition	50~100	$2.8–5.6 \times 10^{-3}$	~570	Large inner stress, pores and high deposition rate	(98, 102)
CVD	10	$0.28~0.56 \times 10^{-3}$	700~800	Dense and low deposition rate	(103–106)
MOCVD	5~50	$0.05~6.94 \times 10^{-3}$	500~600	Small grains and some pinholes	(13, 92, 107, 108)
PLD	~0.1	–	25~400	Well crystallised, smooth surface and low deposition rate	(100, 109)
DGP	5~50	$0.56~5.6 \times 10^{-3}$	800~1100	High deposition rate, strong bond and pinholes	(6, 12, 48, 51, 110)
ALD	0.009–0.175	0.02~0.06 nm per cycle	165~400	Low deposition rate, smooth surface, adhered well to the different substrate	(95)

surface to form solid deposits. Dense and adherent coatings depend on optimal deposition parameters and the choice of gaseous compound of the deposited material. The deposition parameters include temperature, gas concentration, carrier and co-reagent gas flow rate, precursor flow rate and gas pressure. Dense Ir coatings are essential to offer effective corrosion or oxidation protection. For generalised perturbation method (GPM) coatings by MOCVD, most of the precursors are metal organic complexes. Garcia and Goto (103) reviewed MOCVD operating conditions for Ir with different precursors such as metal β-diketonates, carbonyl complexes and allyl complexes. Ir coatings obtained by this route may contain carbon impurities from the thermal decomposition of organic precursors. It is very important to eliminate these carbon impurities for high-temperature applications. However, carbon can prevent the grain growth of noble metals, which leads to the formation of nanoparticles that may be highly catalytic and reversible as electrodes for solid electrolytes (113).

Some researchers (114, 115) carried out doping with precursor in the presence of oxygen to obtain pure Ir coatings by MOCVD. For the CVD process, halides of Ir as the precursors have poor volatility, the deposition temperatures are high and the reaction products will corrode the equipment (116). At present, Ir coatings made by MOCVD are successfully used in liquid rocket motors operated at ~2200ºC (45). Compared with other processes, Reed, Biaglow and Schneider (117) claimed that MOCVD is the only established process for the fabrication of Ir-coated Re combustion chambers. However, major concerns of this process are high cost, low deposition rate and impurities in the coating.

2.3 Atomic Layer Deposition

ALD is a superior method for thin film deposition which is used for fabrication of highly uniform and conformal Ir films over large and complex substrate areas. ALD is considered to be a special modification of CVD in which the substrate is exposed to one precursor at a time, the precursor pulses being separated by inert gas purging (95). In ALD processing, two or more precursors alternately react with the surface and saturate it with chemisorbed species. This self-limiting mechanism can lead to successful deposition of uniform and conformal films with the desired composition and thickness, as long as appropriate precursors are chosen, suitable reaction temperatures applied and the correct number of deposition cycles performed. For the deposition of Ir, oxygen may be applied as the other precursor together with the metal complex. Molecular oxygen is activated through its dissociative chemisorption producing reactive atomic oxygen on the metal surface. The Ir complex-oxygen ALD process gives the metal only above a certain threshold temperature, which is governed most likely by the dissociative chemisorption of oxygen on the metal surface. When the deposition temperature is below this threshold, no reaction occurs and nothing is deposited (118, 119).

Hämäläinen *et al.* (120–122) reported that Ir films could be obtained using molecular hydrogen as a reducing agent in each ALD cycle after the ozone pulse at low deposition temperatures. Aaltonen *et al.* (95) observed that an Ir film with a preferred **(111)** orientation was grown by ALD in a wide temperature range of 225–375ºC from tris(2,4-pentanedionato)iridium [$Ir(acac)_3$] and oxygen. Christensen and Elam (123) synthesised Ir-Pt films using Ir(III)acetylacetonate-O_2 cycles for Ir ALD and $MeCpPtMe_3$–O_2 cycles for Pt ALD at 300ºC, and found that the growth rates of Pt and Ir remained constant regardless of the dosing ratio, indicating that both Ir and Pt ALD proceeded equally well on either metal surface.

2.4 Physical Vapour Deposition

PVD is a versatile technique and is the most widely used sputtering method. The sputtering process involves the bombardment of a solid target of the material to be coated with ions extracted from a concentrated plasma cloud positioned very close to the surface of the target (89, 124, 125). High energy atoms are dislodged from the target and directed toward the substrate. The advantages of PVD include a high sputtering rate at the target, high deposition rate and superior adhesion of the sputtered coating. Mumtaz *et al.* (90, 91) found that RFMS could obtain a uniform and thorough coverage of Ir with columnar grains. However, a DCMS Ir coating had a porous columnar structure and a rough surface due to the effect of shadowing. The effects of deposition parameters on the structure and properties of the Ir coating have been studied (126).

The PVD process includes electron beam PVD and plasma based ion implantation. Murakami's research group (127–129) investigated Ir-based bond coatings such as Ir-Hf and Ir-Ta prepared by electron beam PVD. An Ir-Re alloy coating created using a plasma based ion implantation process could protect engineering tools from oxidation at high temperatures (130). Lee *et al.* (131) studied Ir film deposition by electron evaporation

with simultaneous bombardment by an argon ion beam and found that the charge injection capability of the Ir film was identical to bulk Ir.

2.5 Electrodeposition

Electrodeposition is promising as a low cost, reliable coating process. The plating of Ir from aqueous solutions has been reviewed by Jones (132). Plating of Ir from Ir chloride solutions with sulfamic acid produces deposits up to 25 μm thick, although the deposits exhibit cracks. Plating of Ir from solution in hydrobromic acid produces crack-free deposits up to 1 μm thick using a deposition rate of ~1 μm h^{-1}. Improved deposition efficiencies and decreased cracking size of the coating were reported for sodium hexabromoiridate(III) baths with additions of oxalic acid. While typical thicknesses of Ir plating of ≤1 μm could minimise corrosion and serve for many electronic applications, thick Ir coatings are necessary for use at elevated temperature. Cohen Sagiv, Eliaz and Gileadi (133) developed suitable plating baths for electroplating of Re-Ir-Ni alloy coating and suggested a mechanism for the electrodeposition process. Wu *et al.* (134) further studied the effects of pH and deposition temperature on the chemical composition, deposition efficiencies and microstructure of Re-Ir-Ni coatings. Qian *et al.* (135–137) reported that an Ir coating could be electrodeposited from aqueous solution, composite ionic liquid and sodium chloride-potassium chloride molten salt systems. However, the quality of the Ir coating was relatively poor.

Dense and ductile Ir coatings were electrodeposited from a molten ternary eutectic of alkali metal chlorides under an argon atmosphere as an alternative to the more generally used molten cyanide, which is toxic and unstable (98). The best electrolyte for Ir coating was a non-toxic ternary eutectic molten salt of sodium chloride-potassium chloride-caesium chloride (138). However, the electrodeposition process was performed either in inert atmosphere or in chlorine, which increased the complexity of the facility. Timofeev, Baraboshkin and Saltykova (139) carried out the electrodeposition of Ir on graphite crucibles from a fused chloride electrolyte. Saltykova (140, 141) studied the effects of electrolysis conditions on the structure of Ir deposits on graphite from a ternary eutectic molten salt using both constant and reverse current. Bai's research group (142) adopted the molten electrodeposition method to obtain a laminar Ir coating and suggested that the Ir-Re coated graphite was oxidised at elevated temperatures from 1600ºC to ~1900ºC in stagnated air for 1 h. Reed and Dickerson (143) found that an electrodeposited Ir coating presented pores and poor adherence, and suggested that the integrity of the coating could be improved by densification of the Ir layer through a post-deposition treatment.

2.6 Double Glow Plasma

The DGP process can be looked on as a new kind of PVD technique, which could be applied to almost all solid metallic elements to realise surface alloying of the metallic substrates (144, 145). A surface alloying experiment was performed in a DGP surface alloying device in which a glow discharge process in a vacuum sputtering chamber produced low-temperature plasma. The general advantages of this process include low operating cost, low pollution, safety, improved stability, high deposition rate, good coating uniformity, controllability of the coating thickness and strong adhesion to complex shaped substrates (146). This process can produce co-deposited coatings with different composition ratios in a controlled manner with simple operating procedures (147–149). The main characteristics of a DGP process are high deposition temperature of 800–1200ºC and resputtering during the deposition process. Chen's research group (150–155) investigated the microstructure, texture evolution, growth mechanism, mechanical properties and ablation resistance of Ir coatings produced by a DGP process on refractory materials and found that the Ir has excellent adhesion, exhibits a <110> texture and presents some micropores or pinholes in the coating after high-temperature treatment. Wu *et al.* (101) studied the effects of bias voltage and gas pressure on the orientation and microstructure of Ir coatings formed by DGP and found that Ir coatings on Ti, Nb and molybdenum substrates all exhibited the preferred **(220)** orientation under the same deposition conditions. The microstructure of the Ir coating was affected by bias voltage, gas pressure and substrate effects. The bias voltages had a significant impact on the crystal orientation of the coating. The increase of bias voltage resulted in a high substrate temperature and high deposition rate. An increase in the coating thickness can affect the microstructure and orientation of the coating.

2.7 Pulsed Laser Deposition

The PLD process can produce high quality films with high purity and good adherence. PLD consists of a target and a substrate in a vacuum chamber. A high

power laser is used as an external energy source to vaporise the target and to deposit a thin film on the substrate. The advantages of PLD are flexibility, fast response, energetic evaporants and congruent evaporation (156). The deposition parameters include the laser characteristics, substrate temperature, degree of vacuum and the distance between target and substrate. PLD Ir films had a polycrystalline structure with average grain size in nano-scale and the PLD process led to higher purity films than RFMS (157). The crystal orientation and surface morphology were investigated by Gong *et al.* (100, 109), and the resistivities of PLD Ir films were determined as a function of substrate temperature. Well-crystallised and single-phase Ir layers with <111> preferred orientation were obtained at low substrate temperatures of 200–300ºC. Chen (158) investigated high purity Ir films deposited on Si **(100)** *via* PLD. A high Ir deposition rate was obtained with pulsed laser power higher than 4.2×10^9 W cm^{-2}. The PLD Ir films exhibited a **(110)** preferentially orientated polycrystalline structure. Their average grain size increased from 30 nm to 110 nm as the deposition temperature was raised from 100ºC to 600ºC. With a substrate temperature of 700ºC, the grain size changed to 500 nm. Ir silicide was found in the film deposited at a substrate temperature of 700ºC.

2.8 Other Processes

The PVD method for Ir coating includes both thermal evaporation and sputtering (5, 159). Bauer *et al.* (160) reported that large area, single-crystalline Ir films on Al_2O_3, strontium titanate ($SrTiO_3$) and magnesium oxide (MgO) substrates are desired for the heteroepitaxial deposition of diamond. These were obtained by e-beam evaporation. Many deposition processes have been investigated for Ir coating of components. A compact Ir coating was deposited on Re by arc ion plating (AIP) (161). The isothermal oxidation resistance of the Ir coating was retained for up to 4 h at 1800ºC and up to 2 h at 2000ºC, respectively. After 120 oxidation test cycles at 1950ºC, the surface and cross-section of the Re-Ir remained compact and no peeling was detected.

Snell *et al.* (7) reported a novel LCVD process to produce an Ir coating, the principle of which is to use a high energy laser beam to dissociate a precursor solid or liquid on the Ir slurry layer. The production of near-net-shape parts with Ir by directed light fabrication has shown some promise (162). In this method, metal powder is transported in a stream of inert gas and fused to a surface in the focus of a high power laser beam, to form fully fused near-net-shape components. Initial work on this process indicates that porosity originating from gases during melting and solidification is an issue. Plasma spray, vacuum plasma spray or low pressure plasma spray of Ir have been proposed as alternative methods for achieving high density coatings. While there is little published literature available on plasma spraying of Ir, it is expected to perform similarly to that of a number of refractory metals.

3. Conclusion

Ir is of great interest to the scientific and technical communities and could be used in several applications. There are a number of processes available to produce thin or thick Ir coatings on various substrates and the quality of the as-deposited Ir coatings vary. Each process has its unique advantages resulting in different coating textures and structures. The effects on texture and structure will be explored in Part II, along with mechanical properties, growth mechanisms and an outlook for applications of Ir coatings.

Acknowledgements

This work has been supported by the National Natural Science Foundation of China (Grant Number: 50872055/E020703) and the Natural Science Foundation of Jiangsu Province (Grant Number: BK20150260). The authors wish to thank the referees for their helpful suggestions, and Editors Ms Sara Coles and Ming Chung for the editing.

References

1 C. Couderc, *Platinum Metals Rev.*, 2010, **54**, (3), 186

2 J. Goswami, C.-G. Wang, P. Majhi, Y.-W. Shin and S. K. Dey, *J. Mater. Res.*, 2001, **16**, (8), 2192

3 F. D. Richardson, *Platinum Metals Rev.*, 1958, **2**, (3), 83

4 J. R. Handley, *Platinum Metals Rev.*, 1986, **30**, (1), 12

5 E. K. Ohriner, *Platinum Metals Rev.*, 2008, **52**, (3), 186

6 Z. F. Chen, W. P. Wu and X. N. Cong, *J. Mater. Sci. Technol.*, 2014, **30**, (3), 268

7 L. Snell, A. Nelson and P. Molian, *Carbon*, 2001, **39**, (7), 991

8 C. A. Brookes, J. H. Greenwood and J. L. Routbort, *J. Appl. Phys*., 1968, **39**, (5), 2391

9 R. Weiland, D. F. Lupton, B. Fischer, J. Merker, C. Scheckenbach and J. Witte, *Platinum Metals Rev.*,

2006, **50**, (4), 158

10 R. W. Douglass and R. I. Jaffee, *Proc. ASTM.*, 1962, **62**, 627

11 B. L. Mordike and C. A. Brookes, *Platinum Metals Rev.*, 1960, **4**, (3), 94

12 Z. F. Chen, W. P. Wu, L. B. Wang and Y. Zhang, *Int. J. Fract.*, 2008, **153**, (2), 185

13 Y. F. Hua, L. T. Zhang, L. F. Cheng and W. B. Yang, *Mater. Sci. Eng. B*, 2005, **121**, (1–2), 156

14 C. Gandhi and M. F. Ashby, *Scripta Metall.*, 1979, **13**, (5), 371

15 P. Panfilov, *J. Mater. Sci.*, 2007, **42**, (19), 8230

16 P. Panfilov and A. Yermakov, *Platinum Metals Rev.*, 2001, **45**, (4), 176

17 P. Panfilov, A. Yermakov, V. Dmitriev and N. Timofeev, *Platinum Metals Rev.*, 1991, **35**, (4), 196

18 P. Panfilov and A. Yermakov, *Int. J. Fract.*, 2004, **128**, (1), 147

19 P. Panfilov and A. Yermakov, *J. Mater. Sci.*, 2004, **39**, (14), 4543

20 P. Panfilov, *J. Mater. Sci.*, 2005, **40**, (22), 5983

21 E. P. George, C. G. McKamey, E. K. Ohriner and E. H. Lee, *Mater. Sci. Eng. A*, 2001, **319–321**, 466

22 R. E. MacFarlane, J. A. Rayne and C. K. Jones, *Phys. Lett.*, 1966, **20**, (3), 234

23 C. N. Reid and J. L. Routbort, *Metall. Trans.*, 1972, **3**, (8), 2257

24 L. Heatherly and E. P. George, *Acta Mater.*, 2001, **49**, (2), 289

25 C. L. White and C. T. Liu, *Scripta Metall.*, 1978, **12**, (8), 727

26 C. L. White, R. E. Clausing and L. Heatherly, *Metall. Trans. A*, 1979, **10**, (6), 683

27 L. Heatherly and E. P. George, *Acta Mater.*, 2001, **49**, (2), 289

28 A. V. Yermakov, V. M. Koltygin and E. V. Fatyushina, *Platinum Metals Rev.*, 1992, **36**, (3), 146

29 A. Yermakov, P. Panfilov and R. Adamesku, *J. Mater. Sci. Lett.*, 1990, **9**, (6), 696

30 A. V. Ermakov, S. M. Klotsman, V. G. Pushin, A. N. Timofeev, V. N. Kaigorodov, P. Ye. Panfilov and L. I. Yurchenko, *Scripta Mater.*, 1999, **42**, (2), 209

31 S. S. Hecker, D. L. Rohr and D. F. Stein, *Metall. Trans. A*, 1978, **9**, (4), 481

32 S. P. Lynch, *Scripta Mater.*, 2007, **57**, (2), 85

33 T. J. Balk and K. J. Hemker, *Phil. Mag. A*, 2001, **81**, (6), 1507

34 J. M. MacLaren, S. Crampin, D. D. Vvedensky and M. E. Eberhart, *Phys. Rev. Lett.*, 1989, **63**, (23), 2586

35 S. Crampin, K. Hampel, D. D. Vvedensky and J. M. MacLaren, *J. Mater. Res.*, 1990, **5**, (10), 2107

36 M. J. Cawkwell, D. Nguyen-Manh, C. Woodward, D. G. Pettifor and V. Vitek, *Science*, 2005, **309**, (5737), 1059

37 C. T. Liu and H. Inouye, "Development and Characterization of an Improved Ir–0.3% W Alloy for Space Radioisotopic Heat Sources", ORNL-5290, Oak Ridge National Laboratory, Tennessee, USA, 1977

38 E. A. Franco-Ferreira, G. M. Goodwin, T. G. George and G. H. Rinehart, *Platinum Metals Rev.*, 1997, **41**, (4), 154

39 C. L. White and C. T. Liu, *Acta Metall.*, 1981, **29**, (2), 301

40 C. T. Liu, H. Inouye and A. C. Schaffhauser, *Metall. Trans. A*, 1981, **12**, (6), 993

41 C. L. White, L. Heatherly and R. A. Padgett. *Acta Metall.*, 1983, **31**, (1), 111

42 E. P. George, C. G. McKamey, E. K. Ohriner and E. H. Lee, *Mater. Sci. Eng.: A*, 2001, **319–321**, 466

43 C. T. Liu and H. Inouye, "Study of Iridium and Iridium-tungsten Alloys for Space Radioisotopic Heat Sources', ORNL-5240, Oak Ridge National Laboratory, Tennessee, USA, 1976

44 H. Jehn, R. Völker and M. I. Ismail, *Platinum Metals Rev.*, 1978, **22**, (3), 92

45 Ultramet Advanced Materials Solutions, Propulsion System Components, liquid rocket engines: http://www.ultramet.com/propulsionsystem_components_liquid_rocket.html (Accessed on 17th October 2016)

46 Z. B. Bao, H. Murakami and Y. Yamabe-Mitarai, *Appl. Surf. Sci.*, 2011, **258**, (4), 1514

47 R. T. Wimber and H. G. Kraus, *Metall. Trans.*, 1974, **5**, (7), 1565

48 Z. F. Chen, W. P. Wu, L. B. Wang and Y. Zhang, *Surf. Eng.*, 2011, **27**, (4), 242

49 J. W. Arblaster, *Platinum Metals Rev.*, 2010, **54**, (2), 93

50 M. B. Weinberger, J. B. Levine, H.-Y. Chung, R. W. Cumberland, H. I. Rasool, J.-M. Yang, R. B. Kaner and S. H. Tolbert, *Chem. Mater.*, 2009, **21**, (9), 1915

51 W. P. Wu, X. Lin, Z. F. Chen, Z. F. Chen, X. N. Cong, T. Z. Xu and J. L. Qiu, *Plasma Chem. Plasma Proc.*, 2011, **31**, (3), 465

52 L. B. Hunt, *Platinum Metals Rev.*, 1987, **31**, (1), 32

53 Y. Ritterhaus, T. Hur'yeva, M. Lisker and E. P. Burte, *Chem. Vap. Deposition*, 2007, **13**, (12), 698

54 S. S. Hecker, D. L. Rohr and D. F. Stein, *Metall. Trans.*

A, 1978, **9**, (4), 481

55 S. M. Sabol, B. T. Randall, J. D. Edington, C. J. Larkin and B. J. Close, "Barrier Coatings for Refractory Metals and Superalloys", B-MT-(SPME)-35, TRN: US0603658, Bettis Atomic Power Laboratory (BAPL), Pennsylvania, USA, 2006, pp. 1–28

56 K. Mumtaz, J. Echigoya, T. Hirai and Y. Shindo, *J. Mater. Sci. Lett.*, 1993, **12**, (18), 1411

57 N. I. Baklanova, N. B. Morozova, V. V. Kriventsov and A. T. Titov, *Carbon*, 2013, **56**, 243

58 J. Merker, B. Fischer, D. F. Lupton and J. Witte, *Mater. Sci. Forum*, 2007, **539–543**, 2216

59 R. H. Tuffias, *Mater. Manuf. Process.*, 1998, **13**, (5), 773

60 G. T. A. Kovacs, C. W. Storment and S. P. Kounaves, *Sens. Actuators B*, 1995, **23**, (1), 41

61 H.-U. Kim, D.-H. Cha, H.-J. Kim and J.-H. Kim, *Int. J. Prec. Eng. Manuf.*, 2009, **10**, (3), 19

62 J. Hagen, F. Burmeister, A. Fromm, P. Manns and G. Kleer, *Plasma Process. Polym.*, 2009, **6**, (S1), 678

63 S. Kohli, D. Niles, C. D. Rithner and P. K. Dorhout, *Adv. X-ray Anal.*, 2002, **45**, 352

64 H. Osamura, 'Development of Long Life and High Ignitability Iridium Spark Plug', F2000A144, Seoul 2000 FISITA World Automotive Congress, Seoul, South Korea, 12th–15th June, 2000

65 S. Horita, S. Horii and S. Umemoto, *Jpn. J. Appl. Phys.*, 1998, **37**, (1), 5141

66 Y. Li and J. A. Woollam, *J. Vac. Sci. Technol. A*, 2004, **22**, (5), 2177

67 Y. Li and J. A. Woollam, *J. Appl. Phys.*, 2002, **92**, (8), 4386

68 E. N. El Sawy and V. I. Birss, *J. Mater. Chem.*, 2009, **19**, (43), 8244

69 X.-Y. Zhu, J.-J. Wei, L.-X. Chen, J.-L. Liu, L.-F. Hei, C.-M. Li and Y. Zhang, *Thin Solid Films*, 2015, **584**, 305

70 S.-C. Liu, Y.-I. Chen, J.-J. Shyu, H.-Y. Tsai, K.-Y. Lin, Y.-H. Chen and K.-C. Lin, *Surf. Coat. Technol.*, 2014, **259**, (B), 352

71 S.-C. Liu, Y.-I. Chen, H.-Y. Tsai, K.-C. Lin and Y.-H. Chen, *Surf. Coat. Technol.*, 2013, **237**, 105

72 M.-W. Cheon, T.-G. Kim and Y.-P. Park, *J. Ceramic Proc. Res.*, 2012, **13**, (2), S328

73 F.-B. Wu, W.-Y. Chen, J.-G. Duh, Y.-Y. Tsai and Y.-I. Chen, *Surf. Coat. Technol.*, 2003, **163–164**, 227

74 H. Fukushima and S. Midorikawa, Canon Kabushiki Kaisha, 'Amorphous Alloy, Molding Die, and Method for Producing Optical Element', *US Appl.* 2014/0,053,606

75 W. Zhang, R. Vargas, T. Goto, Y. Someno and T. Hirai, *Appl. Phys. Lett.*, 1994, **64**, (11), 1359

76 V. G. Bessergenev, N. V. Gelfond, I. K. Igumenov, S. Sh. Ilyasov, R. D. Kangiev, Yu. A. Kovalevskaya, V. S. Kravchenko, S. A. Slobodyan, V. I. Motorin and A. F. Shestak, *Supercond. Sci. Technol.*, 1991, **4**, (7), 273

77 I. K. Igumenov, N. V. Gelfond, P. S. Galkin, N. B. Morozova, N. E. Fedotova, G. I. Zharkova, V. I. Shipachev, E. F. Reznikova, A. D. Ryabtsev, N. P. Kotsupalo, V. I. Titarenko, Yu. P. Dikov, V. V. Distler and M. I. Buleev, *Desalination*, 2001, **136**, (1–3), 273

78 NASA Glenn Research Center at Lewis Field, 'Achieving the Extraordinary', NASA, 2006: http://www.nasa.gov/centers/glenn/pdf/168206main_CenterResume62011.pdf (Accessed on 24th November 2016)

79 C. T. Liu, E. P. George and E. E. Bloom, UT-Battelle, LLC, 'Ir-based Alloys for Ultra-high Temperature Applications', *US Patent* 6,982,122; 2006

80 R. H. Tuffias, J. Harding and R. Kaplan, Ultramet, 'High Temperature Corrosion Resistant Composite Structure', *US Patent* 4,917,968; 1990

81 H.-J. Li, H. Xue, Q.-G. Fu, Y.-L. Zhang, X.-H. Shi and K.-Z. Li, *J. Inorg. Mater.*, 2010, **25**, (4), 337

82 H. Hosoda, 'Smart Coatings – Multilayered and Multifunctional in-situ Ultrahigh-temperature Coatings', in "Nanomaterials: From Research to Applications", eds. H. Hosono, Y. Mishima, H. Takezoe and K. J. D. MacKenzie, Elsevier Ltd, Oxford, UK, 2006, pp. 419–445

83 W. M. Clift, K. F. McCarty and D. R. Boehme, *Surf. Coat. Technol.*, 1990, **42**, (1), 29

84 Y. Yamabe-Mitari, Y. Ro, T. Maruko and H. Harada, *Intermetallics*, 1999, **7**, (1), 49

85 P. Kuppusami, H. Murakami and T. Ohmura, *Surf. Eng.*, 2005, **21**, (1), 53

86 A. Suzuki, Y. Wu, A. Yamaguchi, H. Murakami and C. M. F. Rae, *Oxid. Met.*, 2007, **68**, (1), 53

87 S.-F. Tseng, W.-T. Hsiao, K.-C. Huang, M.-F. Chen, C.-T. Lee and C.-P. Chou, *Surf. Coat. Technol.*, 2010, **205**, (7), 1979

88 S. K. Dey, J. Goswami, C.-G. Wang and P. Majhi, *Jpn. J. Appl. Phys.*, 1999, **38**, (2), 1052

89 M. A. El Khakani, M. Chaker and B. Le Drogoff, *J. Vac. Sci. Technol. A*, 1998, **16**, (2), 885

90 K. Mumtaz, J. Echigoya, H. Enoki, T. Hirai and Y. Shindo, *J. Mater. Sci.*, 1995, **30**, (2), 465

91 K. Mumtaz, J. Echigoya, T. Hirai and Y. Shindo, *Mater. Sci. Eng.: A*, 1993, **167**, (1–2), 187

92 F. Maury and F. Senocq, *Surf. Coat. Technol.*, 2003, **163–164**, 208

93 X. Yan, Q. Zhang and X. Fan, *Mater. Lett.*, 2007, **61**, (1), 216

94 Y.-L. Chen, C.-C. Hsu, Y.-H. Song, Y. Chi, A. J. Carty, S.-M. Peng and G.-H. Lee, *Chem. Vap. Deposition*, 2006, **12**, (7), 442

95 T. Aaltonen, M. Ritala, V. Sammelselg and M. Leskelä, *J. Electrochem. Soc.*, 2004, **151**, (8), G489

96 Y.-N. Wu, A. Suzuki, H. Murakami and S. Kuroda, *Mater. Trans.*, 2005, **46**, (10), 2176

97 L.-A. Zhu, S.-X. Bai and H. Zhang, *Surf. Coat. Technol.*, 2011, **206**, (6), 1351

98 A. Etenko, T. McKechnie, A. Shchetkovskiy and A. Smirnov, *ECS Trans.*, 2007, **3**, (14), 151

99 J.-G. Qian and T. Zhao, *Trans. Nonferrous Met. Soc. China*, 2012, **22**, (11), 2855

100 Y.-S. Gong, C.-B. Wang, Q. Shen and L.-M. Zhang, *Appl. Surf. Sci.,* 2008, **254**, (13), 3921

101 W.-P. Wu, Z.-F. Chen, X. Lin, B.-B. Li and X.-N. Cong, *Vacuum*, 2011, **86**, (4), 429

102 D. A. Toenshoff, R. D. Lanam, J. Ragaini, A. Shchetkovskiy and A. Smirnov, 'Iridium Coated Rhenium Rocket Chambers Produced by Electroforming', 36th AIAA/ASME/SAE/ASEE Joint Propulsion Conference and Exhibit, Las Vegas, USA, 24th–28th July, 2000

103 J. R. V. Garcia and T. Goto, *Mater. Trans.*, 2003, **44**, (9), 1717

104 J. T. Harding, V. Fry, R. H. Tuffias and R. B. Kaplan, "Oxidation Resistance of CVD Coatings", AFRPL TR-86-099, Air Force Rocket Propulsion Laboratory (AFRPL), Edwards Air Force Base, California, USA, 1987, p. 29

105 J. T. Harding, R. H. Tuffias and R. B. Kaplan, "High Temperature Oxidation Resistant Coatings", AFRPL TR-84-036, Air Force Rocket Propulsion Laboratory (AFRPL), Edwards Air Force Base, California, USA, 1984

106 J. P. Endle, Y.-M. Sun, N. Nguyen, S. Madhukar, R. L. Hance, J. M. White and J. G. Ekerdt, *Thin Solid Films*, 2001, **388**, (1–2), 126

107 N. V. Gelfond, P. S. Galkin, I. K. Igumenov, N. B. Morozova, N. E. Fedotova, G. I. Zharkova and Yu. V. Shubin, *J. Phys. IV France*, 2001, **11**, (Pr3), 593

108 I. K. Igumenov, N. V. Gelfond, N. B. Morozova and H. Nizard, *Chem. Vapor Depos.*, 2007, **13**, (11), 633

109 Y.-S. Gong, C.-B. Wang, Q. Shen and L.-M. Zhang, *Vacuum*, 2008, **82**, (6), 594

110 W.-P. Wu, Z.-F. Chen, X.-N. Cong and L.-B. Wang, *Rare Metal Mater. Eng.*, 2013, **42**, (2), 435 (In Chinese)

111 J. M. Criscione, R. A. Mercuri, E. P. Schram, A. W. Smith and H. F. Volk, 'High Temperature Protective Coatings for Graphite', ML-TDR-64-173, Part I, Union Carbide Corporation, Parma, Ohio, USA, 1964

112 J. M. Criscione, R. A. Mercuri, E. P. Schram, A. W. Smith and H. F. Volk, 'High Temperature Protective Coatings for Graphite', ML-TDR-64-173, Part II, Union Carbide Corporation, Parma, Ohio, USA, 1964

113 T. Goto, T. Ono and T. Hirai, *Scripta Mater.*, 2001, **44**, (8–9), 1187

114 Y.-M. Sun, J. P. Endle, K. Smith, S. Whaley, R. Mahaffy, J. G. Ekerdt, J. M. White and R. L. Hance, *Thin Solid Films*, 1999, **346**, (1–2), 100

115 J. B. Hoke, E. W. Stern and H. H. Murray, *J. Mater. Chem.*, 1991, **1**, (4), 551

116 H.-Z. Cai, L. Chen, Y. Wei and C.-Y. Hu, *Rare Metal Mater. Eng.*, 2010, **39**, (2), 209

117 B. D. Reed, J. A. Biaglow and S. J. Schneider, *Mater. Manuf. Proc.*, 1998, **13**, (5), 757

118 K. Knapas and M. Ritala, *Chem. Mater.*, 2011, **23**, (11), 2766

119 J. Hämäläinen, E. Puukilainen, T. Sajavaara, M. Ritala and M. Leskelä, *Thin Solid Films*, 2013, **531**, 243

120 J. Hämäläinen, M. Ritala and M. Leskelä, *Chem. Mater.*, 2014, **26**, (1), 786

121 J. Hämäläinen, T. Hatanpää, E. Puukilainen, T. Sajavaara, M. Ritala and M. Leskelä, *J. Mater. Chem.*, 2011, **21**, (41), 16488

122 J. Hämäläinen, E. Puukilainen, M. Kemell, L. Costelle, M. Ritala and M. Leskelä, *Chem. Mater.*, 2009, **21**, (20), 4868

123 S. T. Christensen and J. W. Elam, *Chem. Mater.*, 2010, **22**, (8), 2517

124 J. A. Venables, "Introduction to Surface and Thin Film Processes", Cambridge University Press, Cambridge, UK, 2000

125 M. Ohring, "Materials Science of Thin Films: Deposition and Structure", 2nd Edn., Academic Press, San Diego, California, USA, 2002

126 K. Mumtaz, J. Echigoya, H. Enoki, T. Hirai and Y. Shindo, *J. Alloys Compd.*, 1994, **209**, (1–2), 279

127 H. Murakami, T. Yano and S. Sodeoka, *Mater. Trans.*, 2004, **45**, (9), 2886

128 F. Wu, H. Murakami and A. Suzuki, *Surf. Coat. Technol.*, 2003, **168**, (1), 62

129 K. Kamiya and H. Murakami, *J. Japan Inst. Metals*

Mater., 2005, **69**, (1), 73

130 S. Isogawa, H. Tojo, A. Chayahara and Y. Horino, *Surf. Coat. Technol.*, 2002, **158–159**, 186

131 I.-S. Lee, C.-N. Whang, J.-C. Park, D.-H. Lee and W.-S. Seo, *Biomater.*, 2003, **24**, (13), 2225

132 T. Jones, *Metal Finish.*, 2004, **102**, (6), 87

133 M. Cohen Sagiv, N. Eliaz and E. Gileadi, *Electrochim. Acta*, 2013, **88**, 240

134 W.-P. Wu, N. Eliaz and E. Gileadi, *J. Electrochem. Soc.*, 2015, **162**, (1), D20

135 J.-G. Qian, S.-M. Xiao, T. Zhao and H.-J. Luan, *Rare Metal Mater. Eng.*, 2012, **41**, (7), 1139

136 J.-G. Qian, Y. Yin, X. Li and T.-J. Li, *Trans. Nonferrous Metals Soc. China*, 2015, **25**, (5), 1685

137 J.-G. Qian and T. Zhao, *Trans. Nonferrous Metals Soc. China*, 2012, **22**, (11), 2855

138 N. A. Saltykova and O. V. Portnyagin, *Russ. J. Electrochem.*, 2001, **37**, (9), 924

139 N. I. Timofeev, V. E. Baraboshkin and N. A. Saltykova, 'Production of Iridium Crucibles by Electrolysis of Molten Salts', in "Iridium", eds. E. K. Ohriner, R. D. Lanam, P. Panfilov and H. Harada, Proceedings of the International Symposium held During the 129th Annual Meeting & Exhibition of The Minerals, Metals & Materials Society (TMS), Nashville, Tennessee, USA, TMS, Warrendale, Pennsylvania, 2000, pp. 175–179

140 N. A. Saltykova, *J. Min. Metall. B: Metall.*, 2003, **39**, (1–2), 201

141 N. A. Saltykova, S. N. Kotovskii, O. V. Portnyagin, A. N. Baraboshkin and N. O. Esina, *Sov. Electrochem.*, 1990, **26**, (3), 338

142 Y.-L. Huang, S.-X. Bai, H. Zhang and Y.-C. Ye, *Appl. Surf. Sci.*, 2015, **328**, 436

143 B. D. Reed and R. Dickerson, 'Testing of Electroformed Deposited Iridium/Powder Metallurgy Rhenium Rockets', NASA Technical Memorandum 107172, National Aeronautics and Space Administration, Cleveland, Ohio, USA, 1995

144 L.-B. Wang, Z.-F. Chen, P.-Z. Zhang, W.-P. Wu and Y. Zhang, *J. Coat. Technol. Res.*, 2009, **6**, (4), 517

145 L.-B. Wang, Z.-F. Chen, Y. Zhang and W.-P. Wu, *Int. J. Refract. Metals Hard Mater.*, 2009, **27**, (3), 590

146 Y. Zhang, Z.-F. Chen, L.-B. Wang, W.-P. Wu and D. Fang, *J. Coat. Technol. Res.*, 2009, **6**, (2), 237

147 X.-N. Cong, Z.-F. Chen, W.-P. Wu, J. Xu and F. E. Boafo, *Appl. Surf. Sci.*, 2012, **258**, (12), 5135

148 X.-N. Cong, Z.-F. Chen, W.-P. Wu, Z. F. Chen and F. E. Boafo, *Acta Astronaut.*, 2012, **79**, 88

149 W.-P. Wu, Z.-F. Chen and X.-N. Cong, 'Protective Ir-Zr and Ir Coatings for Refractory Metals', 26th International Conference on Surface Modification Technologies, Écully-Lyon, France, 20th–22nd June, 2012, in "Surface Modification Technologies XXVI: Proceedings of the Twenty Sixth International Conference on Surface Modification Technologies", eds. T. S. Sudarshan, M. Jeandin and V. Fridrici, Valardocs, Chennai, India, 2013, pp. 395–406

150 J.-M. Wang, Z.-W. Zhang, Z.-H. Xu, X. Lin, W.-P. Wu and Z. F. Chen, *Corros. Eng. Sci. Technol.,* 2011, **46**, (6), 732

151 Z.-W. Zhang, Z.-H. Xu, J.-M. Wang, W.-P. Wu and Z.-F. Chen, *J. Mater. Eng. Perf.*, 2012, **21**, (10), 2085

152 W.-P. Wu, Z.-F. Chen and Y. Liu, *Plasma Sci. Technol.*, 2012, **14**, (10), 909

153 W.-P. Wu and Z.-F. Chen, *J. Wuhan Univ. Technol.-Mater. Sci. Ed.,* 2012, **27**, (4), 652

154 W.-P. Wu, Z.-F. Chen, X.-W. Cheng and Y.-W. Wang, *Nucl. Instr. Meth. Phys. Res. Sect. B: Beam Int. Mater. Atoms*, 2013, **307**, 315

155 W.-P. Wu, Z.-F. Chen and X. Lin, *Adv. Mater. Res.*, 2011, **189–193**, 688

156 D. H. Lowndes, D. B. Geohegan, A. A. Puretzky, D. P. Norton and C. M. Rouleau, *Science*, 1996, **273**, (5277), 898

157 M. Galeazzi, C. Chen, J. L. Cohn and J. O. Gundersen, *Nucl. Instrum. Meth. Phys. Res. Sect. A: Accel., Spectr., Detect. Assoc. Equip.*, 2004, **520**, (1–3), 293

158 C.-L. Chen, 'Iridium Thin Films Deposited *via* Pulsed Laser Deposition', PhD Thesis, University of Miami, USA, Dissertations from ProQuest, Paper 2456, 2006

159 H. Herzig, *Platinum Metals Rev.*, 1983, **27**, (3), 108

160 T. Bauer, S. Gsell, M. Schreck, J. Goldfuß, J. Lettieri, D.G. Schlom and B. Stritzker, *Diam. Relat. Mater.*, 2005, **14**, (3–7), 314

161 H.-Q. Li, D.-Y. Chen, F.-T. Xu, Z.-H. Jia and X.-H. Zhang. *Aerospace Mater. Technol.*, 2013, (6), 64 (in Chinese)

162 J. O. Milewski, D. J. Thoma, J. C. Fonseca and G. K. Lewis, *Mater. Manuf. Process.*, 1998, **13**, (5), 719

The Authors

Wang-ping Wu received his doctorate in Materials Processing Engineering at Nanjing University of Aeronautics and Astronautics, China, in 2013 and held a Pikovsky Valazzi Scholarship at Tel Aviv University, Israel, where he was a Postdoctoral Fellow. He is now a Senior Lecturer at the School of Mechanical Engineering in Changzhou University, China. His research interests are mainly directed towards the synthesis and characterisation of films and coatings of the noble metals and their alloys.

Zhao-feng Chen is Professor of Materials Science and Director of the International Laboratory for Insulation and Energy Efficiency Materials at the College of Material Science and Technology at Nanjing University of Aeronautics and Astronautics. His research interests include advanced insulation composite materials and the application of coatings of noble metals.

http://dx.doi.org/10.1595/205651317X693750 *Johnson Matthey Technol. Rev.*, 2017, **61**, (1), 29–31

JOHNSON MATTHEY
TECHNOLOGY REVIEW

www.technology.matthey.com

World Hydrogen Energy Conference 2016

Recent advances in a range of topics related to hydrogen and fuel cells

Reviewed by David Wails
Johnson Matthey Technology Centre, Blounts Court, Sonning Common, Reading, RG4 9NH, UK

Email: david.wails@matthey.com

1. Introduction

The World Hydrogen Energy Conferences (WHEC) are biennial events focusing primarily on the hydrogen for fuel cells sector. The 2016 event, the 21st in the series, was held in Zaragoza, Spain, from the 13th–16th June 2016 and attracted approximately 1000 delegates (mainly academic) from around 60 countries. The conference was organised by the Spanish Hydrogen Association on behalf of the International Association for Hydrogen Energy. 1134 accepted abstracts in eight parallel sessions covered a range of topics including:

- hydrogen production: fossil sources, solar hydrogen and renewable hydrogen, bio hydrogen and bio gasification, electrolysis/electrolysers, catalysts
- hydrogen storage: chemical carriers and hydrides, gas and liquefaction
- electrocatalysts and electrodes (fuel cells and electrolysers)
- fuel cell components: polymer electrolyte membrane (PEM), solid oxide, molten carbonate, alkaline, stacks
- modelling: systems, hydrogen systems, infrastructure systems
- applications: transportation and aerospace, stationary applications, other applications of hydrogen as a fuel, other applications of fuel cells
- purification, separation, membranes
- safety, sensors, hydrogen properties
- environmental impact and emissions
- pipelines, hydrogen infrastructure, distribution, filling stations
- hydrogen economy, commercialisation, codes and standards
- countries strategies, associations and assessments.

Parallel poster sessions, a trade fair (**Figure 1**) and a ‘test and drive’ area were also included in the conference, where participants were able to drive a Toyota Mirai (the world’s first mass produced fuel cell electric vehicle (FCEV)) or ride in a BMW 5GT FCEV (**Figure 2**), as well as see a hydrogen refuelling station in operation. Highlights of the conference included sessions on fuel cell vehicles, the use of hydrogen in electricity grid balancing and alternative hydrogen carriers being considered in particular markets.

2. Fuel Cell Vehicles

Keynote talks from Matthias Klietz (BMW AG, Germany) and Jacques Pieraerts (Toyota Motor Europe, Belgium) focused on their introduction of FCEVs. BMW’s view is that their customers no longer simply want zero emission FCEVs but want well to wheels zero emission vehicles (ZEV). This means that the hydrogen to refuel these vehicles will need to come from renewable energy sources (wind, solar)

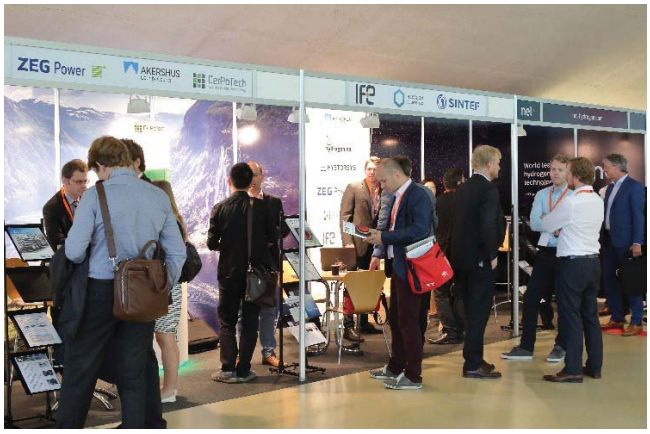

Fig. 1. Attendees at the trade fair during WHEC (Reproduced by courtesy of the Spanish Hydrogen Association, Spain)

Fig. 2. BMW 5GT FCEV and Toyota Mirai were available for a test drive during WHEC (Reproduced by courtesy of the Spanish Hydrogen Association)

via electrolysis rather than from fossil fuels. Toyota reiterated this view, adding that their 2050 roadmap has only hybrid internal combustion engine vehicles (possibly fuelled by hydrogen or biogas rather than gasoline or diesel) including plug in hybrids alongside battery and FCEV. Toyota and BMW are engaged in a pre-competitive collaboration looking at joint development of fuel cell stacks, systems and hydrogen storage tanks.

3. The Role of Hydrogen in Grid Balancing

Other keynote talks focused on the role of hydrogen in balancing electricity transmission grids. Klaus Bonhoff (National Organisation Hydrogen and Fuel Cell Technology (NOW) GmbH, Germany) discussed Germany's 2050 targets (based on European Union (EU) 2050 targets) to have a 90% reduction in greenhouse gas emissions, with renewables accounting for 60% of energy requirements by then, compared to their 18% contribution today. This is expected to be achieved *via* electrolysis using renewable electricity (wind, solar) with storage *via* power to gas (P2G) and batteries. A number of German initiatives including market preparation for residential fuel cell systems, technology validation for fuel cell vehicles (including a programme involving 50 refuelling stations) and 30 P2G schemes were discussed.

Simon Bourne (ITM Power, UK) discussed the increasing use of renewable electricity in the UK and issues with curtailment, where renewable electricity (from wind) is available but there is no demand for the power. Electrolysers can be a useful transducer between power and gas particularly if the electrolysers have a rapid (<1 second) response to enable the grid frequency to also be balanced. At a 1 MW scale, 72% efficiency is typical and can be up to 86% where waste heat is also utilised. Storage capacity in the UK's gas network is five times that of the electricity grid. Rather than converting hydrogen into methane (*via* reaction with carbon dioxide), a UK safety laboratory reported that up to 20% hydrogen in the natural gas network would not impact on polyethylene pipework or gas appliance performance and provide no additional safety issues compared to natural gas alone. However, the regulations on natural gas composition in many countries specifically limit the hydrogen content to very low levels and so there are political as well as technical limitations to be overcome.

Gregor Waldstein (ETOGAS GmbH, Germany), discussed experiences from some successful P2G projects, including Audi's 'e-gas' plant, which upgrades biogas to synthetic natural gas (SNG) using hydrogen from electrolysis with renewable electricity. Owners purchase compressed natural gas (CNG) using a top-up card and the plant adds the amount of CNG used to the gas network. It was commented that the mobility market is willing to pay the higher cost of gas compared to the electricity market. Considering well to well emissions (including battery manufacture) the technology is considered to have similar carbon dioxide emissions to wind electricity plus battery systems, although exactly where and how total emissions are defined remains a contentious issue. Everett Anderson (Proton OnSite,

USA) described how in some US locations, continuing wind turbine construction is leading to extremely cheap electricity in significant quantities, meaning that the cost of hydrogen *via* electrolysis can compete with the hydrogen cost from steam methane reforming traditionally used for hydrogen production and without carbon dioxide emissions.

4. Country Specific Sessions

Eiji Ohira (New Energy and Industrial Technology Development Organization (NEDO), Japan) presented Japan's policy on hydrogen energy, which is intended to act against climate change without sacrificing economic growth. Japan is aiming for 24% renewable electricity production by 2030, including 5.3 million micro combined heat and power (mCHP) units and 800,000 FCEVs with 320 hydrogen refuelling stations.

Hydrogen resources overseas, including fossil and renewable sources would produce hydrogen which will be transported to Japan. Tankers will be used to import hydrogen *via* liquid hydrogen (Kawasaki Heavy Industries, Japan) or through organic carriers such as methyl cyclohexane. Yoshimi Okada (Chiyoda Corporation, Japan) discussed a toluene-methylcyclohexane hydrogenation-dehydrogenation system which is already being introduced at a significant scale by the Chiyoda Corporation using a platinum group metal catalyst.

Mina Jeon (Korea Institute of Science and Technology, South Korea) explored the topic of ammonia, one of the world's largest commodity chemicals which is also considered to be a vector for hydrogen transportation, having 17.7 wt% hydrogen storage density and can be easily liquefied. The ammonia can be decomposed to generate hydrogen, or as Osamu Kurata (National Institute of Advanced Industrial Science and Technology (AIST), Japan) discussed, can be used to generate electricity directly by combustion in a gas turbine power station. Oren Elishav (Technion – Israel Institute of Technology, Israel) looked at alternative nitrogen based carriers which include urea, ammonium hydroxide or ammonium nitrate mixtures. Ammonium hydroxide or urea mixtures were considered to be safer alternatives to ammonia and are also suitable for combustion processes.

Alternative organic hydrogen carriers being considered in Germany, such as dibenzyl toluene, were discussed by Daniel Teichmann (Hydrogenious Technologies GmbH, Germany). These are liquid at operating temperature, non-flammable and non-toxic so are considered safer than existing hydrocarbons handled in the fuel transportation industry. Hydrogenation is carried out using a photovoltaic system coupled to an electrolyser. A demonstration system is currently supplying a FCEV refuelling station in Stuttgart. Economically, the technology is considered to be more expensive than cryogenic hydrogen transportation but significantly more flexible.

5. Conclusions

WHEC 2016 attracted a large number of delegates to participate in a range of topics related to hydrogen and fuel cells, including fuel cell electric vehicles, hydrogen production, hydrogen storage and hydrogen distribution. Other, emerging uses for hydrogen such as applications in electricity grid balancing and power to gas applications also received significant coverage. Owing to the large number of talks across eight parallel sessions, this review has only covered a small proportion of the presentations given.

The next WHEC will be held in Rio de Janeiro, Brazil, in 2018.

The Reviewer

David Wails is a Senior Principal Scientist in the Low Carbon Technology group at Johnson Matthey Technology Centre, Sonning Common, UK. His areas of research include hydrogen production for fuel cell vehicles and stationary fuel cells, and hydrogen utilisation in power to gas and power to chemical applications.

http://dx.doi.org/10.1595/205651317X693741 Johnson Matthey Technol. Rev., 2017, 61, (1), 32–39

JOHNSON MATTHEY
TECHNOLOGY REVIEW
www.technology.matthey.com

Health Impact Analysis of Cisplatin, Carboplatin and Oxaliplatin

Quantifying the health impact of platinum compounds

By Matthew Taylor and Alex Filby*
York Health Economics Consortium, Enterprise House, Innovation Way, University of York, YO10 5NQ, UK

***Email:** alex.filby@york.ac.uk

A literature based study on the health impacts of three platinum anticancer drugs (cisplatin, carboplatin and oxaliplatin) was undertaken. The published evidence for health benefits is presented and assessed. A model was developed to quantify the health gain of adding platinum based drugs to cancer treatment at the population level for the UK and the USA. The economic value of using platinum drugs (in terms of quality-adjusted life year (QALY)) in addition to other cancer treatments can be estimated at over £556 million for the UK and over US$4.8 billion for the USA, depending on the scenario chosen.

Introduction

Cisplatin, carboplatin and oxaliplatin are platinum compounds used intravenously in the chemotherapy treatment of eight types of cancer where solid tumours are present (1).

A solid tumour is an abnormal mass of tissue that usually does not contain cysts or liquid areas. Solid tumours may be benign or malignant. Examples of solid tumours are sarcomas, carcinomas and lymphomas. Leukaemias (cancers of the blood) generally do not form solid tumours (2).

The use of cisplatin, carboplatin and oxaliplatin by type of cancer according to the British National Formulary (BNF) (3) is shown in **Table I**.

Even allowing for clinical decisions to use other treatments, the use of platinum compounds in the types of cancer listed in **Table I** suggests that treatment using cisplatin, carboplatin or oxaliplatin could offer significant benefit to the UK and US populations.

The aim of the present research is to quantify the health impact of key pharmaceutical compounds (cisplatin, carboplatin and oxaliplatin) on population health. The specific objectives were to undertake a targeted literature review on the health benefits of using platinum compounds in oncology treatment and to develop a *de novo* model to show the health impacts on population-level health in the UK and USA.

Method: Targeted Literature Searches

In order to capture the data necessary to populate the model a targeted literature search and literature review were carried out.

The literature search and review were targeted to capture evidence on any existing effectiveness analyses for any of the treatments (reported as progression-free survival (PFS) or overall survival (OS)); quality of life

Table I The use of Cisplatin, Carboplatin and Oxaliplatin by Type of Cancer

Type of Cancer	Cisplatin	Carboplatin	Oxaliplatin
Ovarian	✓[a]	✓	×
Lung (particularly the small cell type)	✓	✓	×
Testicular	✓	×	×
Cervical	✓	×	×
Bladder	✓	×	×
Head and neck	✓	×	×
Colorectal (metastatic)	×	×	✓
Colon (adjuvant)	×	×	✓

[a]Cisplatin can be used but carboplatin is preferred for ovarian cancer (1)

data associated with the treatments or disease area and UK and USA epidemiology data.

An initial search strategy was developed and run and this was then followed up with further targeted searches. The aim was to identify papers that used platinum compounds as an add-on treatment for each cancer type identified in **Table I** in order to calculate the additional benefit gained from platinum compound usage.

The search strategy was developed to be as sensitive as possible in order to retrieve all relevant records. Any record containing the words 'cisplatin', 'carboplatin' or 'oxaliplatin' was returned. The search was limited to records indexed as review papers, English language papers and the date was limited from 2002 until present. These limits were applied to identify the most relevant and current research and to make the amount of results retrieved manageable within the constraints of the project. This search strategy was run in Ovid MEDLINE® In-Process and Ovid MEDLINE® with over 300 records retrieved.

Next, targeted searches of PubMed®, Google™ and Google Scholar™ were carried out. Searches on each database included the type of platinum compound, the type of cancer and phrases 'plus' and 'with or without'.

These searches were carried out for each combination of platinum compound and type of cancer. The first three to five pages of search results were reviewed based on title. Any articles that appeared relevant were then reviewed based on abstract. If the abstract appeared useful or if it was not possible to tell if it would be useful, the full paper was obtained (where possible).

If no literature was identified in the above searches then further targeted searching of the specific area of interest (i.e. the cancer type and drug type) were carried out.

The Model

A model was developed in Microsoft® Excel® to calculate the health gain of adding platinum to cancer treatment. The structure of the model is outlined in **Figure 1**. The model aims to capture the health gains and the value of these health gains achieved by using platinum compounds in cancer treatment. The analysis modelled a hypothetical cohort of patients in order to show the potential health benefits that could arise from using platinum compounds. It is assumed that all patients in a cancer category are treated with platinum compounds and that all accrue the QALY gain. This is calculated for UK and USA populations in the model.

The model inputs were identified from the targeted literature searches. Generally, for carboplatin and cisplatin it seemed that these compounds were already established as effective and so were often used in standard care rather than as an add-on. Otherwise, articles tended to compare the two types of platinum compound and so could not be included. Various strategies to deal with 'poor' evidence were employed. For example, research on small cell lung cancer was not identified for carboplatin so this was replaced with research on non-small cell lung cancer. In many groups (for instance, ovarian and lung) data were found for one type of platinum compound but not another so this

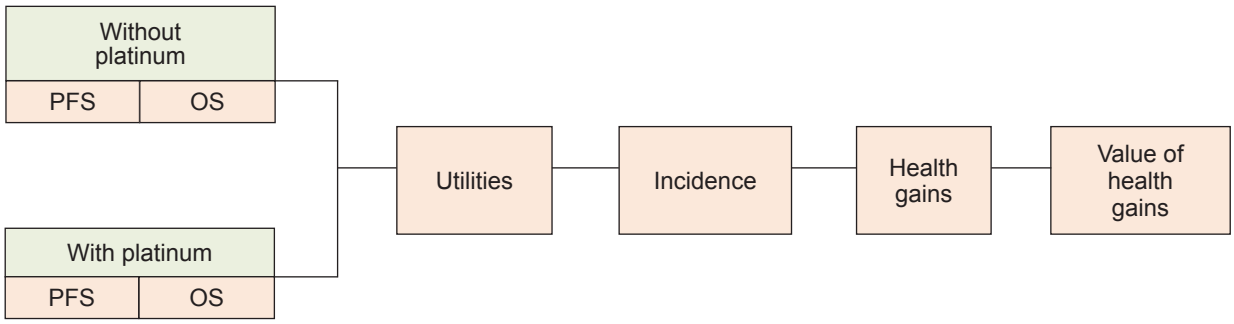

Fig. 1. Structure of the model. PFS = progression free survival, OS = overall survival

patient group was still accounted for. Testicular cancer and bladder cancer were excluded due to a lack of data.

One article that investigated cisplatin as an add-on treatment for bladder cancer was identified (4). However, this study reported a negative difference in overall survival for using platinum as an add-on treatment. The decision was made to exclude this article based on the fact that it appears that platinum compounds are well-established first line therapies for bladder cancer, suggesting that cisplatin is effective in improving cancer health outcomes. In addition, the trial failed to meet its recruitment targets and a larger study was recommended. Cisplatin is already a well-established standard therapy which may explain why no further studies were identified investigating cisplatin as an add-on treatment.

Table II shows the PFS and OS with and without platinum and the sources from which the data were extracted. Where more than one source is given, a weighted average based on sample size was calculated.

For cervical cancer the results show that there is a gain in PFS in the 'with platinum' arm while there is a reduction in OS. Two of the three studies identified showed lower PFS and lower OS in the treatment arm (9, 10) while the third study (8) showed an improvement in both PFS and OS when platinum was used (see **Appendix A**). The combination of the weighting (one study has a much larger sample size) and the relative difference in survival in each study results in this weighted average result. **Appendix B** shows the significance levels between treatment arms reported in the study.

Health-related quality of life inputs (utilities) were applied to each health state in order to generate QALYs. The utilities that were used in the model for PFS and post-progression survival (PPS) are outlined in **Table III**.

Table II Weighted Averages of PFS and OS Included in the Model

		Weighted averages (months)				
		Without platinum		With platinum		
Cancer type	Platinum compound	PFS	OS	PFS	OS	Source
Lung	Carboplatin	4.62	11.83	5.55	12.41	(5, 6)
Ovarian	Cisplatin	15.58	37.37	20.34	37.94	(7)
Cervical	Cisplatin	101.39	121.17	105.64	117.22	(8–10)
Head and neck	Cisplatin	24.24	41.84	34.62	67.81	(11)
Colorectal	Oxaliplatin	6.50	22.61	9.65	22.92	(12–18)

Table III Utilities Included in the Model

Cancer type	Utility PFS	Source	Utility PPS	Source
Lung	0.653	(19)	0.473	(19)
Ovarian	0.85	(20)	0.65	(20)
Cervical	0.72	(21)	0.29	(21)
Head and neck	0.65	(22)	0.51	(22)
Colorectal	0.8	(23)	0.46	(24)

Results for UK

In the base case model, it has been assumed that 100% of the patients from the population cancer incidence statistics are treated with platinum. The results show that using platinum compounds in cancer treatment offers potential health gains over cancer treatment not including platinum compounds. **Table IV** shows that, based on the base case inputs in the model, using platinum compounds could result in a potential gain of over 27,000 QALYs per year in the UK. In the UK a value of £20,000 per QALY is considered to be cost-effective (1). Therefore, assuming a threshold of up to £20,000 per QALY, the total QALYs gained would be valued at over £556 million.

Results for USA

Based on the base case inputs in the model, platinum compounds in cancer treatment could result in potential health gains of over 97,000 QALYs in the US population. Although there is no official published estimate of the value of QALYs in the USA, if it is assumed that the USA values QALYs at US$50,000 this would result in potential health gains valued at over US$4.8 billion.

Analysis of Uncertainty for UK

Bladder cancer and testicular cancer were excluded because the data were not available in the literature to populate the model. A sensitivity analysis including these sub-groups was run. This is based on the assumptions that 100% of patients in this disease sub-group are treated with platinum compounds, and that the per patient QALY gain is based on an average of the QALY gain in the other disease areas included in the model. The results showed that this may add over 3800 additional QALYs with a value of over £77 million.

If treatment uptake in the base case results was reduced to 50% the health gain from the use of platinum compounds would be valued at over £278 million. If head and neck cancer uptake of platinum treatment was lowered to just 10% (note: this is the third highest incidence and has by far the highest QALY gain per

Table IV Summary of QALY Gain for the UK

Cancer type	Platinum compound	QALY gain per patient if using drug	Incidence UK	Potential QALYs gained
Lung	Carboplatin	0.03	42,026	1547
Ovarian	Cisplatin	0.08	7,011	776
Cervical	Cisplatin	0.04	2,851	166
Head and neck	Cisplatin	0.85	17,353	21,255
Colorectal	Oxaliplatin	0.07	40,695	4102
			Total QALYs gained	**27,845**
			UK total value of QALYs gained	£556,900,453

patient), the total value of the QALYs gained would be around £174 million. Finally, in a more pessimistic scenario, in which all uptake is lowered to 50% and 10% in head and neck cancer, the value of QALYs gained would be over £108 million.

Discussion

The results of the analysis depend on the inputs and assumptions that the model user has selected. However, the model demonstrates that using platinum compounds in the five cancer types included in the model results in QALY gains from which a monetary value of health gain is calculated.

A key strength of the modelling approach is that it allows the decision maker to combine evidence from a variety of sources in order to derive a single assessment of the intervention's impact upon quality of life and survival. In addition, sensitivity analyses were carried out on uncertain input parameters which showed that even in the most pessimistic scenarios; platinum compounds were associated with quantitative health benefits.

A key limitation of this analysis is the lack of robust data with which to populate the model. The literature investigating platinum compounds as an add-on to standard treatment is sparse. This is likely because platinum is already accepted as a standard treatment and is usually included in both arms of the trial or study in combination with other chemotherapy drugs. This would result in the current analysis underestimating the health value of platinum compounds. However, it should be noted that in all cancer types and platinum compound sub-groups (with the exception of one underpowered study (4)) the weighted average survival gain extracted from the literature showed that platinum as an add-on offered health benefits.

Finally, this research focuses on the health outcomes only and does not consider the costs associated with the use of cisplatin, carboplatin or oxaliplatin. Further research could extend the current work to include these costs to determine if the added health benefits outweigh the costs associated with platinum compound use in oncology treatment.

Conclusion

The study showed that platinum compounds are associated with population health gains when used in oncology treatment. This health benefit has been quantified using the value associated with a QALY. The results showed that, even in the most pessimistic scenarios, cisplatin, carboplatin and oxaliplatin were associated with a positive monetary value of health gain when used to treat a number of different solid tumours.

Funding Statement

This project was supported by funding from Johnson Matthey.

References

1. "Developing NICE Guidelines: The Manual", Process and Methods, PMG20, National Institute for Health and Care Excellence, London, UK, October, 2014
2. 'Appraising Life-Extending, End of Life Treatments', National Institute for Health and Clinical Excellence, London, UK, 2009
3. National Institute for Health and Care Excellence (NICE), British National Formulary (BNF), 'Platinum Compounds', October, 2016: https://www.evidence.nhs.uk/formulary/bnf/current/8-malignant-disease-and-immunosuppression/81-cytotoxic-drugs/815-other-antineoplastic-drugs/platinum-compounds (Accessed on 10th November 2016)
4. D. M. A. Wallace, D. Raghavan, K. A. Kelly, T. F. Sandeman, I. G. Conn, N. Teriana, J. Dunn, J. Boulas and T. Latief, *British J. Urology*, 1991, **67**, (6), 608
5. E. F. Smit, S. A. Burgers, B. Biesma, H. J. M. Smit, P. Eppinga, A.-M. C. Dingemans, M. Joerger, J. H. Schellens, A. Vincent, N. van Zandwijk and H. J. M. Groen, *J. Clin. Oncol.*, 2009, **27**, (12), 2038
6. A. Ardizzoni, M. Tiseo, L. Boni, A. D. Vincent, R. Passalacqua, S. Buti, D. Amoroso, A. Camerini, R. Labianca, G. Genestreti, C. Boni, L. Ciuffreda, F. Di Costanzo, F. de Marinis, L. Crinò, A. Santo, A. Pazzola, F. Barbieri, N. Zilembo, I. Colantonio, C. Tibaldi, R. Mattioli, M. A. Cafferata, R. Camisa and E. F. Smit, *J. Clin. Oncol.*, 2012, **30**, (36), 4501
7. F. M. Muggia, P. S. Braly, M. F. Brady, G. Sutton, T. H. Niemann, S. L. Lentz, R. D. Alvarez, P. R. Kucera and J. M. Small, *J. Clin. Oncol.*, 2000, **18**, (1), 106
8. R. Pearcey, M. Brundage, P. Drouin, J. Jeffrey, D. Johnston, H. Lukka, G. MacLean, L. Souhami, G. Stuart and D. Tu, *J. Clin. Oncol.*, 2002, **20**, (4), 966
9. M. Garipağaoğlu, F. Kayikçioğlu, M. F. Köse, M. Adli, K. H. Gülkesen, Z. Koçak and G. Tulunay, *British J.*

Radiol., 2004, **77**, (919), 581

10. S. Chiara, M. Bruzzone, L. Merlini, P. Bruzzi, R. Rosso, P. Franzone, M. Orsatti, V. Vitale, G. Foglia, F. Odicino, N. Ragni, S. Rugiati and P. Conte, *Am. J. Clin. Oncol.*, 1994, **17**, (4), 294
11. P. Ghadjar, M. Simcock, G. Studer, A. S. Allal, M. Ozsahin, J. Bernier, M. Töpfer, F. Zimmermann, M. Betz, C. Glanzmann and D. M. Aebersold, *Int. J. Radiat. Oncol. Biol. Phys*., 2012, **82**, (2), 524
12. A. Ibrahim, S. Hirschfeld, M. H. Cohen, D. J. Griebel, G. A. Williams and R. Pazdur, *The Oncologist*, 2004, **9**, (1), 8
13. A. de Gramont, A. Figer, M. Seymour, M. Homerin, A. Hmissi, J. Cassidy, C. Boni, H. Cortes-Funes, A. Cervantes, G. Freyer, D. Papamichael, N. Le Bail, C. Louvet, D. Hendler, F. de Braud, C. Wilson, F. Morvan and A. Bonetti, *J. Clin. Oncol*., 2000, **18**, (16), 2938
14. S. Giacchetti, B. Perpoint, R. Zidani, N. Le Bail, R. Faggiuolo, C. Focan, P. Chollet, J.F. Llory, Y. Letourneau, B. Coudert, F. Bertheaut-Cvitkovic, D. Larregain-Fournier, A. Le Rol, S. Walter, R. Adam, J.L. Misset and F. Lévi, *J. Clin. Oncol*., 2000, **18**, (1), 136
15. G. A. P. Hospers, M. Schaapveld, J. W. R. Nortier, J. Wils, A. van Bochove, R. S. de Jong, G. J. Creemers, Z. Erjavec, D. J. de Gooyer, P. H. Th. J. Slee, C. J. H. Gerrits, J. M. Smit and N. H. Mulder, *Ann. Oncol*., 2006, **17**, (3), 443
16. N. Kemeny, C. A. Garay, J. Gurtler, H. Hochster, P. Kennedy, A. Benson, D. S. Brandt, J. Polikoff, M. Wertheim, G. Shumaker, D. Hallman, B. Burger and S. Gupta, *J. Clin. Oncol*., 2004, **22**, (23), 4753
17. D. Damjanovic, P. Thompson and M. P. Findlay, *ANZ J. Surg.*, 2004, **74**, (9), 781
18. M. L. Rothenberg, A. M. Oza, R. H. Bigelow, J. D. Berlin, J. L. Marshall, R. K. Ramanathan, L. L. Hart, S. Gupta, C. A. Garay, B. G. Burger, N. Le Bail and D. G. Haller, *J. Clin. Oncol*., 2003, **21**, (11), 2059
19. B. Nafees, M. Stafford, S. Gavriel, S. Bhalla and J. Watkins, *Health Qual. Life Outcomes*, 2008, **6**, 84
20. J. P. Greving, F. Vernooij, A. P. Heintz, Y. van der Graaf and E. Buskens, *Gynecol. Oncol*., 2009, **113**, (1), 68
21. I. M. C. M. de Kok, J. van Rosmalen, J. Dillner, M. Arbyn, P. Sasieni, T. Iftner and M. van Ballegooijen, *Brit. Med. J.*, 2012, **344**, e670
22. J. Greenhalgh, A. Bagust, A. Boland, N. Fleeman, C. McLeod, Y. Dundar, C. Proudlove and R. Shaw, 'Cetuximab for Recurrent and/or Metastatic Squamous Cell Carcinoma of the Head and Neck (SCCHN)', ERG report, National Institute for Health and Clinical Excellence, London, UK, 2008
23. T. Shiroiwa, T. Takeuchi, T. Fukuda, K. Shimozuma and Y. Ohashi, *Value Health*, 2012, **15**, (2), 255
24. S. J. Heitman, R. J. Hilsden, F. Au, S. Dowden and B. J. Manns, *PLoS Med.*, 2010, **7**, (11), e1000370

The Authors

Matthew Taylor is the Director of York Health Economics Consortium (YHEC) and leads the Consortium's health technology assessment programme. He has a PhD degree in Quality of Life Measurement and an MSc in Health Economics from the University of York. Matthew has led more than one hundred economic evaluations for National Institute for Health and Care Excellence (NICE), Scottish Medicines Consortium (SMC) and All Wales Medicines Strategy Group (AWMSG), plus industry submissions as well as health technology submissions in various international settings. Matthew's work at YHEC includes economic evaluations, model adaptations, budget impact modelling, cost-of-illness studies, quality of life research and theoretical research for clients in both the private and public sectors. He is a Scientific Advisor to NICE, and a former member of NICE's Public Health Advisory Committee. He is also Managing Director (Europe) of Minerva, an international network of health economics consultancies.

Alexandra Filby has an MSc in Health Psychology from Sheffield Hallam University, UK, and a PGCert in Health Economics for Health Care Professionals from the University of York. Alex works as a Research Consultant at YHEC. Alex works on projects for both private and public sector clients. She has developed a range of different economic models for various clients.

Appendix A
All Studies Included in Weighted Average Calculations

Carboplatin - Non small cell lung cancer

	Without platinum median (mean)		With platinum median (mean)		Sample size
Author, year (Ref.)	**PFS**	**OS**	**PFS**	**OS**	
Smit, 2008 (5)	2.8 (4.04)	7.6 (10.96)	4.2 (6.06)	8 (11.54)	240
Ardizzoni, 2012 (6)	3.6 (5.19)	8.8 (12.70)	3.5 (5.05)	9.2 (13.27)	240
Weighted average	**3.20 (4.62)**	**8.20 (11.83)**	**3.85 (5.55)**	**8.60 (12.41)**	–

Cisplatin - Ovarian

	Without platinum median (mean)		With platinum median (mean)		Sample size
Author, year (Ref.)	**PFS**	**OS**	**PFS**	**OS**	
Muggia, 2000 (7)	10.8 (15.58)	25.9 (37.37)	14.1 (20.34)	26.3 (37.94)	414

Cisplatin - Cervical

	Without platinum median (mean)		With platinum median (mean)		Sample size
Author, year (Ref.)	**PFS**	**OS**	**PFS**	**OS**	
Pearcey, 2002 (8)	74 (106.76)	76 (109.64)	86 (124.07)	87 (125.51)	253
Garipağaoğlu, 2004 (9)	40 (57.71)	64 (92.33)	33 (47.61)	55.1 (79.49)	44
Chiara, 1994 (10)	77 (111.09)	134 (193.32)	48 (69.25)	76 (109.64)	58
Weighted average	**70.28 (101.39)**	**83.99 (121.17)**	**73.22 (105.64)**	**81.25 (117.22)**	–

Cisplatin - Head and neck

	Without platinum median (mean)		With platinum median (mean)		Sample size
Author, year (Ref.)	**PFS**	**OS**	**PFS**	**OS**	
Ghadjar, 2012 (11)	16.8 (24.24)	29 (41.84)	24 (34.62)	47 (67.81)	224

Oxaliplatin - Colorectal

	Without platinum median (mean)		With platinum median (mean)		Sample size
Author, year (Ref.)	**PFS**	**OS**	**PFS**	**OS**	
Ibrahim, 2004 (12)	2.7 (3.90)	NR	4.6 (6.64)	NR	303
de Gramont, 2000 (13)	6.2 (8.94)	14.7 (21.21)	9 (12.98)	16.2 (23.37)	420
Giacchetti, 2000 (14)	6.1 (8.80)	19.9 (28.71)	8.7 (12.55)	19.4 (27.99)	200
Hospers, 2006 (15)	5.6 (8.08)	13.3 (19.19)	6.7 (9.67)	13.8 (19.91)	302
Kemeny, 2004 (16)	2.4 (3.46)	11.4 (16.45)	4.8 (6.92)	9.9 (14.28)	214
Grothy, 2002 in Damjanovic, 2004 (17)	5.3 (7.65)	16.1 (23.23)	7.9 (11.40)	20.4 (29.43)	238
Rothenberg, 2003 (18)	2.7 (3.90)	NR	4.6 (6.64)	NR	303
Weighted average	**4.51 (6.50)**	**15.67 (22.61)**	**6.69 (9.65)**	**15.88 (22.92)**	–

Appendix B

Carboplatin - Non small cell lung cancer

	Significance levels pre-post	
Author, year (Ref.)	**PFS**	**OS**
Smit, 2008 (15)	HR 0.67; 95% CI 0.51 to 0.89, p = 0.005	HR, 0.85; 95% CI 0.63 to 1.2; p not significant
Ardizzoni, 2012 (6)	HR 1.05; 95% CI 0.81 to 1.36; p = 0.706	HR, 0.97; 95% CI, 0.73 to 1.30; p = 0.834

Cisplatin - Ovarian

	Significance levels pre-post	
Author, year (Ref.)	**PFS**	**OS**
Muggia, 2000 (7)	Statistics are not reported for paclitaxel *vs.* cis + pac	Statistics are not reported for paclitaxel *vs.* cis + pac

Cisplatin - Cervical

	Significance levels pre-post	
Author, year (Ref.)	**PFS**	**OS**
Pearcey, 2002 (8)	No significant difference was found in progression-free survival (p = 0.33)	No significant difference in survival. The HR for survival (arm 2 to arm 1) was 1.10 (95% confidence interval, 0.75 to 1.62)
Garipağaoğlu, 2004 (9)	p = 0.3	p = 0.7
Chiara, 1994 (10)	No significant difference was observed	No significant difference was observed

Cisplatin - Head and neck

	Significance levels pre-post	
Author, year (Ref.)	**PFS**	**OS**
Ghadjar, 2012 (11)	HR, 1.6; 95% CI, 1.1–2.5; p = 0.02	HR, 1.3; 95% CI, 0.9–1.8; p = 0.11

Oxaliplatin - Colorectal

	Significance levels pre-post	
Author, year (Ref.)	**PFS**	**OS**
Ibrahim, 2004 (12)	p < 0.0001	NR
de Gramont, 2000 (13)	p = 0.0003	p = 0.12
Giacchetti, 2000 (14)	p = 0.048	No significant difference was observed
Hospers, 2006 (15)	p = 0.016	p = 0.619
Kemeny, 2004 (16)	p = 0.0001	p = 0.20
Grothy, 2002 in Damjanovic, 2004 (17)	p ≤ 0.0001	No significant difference was observed
Rothenberg, 2003 (18)	p < 0.0001	NR

http://dx.doi.org/10.1595/205651316X693652 *Johnson Matthey Technol. Rev.*, 2017, **61**, (1), 40–42

JOHNSON MATTHEY
TECHNOLOGY REVIEW

www.technology.matthey.com

Electron Physical Science Imaging Centre Launch Event

Highlights from the launch of the new electron Physical Science Imaging Centre (ePSIC) at Diamond Light Source

Reviewed by Dan Carter
Johnson Matthey Technology Centre, Blounts Court, Sonning Common, Reading RG4 9NH, UK

Email: dan.carter@matthey.com

An invitation-only event was held from 5th–6th September 2016 to launch the new state-of-the-art imaging facility, opened on 5th September 2016, which will see the University of Oxford, UK, Johnson Matthey Plc, UK, and Diamond Light Source, UK, in close collaboration on the study of nanoscale materials. The ePSIC is located at the Harwell Science and Innovation Campus in Oxfordshire, UK, and was officially opened by Sir John Meurig Thomas from the University of Cambridge, UK, alongside senior representatives from both Johnson Matthey and Diamond Light Source. Sir John is a world renowned expert in materials and surface chemistry, having authored over a thousand research papers, co-authored 30 patents and, in 1991, was knighted by Queen Elizabeth II for “services to chemistry and the popularisation of science” (1, 2).

ePSIC Launch Conference

The launch event was planned to coincide with an invitation-only conference in the field of microscopy and the study of novel materials at the atomic scale. Approximately 90 delegates attended from six different countries, with an even mix of academic and industrial backgrounds. The first session began with a welcome from Professor Andrew Harrison, the Chief Executive Officer of Diamond Light Source, who stated that the inauguration of this facility was the “most auspicious day since the opening of Diamond” before going on to exemplify the work at Diamond as a fruitful interface between industry and academia.

The scientific programme began with a plenary lecture from Sir John, who presented an entertaining and roughly chronological account of the evolution of electron microscopy from its early use, for example to verify Frank’s theory of crystal growth (3), through to more modern applications, touching for example on the study of zeolites in the petrochemical sector and the understanding of novel materials such as metal-organic frameworks (MOFs). Sir John’s plenary lecture was dedicated to the memory of his fellow scientist and long-time friend, Ahmed Zewail (4), an internationally renowned scientist and world expert in the field of femtosecond chemistry who died in August 2016.

Dogan Ozkaya, Senior Principal Scientist at Johnson Matthey, discussed how the company plans to benefit from its involvement in this collaboration. One of its main areas of interest is catalysis, and understanding how molecules come together and react on surfaces is a fundamental aspect of optimising existing products and designing the next generation of improved processes. Combining electron microscopy with computational

Facilities at ePSIC

The ePSIC facility features two electron microscopes which can image materials with atomic resolution down to 10–30 nm. The centre will operate in the same manner as Diamond's beamlines, being open to scientists from around the world. The beamtime and time on the microscopes are accessed *via* peer reviewed applications.

The two electron microscopes will enable researchers to see the detailed structure of materials such as catalysts (**Figure 1**), but also to take slow-motion images of reactions at an atomic scale. The new building also houses the I14 hard X-ray nanoprobe beamline, a dedicated facility for micro-nano small-angle X-ray scattering (SAXS) and nanoscale microscopy at the Diamond Light Source synchrotron. This nanoprobe can penetrate further into a material than other methods, allowing two-dimensional (2D) and three-dimensional (3D) structural analysis of catalysts down to the nanoscale. The analysis lengthscales of the microscopes and beamline are highly complementary and significant interaction between the two are expected.

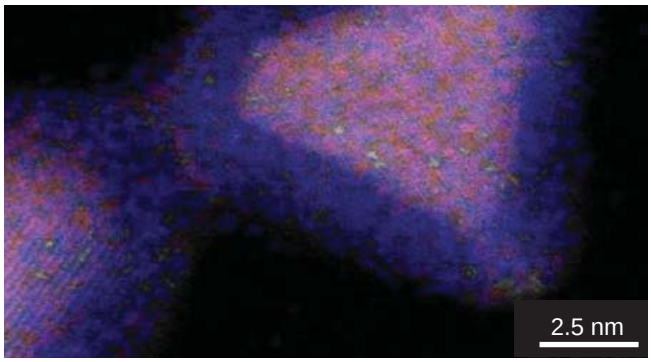

Fig. 1 The new atomic resolution microscope allows analysis down to individual atoms within materials. Image © 2016 Johnson Matthey Plc

Accompanying the two microscopes for the physical sciences will be microscopes to support research in the life sciences. Known as the electron Bio-Imaging Centre (eBIC), this centre will provide similar tools to ePSIC for cryoelectron microscopy research into biological matter such as viruses and bacteria.

techniques, such as density functional theory (DFT), can enable the visualisation of individual surface atoms and help generate an understanding of how they influence catalysis. The ePSIC is the first facility in the world with the dual capability to study samples on both an electron microscope and the hard X-ray nanoprobe beamline at the same location.

One physical occurrence during analysis using high energy electrons is the potential for energy transfer to affect the properties of the sample. Professor Jamie Warner from the University of Oxford is looking to exploit this phenomenon in his work on 2D materials. These materials have a range of potential applications, from optoelectronics and electronics through to various energy applications. Graphene is a commonly known 2D material and has been the focus of Warner's recent work (5) alongside other 2D materials such as molybdenum disulfide and tungsten disulfide. The Warner group introduces and studies defects in these 2D materials in order to understand how they affect the mechanical properties and influence deformation under loads. By selectively removing atoms to create defects in MoS_2 and WS_2 it is possible to either dope catalytically active atoms into these defects or potentially use these materials as highly selective filtration membranes. The use of electron microscopy could displace conventional techniques such as chemical exfoliation.

Professor Joachim Mayer next outlined the use of aberration corrected techniques in developing materials for energy applications. Correcting aberration is vital to achieve the necessary image resolution for microscopy at the atomic scale. One example involved the fundamental understanding of platinum-nickel and platinum-nickel-cobalt nanoparticle growth, which is key to developing catalytically active species for fuel cell applications. Aberration corrected techniques are also being applied to next-generation solar cells. Currently the maximum efficiency can reach around 28% but it is hoped new developments of layered systems, which can convert a broader wavelength range from the incident light, could increase this efficiency up to 60%. Other applications include the development of novel steel materials with the combination of high strain properties and increased hardness. The desired outcome would be to develop stronger, more lightweight materials.

Just as the use of high energy in microscopy can affect surfaces (described above) it can also affect the *in situ* measurement of reactions by imparting additional energy to the system. Nigel Browning, from Pacific Northwest National Laboratory, USA,

highlighted his work to mitigate these effects and enable the capture of highly resolved images at low energy doses using techniques such as inpainting (6). The use of mathematical techniques like this as well as Fourier transforms can allow for lower incident energy dosages, and therefore less physical interaction with the sample, while maintaining the necessary resolution to observe molecular transformations. His work on *in situ* transmission electron microscopy (TEM) is applied across many disciplines including biomedicine, batteries, materials synthesis and corrosion.

The second half of the conference programme diverged from pure microscopy to touch upon related areas of advanced characterisation techniques, including electron tomography, where John (Jianwei) Miao from the University of California, Los Angeles (UCLA), USA, pointed out that advances in this field have taken place at a faster rate than Moore's Law in terms of increased resolution. Peter van Aken from the Max Planck institute in Stuttgart, Germany, introduced his work studying the imaging of plasmonic modes of gold tapers. Quentin Ramasse of SuperSTEM, Daresbury Laboratory, UK, discussed work being carried out at the SuperSTEM project on electron energy loss spectroscopy (EELS) and the final scientific presentation from Cambridge University's Paul Midgley reviewed his group's use of analytical electron tomography for the study of superalloys.

Conclusion

The conference was formally brought to a close by Professor Angus Kirkland from the University of Oxford, followed by tours of the facilities. The ePSIC participants are looking forward to working together to exploit this unique facility. Professor Andrew Hamilton, Vice-Chancellor of Oxford University, said:

> "Bringing together these powerful instruments in one place will be hugely beneficial to researchers, both in academia and industry, who are studying materials at the atomic scale. This new facility could lead to advances in many exciting research areas including graphene technology and the development of cleaner, greener fuels." (7)

References

1. 'Curriculum Vitae, Awards and Honours, Professor Sir John Meurig Thomas', VIII.11, Electron Microscopy Group, Department of Materials Science & Metallurgy, University of Cambridge, UK: http://www-hrem.msm.cam.ac.uk/people/thomas/CV5.pdf (Accessed on 31st October 2016)
2. *The London Gazette (Suppl.)*, No. 52563, 14th June, 1991, B2
3. K. Wada, *Nature*, 1966, **211**, (5056), 1427
4. J. Meurig Thomas, 'Ahmed Zewail Obituary', *The Guardian*, Monday 22nd August, 2016
5. J. H. Warner, E. R. Margine, M. Mukai, A. W. Robertson, F. Giustino and A. I. Kirkland, *Science*, 2012, **337**, (6091), 209
6. A. Stevens, H. Yang, L. Carin, I. Arslan and N. D. Browning, *Microscopy (Tokyo)*, 2014, **63**, (1), 41
7. Science, Integrated Facilities, ePSIC, Facility Partners: http://www.diamond.ac.uk/Science/Integrated-facilities/ePSIC/Facility-Partners.html (Accessed on 3rd November 2016)

The Reviewer

Dan Carter has a PhD in Inorganic Chemistry from the University of Nottingham, UK. He currently manages Johnson Matthey's in-house team of information analysts who support the company's business activities through provision of information and expert searches. This work can range from providing commercial insight to analysing technology platforms or patents and supporting research and development. The team also publishes *Johnson Matthey Technology Review*.

http://dx.doi.org/10.1595/205651317X693868 *Johnson Matthey Technol. Rev.*, 2017, **61**, (1), 43–46

JOHNSON MATTHEY
TECHNOLOGY REVIEW

www.technology.matthey.com

“Surgical Tools and Medical Devices” 2nd Edition

Edited by Waqar Ahmed (University of Central Lancashire, UK) and Mark J. Jackson (Kansas State University, USA), Springer International Publishing, Switzerland, 2016, 691 pages, ISBN: 978-3-319-33487-5, £163.00, €227.76, US$249.00

Reviewed by Alexander Hoppe
Johnson Matthey Advanced Glass Technologies, Fregatweg 38, 6222 NZ Maastricht, The Netherlands

Email: alexander.hoppe@matthey.com

Introduction

“Surgical Tools and Medical Devices” 2nd Edition provides a comprehensive overview containing 23 chapters written by experts in each field. The chapters are not grouped together according to specific topics, but rather each chapter covers a range of aspects of surgical tools, medical device manufacturing and characterisation, surface engineering and interactions between biomaterials and cells. Besides materials science and technology aspects the reader will find information on biological performance and interactions of cells with items such as carbon-based medical devices and bone graft materials.

While the book does not have a specific application focus, cardiovascular devices seem to get slightly more attention with a dedicated chapter (Chapter 5 ‘Cardiovascular Interventional and Implantable Devices’) and several chapters on related topics, for example surface engineering, diamond like carbon (DLC) coatings and cell-cell interactions of carbon based materials, which are particularly relevant for cardiovascular applications.

The overall theme of the book lies in surface engineering and coatings, aimed at covering recent developments in nanotechnology including nanocoatings and nanostructuring of biomedical devices. The goal of the book is to provide scope for future advances in the field, combining nanomaterials and nanotechnologies with the development of biomedical devices and tools.

Medical devices discussed in this book mainly relate to non-resorbable materials, like titanium based alloys and nanoengineering of their surfaces. Hence, readers looking for information on bioactive, resorbable bone grafts and devices might fall short on expectations. Only a single chapter covers resorbable bone-like grafts.

As the book is a comprehensive overview on a broad variety of topics this review will include only selected chapters related to the reviewer’s fields of interest.

Anodisation of Titanium Based Alloys

Chapter 2 by Thomas Webster and Chang Yao (Brown University, USA) describes anodisation and nanostructuring of Ti alloys which is an approach to improve the biocompatibility of Ti-based implant

materials. Nanostructured Ti surfaces have been shown to improve the adhesion of relevant cell types involved in osseointegration of metal implants. Anodisation can be used to create nanoscale roughness or nanotubes on Ti surfaces. By controlling the type of electrolyte (for instance sulfuric acid, sodium hydroxide or hydrogen fluoride) and the process parameters like voltage, current density, pH and temperature, the size and morphology of surface nanostructures can be adjusted. The authors give an overview of available studies reporting on nanostructures ranging from nanopores, high aspect ratio nanotubes and regular nano void arrays which can be achieved through tailoring the process parameters and electrolyte type. **Figure 1** shows examples of nanotube morphologies obtained through anodisation of Ti surfaces.

The chapter also provides an overview of selected *in vitro* studies on cell compatibility of nanostructured Ti surfaces. Generally, nanostructured surfaces obtained through anodisation show improved cell adhesion and cell proliferation behaviour which can be attributed to the nano topography corresponding to the exact dimensions for the cell attachment mechanism provided through integrin molecules.

Regarding future directions, the authors suggest that Ti surfaces should have roughness and structuring on all scales ranging from macro to nano which could be achieved through a combination of mechanical grinding and anodisation steps. Furthermore, anodisation could be used as a tool for incorporating drug delivery capabilities into Ti based surfaces by using the nano topography as a reservoir for chemical signalling molecules like bone morphogenetic proteins (BMPs) to stimulate bone regeneration.

Corrosion Behaviour of Nitinol

Chapter 4 by Frank Placido *et al.* (University of Paisley, Scotland, UK) describes a particular study on the influence of surface finish on corrosion behaviour of nitinol. Beside concerns on biocompatibility which is a basic requirement of biomaterials, metals bear the additional risk of corrosion when exposed to the physiological environment. The authors evaluated the influence of different surface finishes, for example those created by chemical etching and mechanical polishing, on the corrosion of nitinol. The corrosion test was performed in 0.9% saline solution and was evaluated in terms of electrochemical potential, open circuit potential (OCP), corrosion pits and current density measurements. The authors showed that chemically etched nitinol wires were most stable (compared to untreated reference and mechanically etched wires) with the highest corrosion potential, a low corrosion rate and a low corrosion current. Additionally, pitting corrosion behaviour was evaluated based on anodic polarisation treatment of the differently treated wires and a ‘pitting potential’ as well as a ‘passivation potential’ were determined. It has been shown that the values for the ‘pitting potential’ and the ‘passivation behaviour’ were closer for the chemically etched wires indicating lower susceptibility to pitting

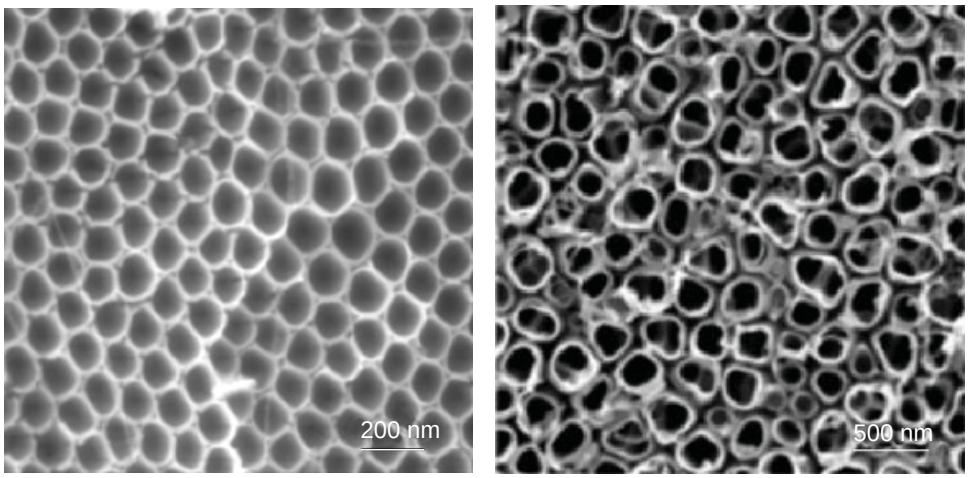

Fig. 1. Examples of nanotube morphologies formed on Ti using anodisation under different process conditions varying the electrolyte type (1)

corrosion. This observation was confirmed through electron microscopic evaluation showing severe pitting corrosion attack accompanied by crack formation on the mechanically treated sample while the chemically etched sampled seemed to be almost unaffected by the anodic treatment. Overall, the authors concluded chemical etching to be a suitable technique to provide enhanced corrosion protection to nitinol materials exposed to corrosive saline environments.

Interventional and Implantable Devices

Chapter 5 by Michael Whitt (California State Polytechnic University, USA) *et al.* gives an overview of generic materials requirements for cardiovascular applications and gives examples of currently used materials and devices. For interventional devices (typically guiding catheters and guiding wires) two most critical parameters are 'track ability' (ease of tracking the device up to the target lesion) and 'push ability' (ability to advance the device across the lesion) which are challenging to measure *in vitro*. Friction can be improved by using hydrophilic coatings as well as hydrophobic coatings like silicon or polytetrafluoroethylene (PTFE) which act as lubricants.

Implantable devices include mechanical (stents) and electrical devices (pacemakers). The main concerns for permanently implanted devices are related to potential thrombus formation (clogging) and blood compatibility (haemocompatibility). Hence, for implantable devices surface properties are key for minimising thrombose risk targeting reduced coagulation, platelet adhesion and platelet activation. In this chapter the reader will find fundamental aspects of thrombus formation and blood cell physiology. For example, a relationship between the haemocompatibility of a material and its electronic structure has been proposed which is based on the theory that fibrinogen denatures (which initiates the cascade reaction leading to thrombus formation) upon electron exchange with an artificial material surface. Hence, the scope for development of haemocompatible implants is targeting materials with semiconducting properties with a band gap of greater than 1.8 eV which is associated with the band gap of fibrinogen (which can be described as a semiconducting material).

Nature's most haemocompatible surface is the endothelium, a thin layer of flat cells lining the interior of blood vessels which, under normal circumstances, prevent blood clogging and allow smooth blood flow. Consequently, a logical and promising approach to increase a material's haemocompatibility is to seed the graft material with endothelial cells prior to implantation. In this context, the compatibility of a graft material with endothelial cells, affecting properties such as their adhesion and proliferation, is essential for adequate performance of cardiovascular device materials. Endothelial cell adhesion on an artificial surface involves distinct molecular interactions which need to be carefully controlled in order to enable confluent cell layer formation, avoiding shear stress and possible complications.

Surface properties of biomaterials are essential for the performance of biomedical devices since the outermost surface (a few atomic layers) are crucial for their interfacial interaction *in vivo*. Surface modifications are widely proposed in order to improve the biocompatibility of material surfaces used for cardiovascular applications.

Surface Engineering of Cardiovascular Devices using Diamond Like Carbon (DLC)

Chapter 6 by Nasar Ali (University of Aveiro, Portugal) *et al.* elaborates on surface compatibility of cardiovascular device materials, describing surface engineering approaches for improving materials biocompatibility based on DLC. DLC coatings are used on prosthetic heart valves since they are chemically inert, hard, wear resistant and biocompatible. It has been shown that DLC reduces platelet adhesion compared to Ti surfaces hence being more haemocompatible. *In vitro* studies have shown reduced platelet adhesion on DLC compared to Ti, TiN and TiC. Typically, no platelet activation, clotting of platelets or thrombus formation are observed on DLC coatings which can be related to a higher ratio of albumin and fibrinogen observed on the DLC coatings.

DLC coatings can also be modified through doping with chromium or silicon. Doping of DLC with silicon has been shown to improve the vitality of endothelial cells and it has been shown that Cr-doped DLC coatings yielded higher endothelial cell attachment. Based on Raman spectroscopy and evaluation of intensities for the D and G graphitic bands, the authors suggest that disordered graphitic phases present in the DLC are responsible for improved endothelial cell viability on Cr-doped DLC coatings.

The interactions of biological entities, for example cells and proteins, with artificial surfaces is key for understanding the performance of biomedical devices.

The book includes a chapter (Chapter 11) dedicated to this topic, exploring the fundamentals of interaction between cell biology and materials which can be greatly appreciated by the reader with an engineering background. The chapter provides a comprehensive overview on material cell interactions in surface engineered carbon based biomedical materials, describing the key aspects dictating the biological response to artificial material surfaces including interactions with proteins, various human cell types and bacteria. As such, this chapter gives scope for the development of suitable materials specifically for cardiovascular applications.

Despite significant advances in the mechanical properties of stents and in implant techniques and antithrombotic therapies, the use of stents and heart valves is still complicated by substantial cases of thrombotic occlusions, stenosis and restenosis. Beyond that mechanical failure, wear or debris, oxidation and corrosion can cause failure of biomedical devices.

Conclusion

Overall, the book is a good overview on materials and surface engineering technologies used for biomedical devices and surgical tools. While it is a comprehensive compilation, as a consequence it remains somewhat superficial regarding technical discussion of specific technologies and materials. However, the book will provide a high level introduction to biomedical devices, biomaterials and biomedical surface engineering. Hence, the book is particularly recommended for (bio) materials researchers and technologists who are interested in an overview and an introduction into the field of biomedical devices, especially in the field of cardiovascular applications. Specialists in biomedical device manufacturing might find less of interest, although they may find use in the comprehensive overview and detailed up to date reference content which will provide scope for expanded research on each topic.

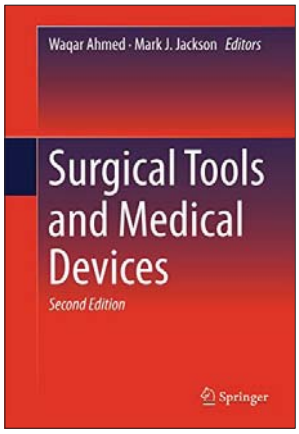

"Surgical Tools and Medical Devices"

Reference

1. X. Zhao, Y. Zhu, Y. Wang, L. Zhu, L. Yang and Z. Sha, *J. Nanomater.*, 2015, 104193

The Reviewer

Alexander Hoppe is Research and Development (R&D) Senior Scientist at Johnson Matthey Advanced Glass Technologies, The Netherlands. His areas of expertise cover materials for biomedical applications, in particular bioglasses and bioceramics, as well as biocompatibility and surface functionalisation.

http://dx.doi.org/10.1595/205651317X693732 *Johnson Matthey Technol. Rev.*, 2017, **61**, (1), 47–51

JOHNSON MATTHEY
TECHNOLOGY REVIEW

www.technology.matthey.com

Durability and Degradation Issues in PEM Electrolysis Cells and its Components

The second international workshop organised by the NOVEL EU-funded programme

Reviewed by Emily Price
Johnson Matthey Technology Centre, Blounts Court, Sonning Common, Reading RG4 9NH, UK

Email: emily.price@matthey.com

The second workshop on "Durability and Degradation Issues in PEM Electrolysis Cells and its Components" was held at Fraunhofer-Institut für Solare Energiesysteme ISE in Freiburg, Germany, from 16th–17th February 2016. The workshop was organised as part of the European Union (EU)-funded 7th Framework Programme, NOVEL, of which project Johnson Matthey Fuel Cells is a partner, along with several other European companies and research institutions. The workshop was attended by over 100 people from all around the world; however, the majority came from Germany.

The talks were given by several NOVEL partners, electrolysis system manufacturers and research institutions or universities, and were followed by short question and answer sessions (**Figure 1**). The presentations described here can be freely accessed on the workshop web page (1).

Polymer Electrolyte Membrane

Magnus Thomassen (SINTEF, Norway) headed up the NOVEL talks, introducing the audience to the project and its main targets and achievements. NOVEL has focused on all areas necessary for improving the performance and reducing the cost of polymer electrolyte membrane (PEM) electrolysis, including degradation protocols, novel membranes and catalysts, bipolar plates and stack testing.

Lorenz Gubler (Paul Scherrer Institut (PSI), Switzerland) spoke to the audience about NOVEL's work on novel membranes for PEM water electrolysis. There is a resistance-gas crossover 'trade-off' with electrolysis membranes, which means that the operational range can be limited. NOVEL has focused on increasing the gas barrier properties of electrolysis membranes and has taken two approaches within the project. The first approach is PSI's radiation grafted membrane, comprising chemically and mechanically robust polymers (such as ethylene tetrafluoroethylene (ETFE) or ethylene chlorotrifluoroethylene (ECTFE)) grafted with a styrenic monomer, which is later sulfonated, a co-monomer and a cross-linker (2). The radiation grafted membrane gave similar performance to Nafion® 117 membrane, but lowered the gas

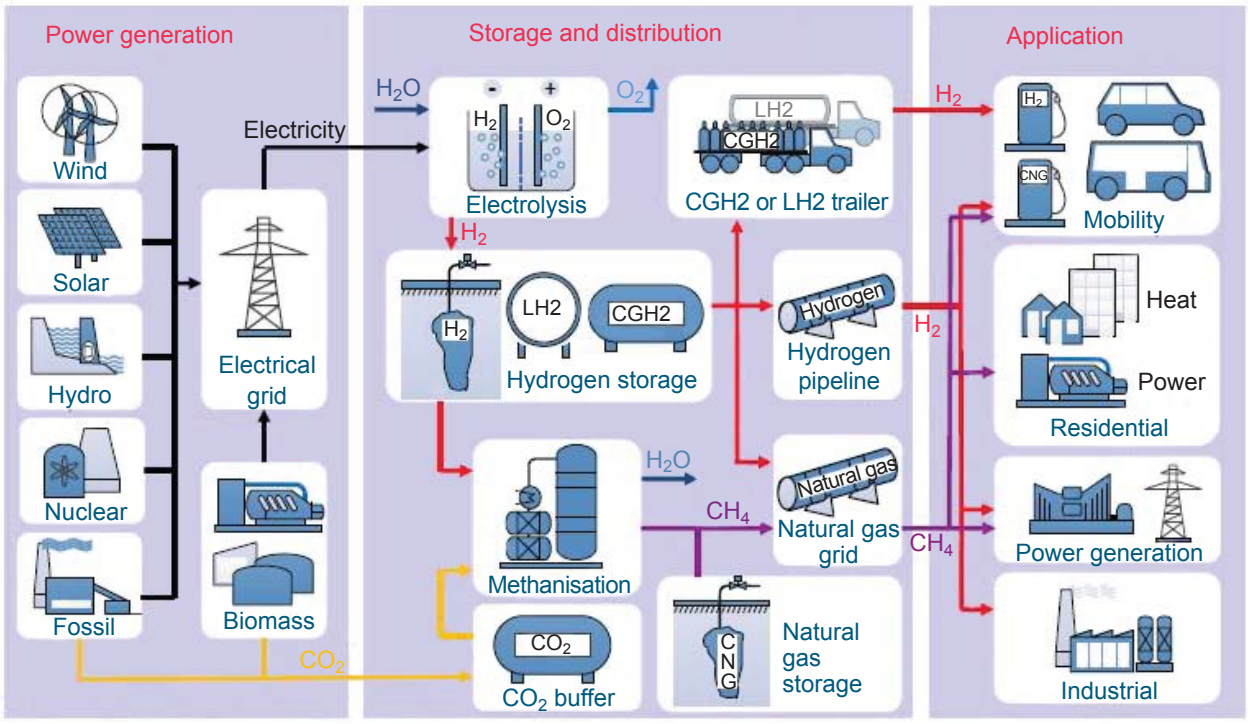

Fig. 1. Why hydrogen? Hydrogen is an energy carrier able to facilitate decarbonisation of the energy system. Coupling renewable energies and hydrogen, new market opportunities for electrolysis (Reproduced from (1) with kind permission from Tom Smolinka, Fraunhofer ISE)

crossover by ~50%, as demonstrated in **Figure 2(a)**. NOVEL's alternative membrane approach is Johnson Matthey's reinforced polyfluorosulfonic acid (PFSA) membrane, which is adapted from an automotive membrane, measures just 60 µm in thickness and has functionality included within it that reduces hydrogen crossover. The effect of the addition of recombination catalyst functionality is shown in **Figure 2(b)**.

Georg Andreas (Fraunhofer ISE) summarised the ongoing work within NOVEL by both Fraunhofer ISE and Teer Coatings Ltd, Miba Coatings Group, UK, on coatings for bipolar plates and current collectors. Titanium is frequently used for electrolyser bipolar plates and current collectors, but when left uncoated, it can form a highly resistive oxide passivation layer. The thickness of the passivation layer can be estimated by its colour. Protective coatings are recommended for use on these parts to prevent the growth of the passivation layer and to prevent drops in conductivity and cell efficiency. Sputtered coatings from Teer Coatings Ltd, Miba Coatings Group have been shown to decrease the contact resistance both before and after corrosion testing.

Membrane Electrode Assembly

Frederic Fouda-Onana (French Alternative Energies and Atomic Energy Commission (CEA), France) talked about the accelerated stress tests designed by CEA to test the NOVEL membrane electrode assemblies (MEA). Historically, there have been fewer research activities aimed at shedding light on durability and degradation in PEM electrolysers than fuel cells. It is believed that most of the cell components of a PEM electrolyser will degrade i.e. the anode and cathode catalyst layers, the membrane and the bipolar plates. Four accelerated stress test (AST) protocols were devised by CEA to focus on different causes of degradation and contributing factors. Ageing was found to be more prominent at high current density due to the increased resistance and higher efficiency losses. AST protocols were also shown to have a number of effects depending on which one was used: membrane thinning, electrode degradation, fluoride transfer from membrane to cathode (3) and increased resistance were all observed.

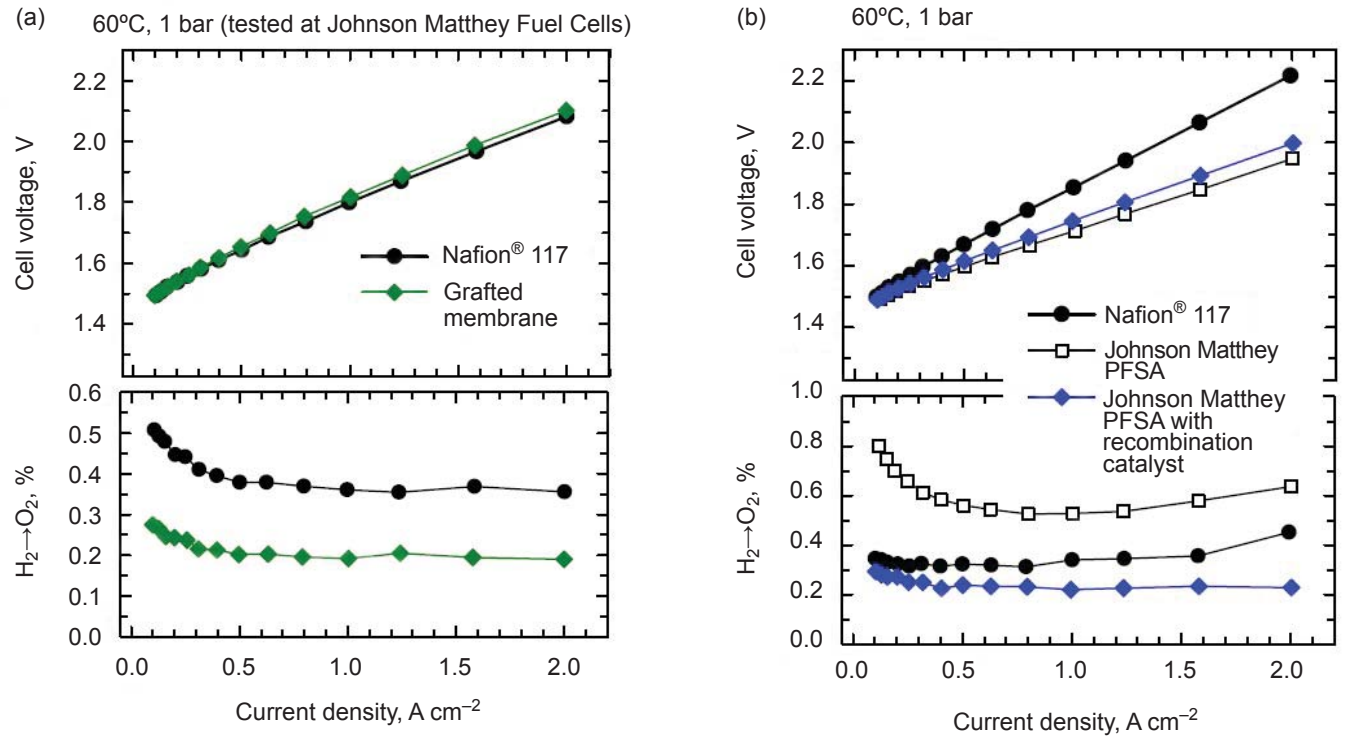

Fig. 2. (a) Cell performance and gas crossover data showing PSI's radiation grafted membrane; (b) cell performance and gas crossover data showing Johnson Matthey Fuel Cells' PFSA membrane with and without recombination catalyst functionality (Reproduced from (1) with kind permission from Lorenz Gubler)

Ed Wright (Johnson Matthey Technology Centre, Sonning Common, UK) spoke about Johnson Matthey Fuel Cells' work on the link between non-uniformity in PEM electrolysis MEAs and high gas crossover. Higher gas crossover was observed with novel anode catalysts and lower loading or thinner anode catalyst layers (**Figure 3**). The effect is believed to be more of a problem with newer, thinner membranes, as they will reduce the ability of the catalyst coated membrane (CCM) to cope with hardware non-uniformity; uneven compression for example. Johnson Matthey Fuel Cells found that hydrogen crossover can be controlled by using thicker or more compressible cathode layers, which are believed to improve tolerance to non-uniformity issues (**Figure 3**).

Moving on to non-NOVEL talks, Tomás Klicpera (Functional Membranes and Plant Technology (FuMA-TECH BWT GmBH, Germany)) presented an overview of the different membranes that FuMA-Tech have available for PEM water electrolysis. Its membranes can swell significantly in the *z*-direction by up to 40% and are very sensitive to cell assembly. Furthermore, it has had to work through performance problems with its membranes – membranes giving bad performance for one customer have been found to give excellent performance for another customer. Klicpera finished off by stating that FuMA-Tech believe that a simpler membrane, such as a woven web reinforced membrane, is a better choice for PEM water electrolysis.

Insights into PEM electrolysis capabilities and requirements at the larger stack-level were provided by National Renewable Energy Laboratory (NREL), USA, and the electrolysis system manufacturer, Proton OnSite, USA. Kevin Harrison (NREL) introduced us

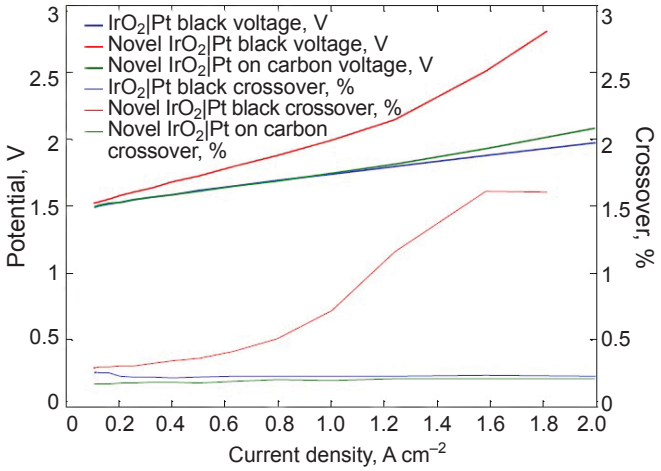

Fig. 3. The effect of both thinner, novel anode layers and thicker, more compressible cathode layers on cell performance and gas crossover, as demonstrated by Johnson Matthey Fuel Cells

to NREL's goal of integrating its renewable hydrogen system to provide support to the grid and to reduce the cost of hydrogen. NREL is currently producing around 50 kg of hydrogen per day, which it intends to double by the end of 2016. It compresses and stores its hydrogen for lab use as well as for fuelling fork lifts and buses, and will produce a 250 kW stack this year.

Proton OnSite has been working with hydrogen energy systems for 20 years and has racked up hundreds of thousands of hours worth of stack testing and data. Everett Anderson (Proton OnSite) stated that it has achieved ~60,000 hours lifetime in its commercial stacks without any detected voltage decay. With its megawatt-scale M-series stack demonstration, it has recently achieved over 500,000 cumulative stack cell testing hours without failures and without any loss in efficiency. Its biggest problem affecting reliability and durability is customer contamination. Anderson stated that Proton OnSite is interested in finding reliable accelerated stress tests to understand the degradation mechanisms of polymer electrolyte membrane water electrolyser (PEMWE) and to shorten development times.

Catalysis

Marcelo Carmo (Forschungszentrum Jülich (FZJ), Germany) spoke about his work on both anode and cathode catalysts for PEMWE and their degradation. Pt_xM_y alloy cathode catalysts (M = cobalt, iron, nickel, bismuth) were de-alloyed *via* acid leaching and compared with standard platinum/carbon. The cathodes were durability tested by cycling for one week in 0.5 M sulfuric acid at 60ºC. FZJ did not observe a difference in durability and performance between cathodes of loading 0.8 mg Pt cm^{-2} and cathodes of loading 0.05 mg Pt cm^{-2}. Additionally, a benchmark iridium black catalyst was used for an anode loading study. Initial performance at a low loading, for example, 0.3–0.6 mg Ir cm^{-2} was similar to initial performance at a high loading, for example, 2.25 mg Ir cm^{-2}. However, the extent of degradation experienced with lower anode loadings was larger than that experienced with higher anode loadings. Carmo recommended that if low anode loadings are to be utilised for PEMWE, then anode supports are required otherwise the layers are too thin to be durable due to low catalyst areas.

Antonino Aricò (Consiglio Nazionale delle Ricerche (CNR)-Instituo di Tecnologie Avanzate per l'Energia (ITAE), Italy) summarised work on degradation mechanisms and low catalyst loadings during the Fuel Cells and Hydrogen Joint Undertaking funded project, ElectroHypem. CNR-ITAE studied MEAs comprising of an $IrRuO_x$ anode, a Pt/C cathode and an Aquivion® membrane (4). The contributing factors to PEM electrolysis performance degradation were found to be: accumulation of Na and Fe in the catalyst; loss of Ru from $IrRuO_x$ anode; degradation of the Ti plates; membrane thinning and restructuring. Aricò suggested mitigation of degradation *via* pre-leaching of catalysts in acid to remove impurities; Ir surface enrichment of the anode catalyst; chemical stabilisation of the membrane and in agreement with NOVEL findings, coating of Ti plates. Similar to Carmo's work, it was found that a reduced total catalyst loading resulted in an increased degradation rate.

Conclusion

The workshop provided an excellent opportunity for review and discussion of the growing area of PEM water electrolysis and was well attended by a range of international researchers. PEM water electrolysis was shown to be a promising area of research that is steadily growing in an effort to provide a fossil-free source of hydrogen. The workshop also provided an opportunity for consortium members of the EU-funded programme, NOVEL, to summarise their progress and achievements within the field before the end of the project. The success of the workshop can be attributed to the large range of topics presented, the variety of speakers and the organisation of Tom Smolinka and Magnus Thomassen.

References

1. NOVEL, Novel materials and system designs for low cost, efficient and durable PEM electrolysers, Second international workshop on durability and degradation issues in PEM electrolysis cells and its components, Presentations: https://www.sintef.no/projectweb/novel/news-and-events/second-international-workshop-on-durabiltiy-and-de/presentations/ (Accessed on 2nd November 2016)
2. L. Gubler, *Adv. Energy Mater.*, 2014, **4**, (3), 1300827
3. M. Chandesris, V. Médeau, N. Guillet, S. Chelghoum, G. Thoby and F. Fouda-Onana, *Int. J. Hydrogen Energy*, 2015, **40**, (3), 1353
4. S. Siracusano, N. Van Dijk, E. Payne-Johnson, V. Baglio and A. S. Aricò, *Appl. Catal. B: Environ.*, 2015, **164**, 488

The Reviewer

Emily Price is a research scientist at Johnson Matthey Technology Centre, Sonning Common, UK. She has a Masters degree in Chemistry from Cardiff University, UK, and joined Johnson Matthey in 2011. She worked for four years in the Fuel Cells Research group on direct ethanol fuel cells, direct methanol fuel cells and PEM water electrolysis. Since April 2016, she has worked in the Emissions Control Research group. Her current area of research is focused on gasoline particulate filters with low platinum group metal content.

http://dx.doi.org/10.1595/205651317X693624 *Johnson Matthey Technol. Rev.*, 2017, **61**, (1), 52–59

JOHNSON MATTHEY
TECHNOLOGY REVIEW

www.technology.matthey.com

Platinum Group Metal Compounds in Cancer Chemotherapy

An overview of the history and the potential of anticancer pgm compounds

By Christopher Barnard
Stoke Row, Oxfordshire, UK

Email: cfj.barnard@yahoo.co.uk

It was some 50 years ago that Barnett Rosenberg and coworkers published their studies on unusual patterns of bacterial growth that led to the identification of platinum compounds as highly effective agents against some cancers, particularly those of genitourinary origin. This sparked a renewed interest around the world in the potential of metal compounds as small molecule therapeutic agents. Some of that history, particularly related to the platinum group metals (pgm) platinum and ruthenium, is described in this overview.

The First Drug – Cisplatin

The application of platinum compounds in cancer therapy was one of the most unexpected developments in pharmaceuticals in the last 50 years. Many reviews have been published previously on this topic; in this journal the most recent being by Reedijk in 2008 (1).

The potential of platinum compounds was discovered by Rosenberg in 1965 (2). He had recently taken up an interdisciplinary post as Professor of Biophysics at Michigan State University, USA. Coming from a physics background with little experience in biological sciences one of his early experiments was to study the effect of electromagnetic fields on cell division. In a fortunate combination of circumstances, he conducted a test experiment with platinum electrodes, an ammoniacal medium and *Escherichia coli* as the test organism. He observed unusual filamentous growth that he was later able to attribute to the formation of soluble platinum ammine complexes. After further study he approached the National Cancer Institute (NCI), USA, to demonstrate whether the key compound, *cis*-$PtCl_2(NH_3)_2$, could also affect the growth of cancer cells. The activity was significant and encouraged the NCI to support the clinical evaluation of cisplatin, as this compound came to be known (3). The action of cisplatin was subsequently determined to arise from its interaction with deoxyribonucleic acid (DNA), in particular forming intrastrand cross-links between neighbouring guanosine residues. Over many years much effort was put into studying the detail of this lesion and its interactions with proteins which might mediate the cell death process (4, 5).

Early clinical results were variable, with occasional patients showing very positive results while others encountered marked toxic effects such as kidney and nerve damage. While these side effects remained uncontrolled there seemed little likelihood of cisplatin achieving regulatory approval, but fortunately a new administration procedure involving pre- and post-hydration significantly reduced the kidney toxicity (but did not eliminate it) (6). This allowed somewhat higher doses to be given to patients with acceptable

toxic risk and pronounced activity in genitourinary cancers (particularly testicular and ovarian cancer) was observed. On this basis, the NCI and Research Corporation (on behalf of Michigan State University) licensed the marketing of cisplatin (**Figure 1**) to Bristol-Myers, USA, with marketing approval being gained in the USA in 1978 and many other countries, including the UK, the following year.

Second Generation – Carboplatin

To raise support for his continuing work at Michigan State University and promote interest in his discovery Professor Rosenberg toured and corresponded widely. This included contact with the platinum companies Rustenburg Platinum Mines Ltd, South Africa (pgm mining and supply), and Engelhard Corp, USA, and Johnson Matthey Plc, UK (both specialised in pgm marketing). To obtain a better understanding of this technology Johnson Matthey and Engelhard sent postgraduate researchers, Michael Cleare and James Hoeschele respectively, to work in Professor Rosenberg's research group. Cleare decided to study the structure-activity relationships of platinum complexes, resulting in the synthesis of various pgm complexes and a series of publications describing this work (see, for example (7–9)). On returning to the UK, Cleare, with Rustenburg's support, coordinated the exchange of results between a number of researchers interested in the new field. After the marketing of cisplatin, he was instrumental in linking Bristol-Myers, Johnson Matthey and the Institute of Cancer Research (ICR), UK, to identify a second generation alternative to cisplatin. The aim of the programme was to increase the therapeutic potential of the drug either by decreasing the toxicity, particularly kidney toxicity, associated with its use or by increasing the potency and thus effectiveness at lower doses.

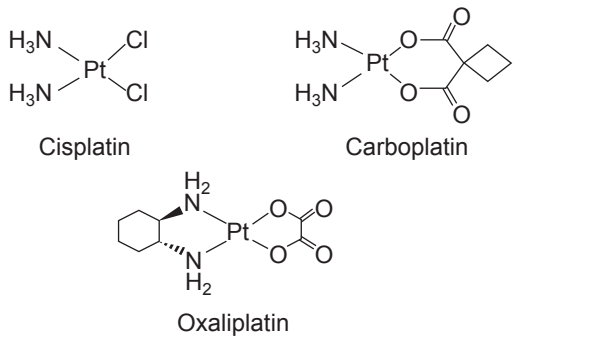

Fig. 1. Globally marketed platinum-containing drugs

Ultimately, it was the former of these targets which proved easier to achieve. From the compounds originally synthesised at Michigan State University by Cleare, diammine-1,1-cyclobutanedicarboxylatoplatinum(II), carboplatin (**Figure 1**), was found by the ICR to have the best balance of antitumour activity and low toxicity for taking forward to clinical trials (10). Due to the close links between the ICR and the Royal Marsden Hospital, London, UK, with the support of Bristol-Myers, the compound was progressed rapidly through clinical trials and granted its first marketing approval for treating ovarian cancer in 1986.

Other Second Generation Compounds – Oxaliplatin

Bristol-Myers and Johnson Matthey investigated another second generation compound, iproplatin (JM-9, **Figure 2**), in this case with the pre-clinical studies being carried out by the Roswell Park Cancer Institute, USA, in addition to work at ICR (11). In clinical trials this drug had similar activity to carboplatin but toxicities proved more difficult to control (12). Bristol-Myers also pursued the development of spiroplatin (TNO-6, **Figure 2**) a compound synthesised at the Dutch Institute of Applied Chemistry, Nederlandse Organisatie Voor Toegepast Natuurwetenschappelijk Onderzoek (TNO), The Netherlands. In this case problems were encountered with kidney toxicity and limited activity (13). Therefore, Bristol-Myers chose to concentrate its further efforts on gaining marketing approval for carboplatin.

A significant number of compounds were investigated in early stage clinical trials by other organisations, both commercial and academic (12, 14). Some examples are given in **Figure 2**. Some of these gained local market approval including nedaplatin (Aqupla™, 254-S), Shionogi Pharmaceuticals, Japan; lobaplatin, Asta Medica, China; heptaplatin (eptaplatin), SK Chemicals Life Sciences, Korea, see **Figure 3**. However, one compound that has achieved widespread use is oxaliplatin (**Figure 1**). This compound incorporates the 1,2-diaminocyclohexane ligand that was favoured in early studies by the NCI, the same ligand being incorporated into JM-82 ((1,2-diaminocyclohexane)(trimellitic acid)platinum(II)) and tetraplatin (ormaplatin, **Figure 2**) which entered clinical trials but were not marketed. Oxaliplatin (named as *l*-OHP) was first reported by Kidani and Mathé (15) who initiated clinical trials (16). Development was continued by Debiopharm Group™, a small Swiss company, with

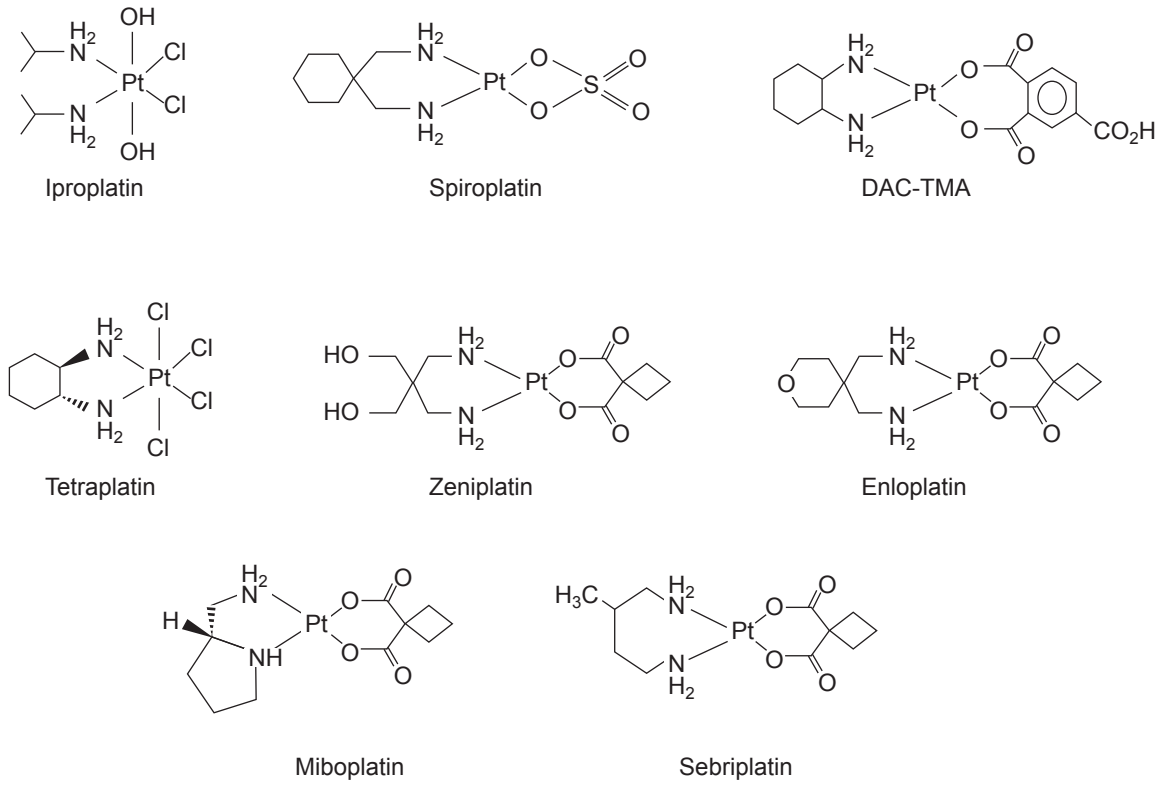

Fig. 2. Second generation platinum compounds evaluated in clinical trials

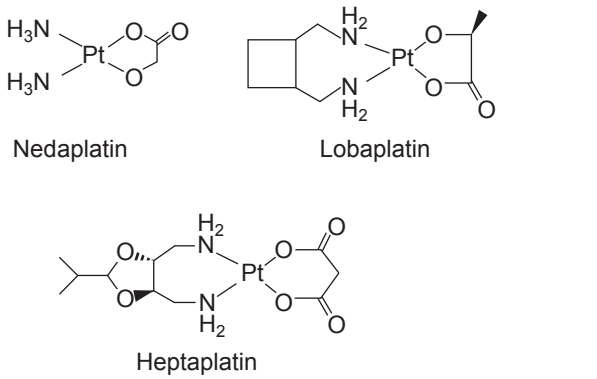

Fig. 3. Regionally marketed platinum-containing drugs

clinicians conducting a number of trials to find the best administration schedule that would maximise the activity while controlling the toxicity. Pre-clinical testing in mice had shown that toxicities could be reduced when the drug was given with circadian periodicity (17). By appropriate scheduling of administration in patients (chronotherapy) it was found that toxicities, such as neutropenia and paraesthesia, were less frequent and improved responses were seen in colon cancer when used together with 5-fluorouracil (18). The drug was then licensed to Sanofi, France, for marketing worldwide with the major indications being adjuvant and metastatic colorectal cancers.

Third Generation – Satraplatin

Following the success of their collaboration on carboplatin, Johnson Matthey, ICR and Bristol-Myers Squibb (following their merger) reviewed their options for further developments in this field. Two targets were identified; firstly, to adapt the platinum agents to provide an orally administered drug as an alternative to the intravenously injectable cisplatin and carboplatin and, secondly, to achieve activity in tumours which were resistant, or had acquired resistance, to cisplatin. Significant progress on the first target came when Giandomenico described versatile routes for converting platinum(IV) hydroxido complexes to their carboxylate counterparts (19). Selecting a compound for clinical trials required careful judgement on balancing the antitumour activity with emetic potential. The compound selected was *cis*-ammine(cyclohexylamine)-*cis*-dichlorido-*trans*(diacetato)platinum(IV), satraplatin (JM-216, **Figure 4**) (20). After some years of clinical trials on hormone resistant prostate cancer, it was determined that the compound did not result in significant life

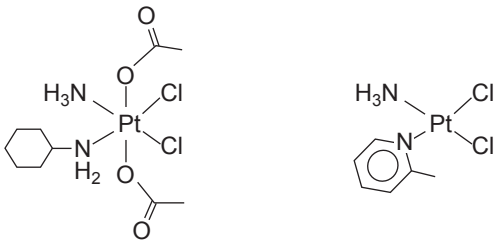

Fig. 4. Third generation platinum compounds

extension for patients and the development was abandoned (21).

Third Generation – Picoplatin

The compound chosen for clinical trials to study the question of activity in cisplatin resistant tumours was *cis*-ammine(2-methylpyridine)dichloridoplatinum(II), picoplatin (**Figure 4**) (22). The 2-methylpyridine ligand reduces the interaction of the complex with strongly binding ligands in an associative ligand substitution pathway. This is important in reducing the likelihood of interaction of the complex with sulfur donors, such as glutathione, which might deactivate the compound (23). Licenses for developing this compound were granted to a number of companies after Bristol-Myers Squibb withdrew from the programme, but none of the trials revealed sufficient activity to warrant marketing approval (21).

'Unconventional' Platinum Compounds

Other options for identifying useful activity were also explored by several groups, in particular through searching for activity outside the spectrum displayed by cisplatin compounds defined by the early structure-activity rules established by Cleare (7). These empirically determined 'rules' identified neutral complexes with *cis* configuration, two am(m)ine or one bidentate chelating diamine carrier ligands and two ligands that could be replaced for subsequent binding to DNA as showing much greater anticancer activity than related complexes. However, with careful choice of compounds it has been shown that most of these 'rules' can be overcome to produce potent compounds. For example, although *trans*-$PtCl_2(NH_3)_2$ is inactive compared with cisplatin, other *trans* compounds such as JM-335 (24–27) or those containing planar organic ligands (28) (see **Figure 5**) do show significant

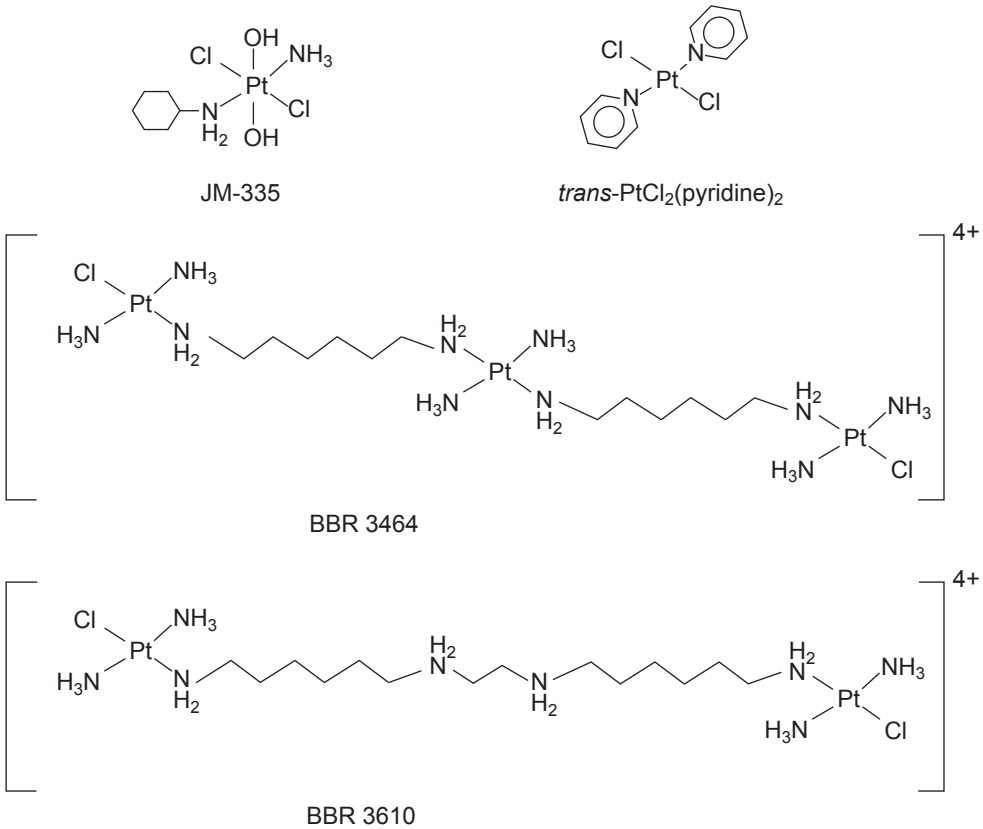

Fig. 5. 'Unconventional' platinum anticancer compounds

activity. However, results from testing cisplatin-resistant xenograft tumours were not sufficiently encouraging for these compounds to be taken forward to clinical study. Dinuclear or oligonuclear complexes of platinum can form different lesions on DNA compared to monomeric cisplatin and this is another area that has been investigated (29). Of particular interest in this regard is the ionic trinuclear complex BBR3464 (**Figure 5**) (30). This compound was developed for clinical trials by Boehringer Mannheim Italia, Italy, but again the level of activity was not sufficient to justify large scale phase III trials (31, 32).

Ruthenium Compounds

As it became increasingly apparent that an immense effort would be required to identify a platinum compound with improved therapeutic properties over cisplatin, carboplatin and oxaliplatin, so many researchers turned to other metals to open up new avenues to identifying compounds which might offer activity where cisplatin was ineffective. Ruthenium complexes were among the first suggested for detailed study (33) and a number of different compounds have been followed up. Early studies of a wide range of metal complexes identified ruthenium dimethylsulfoxide (DMSO) complexes, both *cis*- and *trans*-[$RuCl_4(DMSO)_2$], as being of interest (34). Ruthenium oxidation states II, III and IV are stable in water in various complexes. Ruthenium(III) complexes are relatively inert to substitution compared with ruthenium(II) and this suggested the potential of ruthenium(III) compounds to act as prodrugs for ruthenium(II) species which might be formed by reduction in the body (33). This theory became known as 'activation by reduction' and relied on the fact that tumour masses grow without the associated development of vascularisation systems typical of normal tissue and so offer a less oxygen rich and hence more reducing environment of lower pH than normal tissues. Thus the action of the complexes might be enhanced relative to normal tissue.

Ruthenium(III) Complexes

This theory was evaluated during the development of Na[$RuCl_4$(DMSO)(Im)] (NAMI, Im = imidazole) (34). Results from testing against lung and mammary tumours in mice were encouraging, but NAMI lacked many of the ideal physical characteristics for pharmaceutical development. In particular, the compound is hygroscopic and crystallises with two DMSO molecules of crystallisation resulting in variability in elemental composition and poor stability. Many of these problems were resolved by switching to the imidiazolium salt [ImH][$RuCl_4$(DMSO)(Im)] (NAMI-A, **Figure 6**) (35). This has no molecules of crystallisation resulting in good stability and has good solubility in water. In addition, its synthesis from ruthenium trichloride is a simple and high yielding process. Solution studies showed that the complex is likely to undergo chloride hydrolysis in

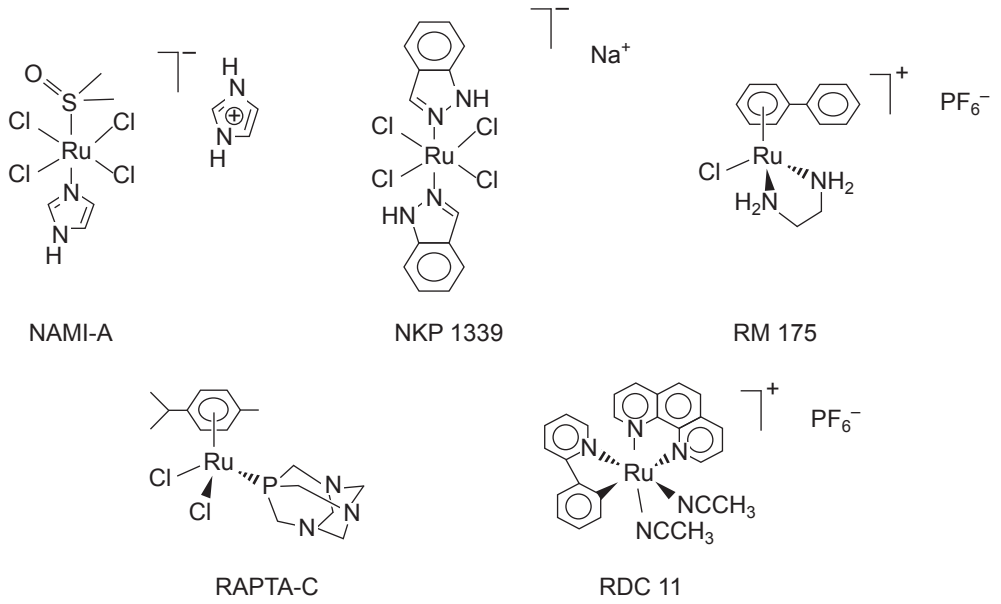

Fig. 6. Ruthenium anticancer compounds

aqueous media either before or after reduction which occurs rapidly in the presence of biological reductants such as ascorbic acid or cysteine. Studies of interaction with DNA suggested a lower and less selective reactivity than cisplatin, but still the potential to interfere with DNA replication. The complex shows significant interaction with plasma proteins albumin and transferrin which might assist its delivery to the tumour. Further research into the mechanism of action has suggested that these complexes do not act primarily by reaction with DNA but provide antimetastatic activity through influencing cell adhesion, motility and invasiveness.

These properties were sufficiently encouraging to initiate single-agent phase 1 clinical trials of NAMI-A in 1999. Twenty-four patients with a variety of tumours were treated and a maximum tolerated dose of 300 mg m^{-2} day^{-1} was determined. Clinical progress since that time has been limited, however, with further phase 1 studies devoted to drug combinations, but no target applications have been identified (35).

Over a similar period the group led by Keppler explored the activity of the related complexes [IndH][$RuCl_4(Ind)_2$] and Na[$RuCl_4(Ind)_2$] (KP1019 and NKP1339, Ind = indazole, **Figure 6**) (36). The initial pre-clinical studies were carried out with the former compound, but a phase 1 study identified the need for a more soluble compound to allow for higher doses and so the second derivative was adopted. As for NAMI-A, rapid binding to plasma proteins is thought to play an important role in tumour targeting. Efforts have been made to demonstrate whether reduction to Ru(II) occurs *in vivo*, but these have not been conclusive. Again, as for NAMI-A, there is evidence that the anticancer activity of these compounds does not arise primarily through direct DNA damage and so they should not be considered as analogues of cisplatin. KP1019 and NKP1339 are believed to induce apoptosis *via* the mitochondrial pathway (37).

Phase 1 trials with KP1019 achieved a dose of 600 mg m^{-2} day^{-1} twice weekly over three weeks. At this level there were limited side effects and the change to NKP1339 for increased solubility was required to take the dose higher. Doses up to 780 mg m^{-2} day^{-1} were administered by infusion on days 1, 8 and 15 of a 28 day cycle. Nausea was dose limiting at this level (36).

Ruthenium(II) Complexes

The ‘activation by reduction’ theory is clearly not applicable if ruthenium(II) complexes are used directly. Ruthenium(II) is the common oxidation state for a variety of organometallic complexes and, although in some cases these have very little aqueous solubility, it is in this area where groups led by Sadler and Dyson have concentrated their efforts. So-called ‘piano stool’ complexes containing arene ligands have a number of useful features for the design of suitable complexes (38). Firstly, the arene group provides the opportunity for variation in hydrophobicity and steric requirements which allow for varying levels of interaction with DNA by intercalation. Of the other three positions (the ‘legs’ of the stool) one position for a monodentate anion provides a site for substitution by biological ligands such as guanine, while the remaining two sites provide the opportunity to tune the kinetics of this substitution. Sadler chose to investigate complexes with one bidentate ligand, such as RM175 containing a neutral 1,2-diaminoethane ligand (see **Figure 6**) (39). After hydrolysis of the chloride ligand, the bidentate ligand is also influential in determining the pK_a of the aqua ligand and preventing the formation of large amounts of hydroxido-complex (as occurs in the cellular hydrolysis of cisplatin). Numerous studies of the interaction of these compounds with nucleobases, oligonucleotides and DNA, in addition to reactions with amino acids and proteins indicate a likelihood of interaction with DNA but suggest that the mechanism(s) of action of these complexes are significantly different from those of cisplatin, offering hope that they can be employed in different treatments in cancer therapy from cisplatin.

The group of Dyson studied ruthenium(II) arene complexes containing 1,3,5-triaza-7-phosphatricyclo-[3.3.1.1] decane (pta) using the acronym RAPTA for this class (40). One example, RAPTA-C, is shown in **Figure 6**. The exchange of the chlorides for a bidentate dicarboxylate ligand gives improved solubility and reduced hydrolysis, as it does in the case of the platinum drugs. Interestingly, through the synthesis of a complex containing 1,4,7-trithiacyclononane $RuCl_2$(P-pta)([9]aneS_3) Alessio was able to show that aromaticity is not required for the face-capping ligand (41, 42). Studies of the intracellular targets for these compounds have suggested that these are predominantly proteins, that they interact only weakly with DNA and that the mechanism of action may be more similar to that proposed for NAMI-A than for the platinum agents (43).

Work is continuing in these groups with the aim of modifying the basic structure to achieve greater

selectivity of action or applications to other treatment methods (44).

Another group of organometallic derivatives with only a single Ru-C linkage has been reported by Pfeffer and coworkers (45). The complex RDC11 (see **Figure 6**) contains a chelating phenylpyridine ligand. As with other ruthenium compounds there is evidence that direct interaction with DNA is less important for the action of this compound than for cisplatin and this opens the way for extending the application of metal-based drugs to additional tumours, creating new possibilities for combination therapies.

Conclusions

It is notable that each of these last investigations is being undertaken in academic groups without the sponsorship of a major pharmaceutical company. With our increasing understanding of genomics in recent years the focus for the pharmaceutical industry is moving towards identifying treatments that play a more direct role in controlling cancer development than can be provided by small molecule chemotherapy. Nevertheless, experience tells us that the opening up of new fields such as this will take longer than anticipated and time still remains for new small molecule drugs to find a place in cancer therapy.

References

1. J. Reedijk, *Platinum Metals Rev.*, 2008, **52**, (1), 2
2. B. Rosenberg, L. Van Camp and T. Krigas, *Nature*, 1965, **205**, (4972), 698
3. B. Rosenberg, L. VanCamp, J. E. Trosko and V. H. Mansour, *Nature*, 1969, **222**, (5191), 385
4. E. R. Jamieson and S. J. Lippard, *Chem. Rev.*, 1999, **99**, (9), 2467
5. U.-M. Ohndorf, M. A. Rould, Q. He, C. O. Pabo and S. J. Lippard, *Nature*, 1999, **399**, (6737), 708
6. E. Cvitkovic, J. Spaulding, V. Bethune, J. Martin and W. F. Whitmore, *Cancer*, 1977, **39**, (4), 1357
7. M. J. Cleare and J. D. Hoeschele, *Bioinorg. Chem.*, 1973, **2**, (3), 187
8. M. J. Cleare, *Coord. Chem. Rev.*, 1974, **12**, (4), 349
9. T. A. Connors, M. J. Cleare and K. R. Harrap, *Cancer Treat. Rep.*, 1979, **63**, (9–10), 1499
10. K. R. Harrap, *Cancer Treat. Rev.*, 1985, **12**, (A), 21
11. C. F. J. Barnard, M. J. Cleare and P. C. Hydes, *Chem. Br.*, 1986, **22**, 1001
12. N. J. Wheate, S. Walker, G. E. Craig and R. Oun, *Dalton Trans.*, 2010, **39**, (35), 8113
13. J. B. Vermorken, W. W. ten Bokkel Huinink, J. G. McVie, W. J. F. van der Vijgh and H. M. Pinedo, 'Clinical Experience with 1,1-Diaminomethylcyclohexane (Sulphato) Platinum (II) (TNO-6)', Platinum Coordination Complexes in Cancer Chemotherapy, Vermont Regional Cancer Center and the Norris Cotton Cancer Center, USA, 22nd–24th June, 1983, "Proceedings of the Fourth International Symposium on Platinum Coordination Complexes in Cancer Chemotherapy", eds. M. P. Hacker. E. B. Douple and I. H. Krakoff, Martinus Nijhoff Publishing, Boston, USA, 1984, p. 330
14. M. C. Christian, *Semin. Oncol.*, 1992, **19**, (6), 720
15. G. Mathé, Y. Kidani, M. Noji, R. Maral, C. Bourut and E. Chenu, *Cancer Lett.*, 1985, **27**, (2) 135
16. G. Mathé, Y. Kidani, K. Triana, S. Brienza, P. Ribaud, E. Goldschmidt, E. Ecstein, R. Despax, M. Musset and J. L. Misset, *Biomed. Pharmacother.*, 1986, **40**, (10), 372
17. A. N. Boughattas, F. Lévi, C. Fournier, G. Lemaigre, A. Roulon, B. Hecquet, G. Mathé and A. Reinberg, *Cancer Res.*, 1989, **49**, (12), 3362
18. F. Lévi, J.-L. Misset, S. Brienza, R. Adam, G. Metzger, M. Itzakhi, J. P. Caussanel, F. Kunstlinger, S. Lecouturier, A. Descorps-Declère, C. Jasmin, H. Bismuth and A. Reinberg, *Cancer*, 1992, **69**, (4), 893
19. C. M. Giandomenico, M. J. Abrams, B. A. Murrer, J. F. Vollano, M. I. Rheinheimer, S. B. Wyer, G. E. Bossard and J. D. Higgins, *Inorg. Chem.*, 1995, **34**, (5), 1015
20. M. J. McKeage, P. Mistry, J. Ward, F. E. Boxall, S. Loh, C. O'Neill, P. Ellis, L. R. Kelland, S. E. Morgan, B. A. Murrer, P. Santabarbara, K. R. Harrap and I. R. Judson, *Cancer Chemother. Pharmacol.*, 1995, **36**, (6), 451
21. A. M. Thayer, *Chem. Eng. News*, 2010, **88**, (26), 24
22. L. R. Kelland and C. F. J. Barnard, *Drugs Fut.*, 1998, **23**, (10), 1062
23. L. R. Kelland, S. Y. Sharp, C. F. O'Neill, F. I. Raynaud, P. J. Beale and I. R. Judson, *J. Inorg. Biochem.*, 1999, **77**, (1–2), 111
24. L. R. Kelland, C. F. J. Barnard, I. G. Evans, B. A. Murrer, B. R. C. Theobald, S. B. Wyer, P. M. Goddard, M. Jones, M. Valenti, A. Bryant, P. M. Rogers and K. R. Harrap, *J. Med. Chem.*, 1995, **38**, (16), 3016
25. L. R. Kelland, C. F. J. Barnard, K. J. Mellish, M. Jones, P. M. Goddard, M. Valenti, A. Bryant, B. A. Murrer and K. R. Harrap, *Cancer Res.*, 1994, **54**, (21), 5618
26. K. J. Mellish, C. F. J. Barnard, B. A. Murrer and L. R. Kelland, *Int. J. Cancer*, 1995, **62**, (6), 717

27. P. M. Goddard, R. M. Orr, M. R. Valenti, C. F. J. Barnard, B. A. Murrer, L. R. Kelland and K. R. Harrap, *Anticancer Res.*, 1996, **16**, (1), 33
28. N. Farrell, L. R. Kelland, J. D. Roberts and M. Van Beusichem, *Cancer Res.*, 1992, **52**, (18), 5065
29. N. Farrell, *Cancer Invest.*, 1993, **11**, 578
30. K. S. Lovejoy and S. J. Lippard, *Dalton Trans.*, 2009, (48), 10651
31. D. I. Jodrell, T. R. J. Evans, W. Steward, D. Cameron, J. Prendiville, C. Aschele, C. Noberasco, M. Lind, J. Carmichael, N. Dobbs, G. Camboni, B. Gatti and F. De Braud, *Eur. J. Cancer*, 2004, **40**, (12), 1872
32. T. A. Hensing, N. H. Hanna, H. H. Gillenwater, M. G. Camboni, C. Allievi and M. A. Socinski, *Anticancer Drugs*, 2006, **17**, (6), 697
33. M. J. Clarke, *Met. Ions Biol. Syst.*, 1980, **11**, 231
34. G. Sava, E. Alessio, A. Bergamo and G. Mestroni, 'Sulfoxide Ruthenium Complexes: Non Toxic Tools for the Selective Treatment of Solid Tumour Metastases', in "Metallopharmaceuticals I", eds. M. J. Clarke and P. J. Sadler, Topics in Biological Inorganic Chemistry, Springer-Verlag, Heidelberg, Germany, 1999, p. 143
35. S. Leijen, S. A. Burgers, P. Baas, D. Pluim, M. Tibben, E. van Werkhoven, E. Alessio, G. Sava, J. H. Beijnen and J. H. M. Schellens, *Invest. New Drugs*, 2015, **33**, (1), 201
36. R. Trondl, P. Heffeter, C. R. Kowol, M. A. Jakupec, W. Berger and B. K. Keppler, *Chem. Sci.*, 2014, **5**, (8), 2925
37. A. Bergamo and G. Sava, *Dalton Trans.*, 2011, **40**, (31), 7817
38. Y. K. Yan, M. Melchart, A. Habtemariam and P. J. Sadler, *Chem. Commun.*, 2005, (38), 4764
39. A. L. Noffke, A. Habtemariam, A. M. Pizarro and P. J. Sadler, *Chem. Commun.*, 2012, **48**, (43), 5219
40. W. H. Ang, E. Daldini, C. Scolaro, R. Scopelliti, L. Juillerat-Jeannerat and P. J. Dyson, *Inorg. Chem.*, 2006, **45**, (22), 9006
41. B. Serli, E. Zangrando, T. Gianferrara, C. Scolaro, P. J. Dyson, A. Bergamo and E. Alessio, *Eur. J. Inorg. Chem.*, 2005, (17), 3423
42. I. Bratsos, S. Jedner, A. Bergamo, G. Sava, T. Gianferrara, E. Zangrando and E. Alessio, *J. Inorg. Biochem.*, 2008, **102**, (5–6), 1120
43. G. Süss-Fink, *Dalton Trans.*, 2010, **39**, (7), 1673
44. C. M. Clavel, E. Paunescu, P. Nowak-Sliwinska, A. W. Griffioen, R. Scopelliti and P. J. Dyson, *J. Med. Chem.*, 2014, **57**, 3546
45. X. Meng, M. L. Leyva, M. Jenny, I. Gross, S. Benosman, B. Fricker, S. Harlepp, P. Hébraud, A. Boos, P. Wlosik, P. Bischoff, C. Sirlin, M. Pfeffer, J.-P. Loeffler and C. Gaiddon, *Cancer Res.*, 2009, **69**, (13), 5458

The Author

Dr Chris Barnard is currently working as an independent consultant after retiring following over 30 years with Johnson Matthey researching primarily biomedical applications of pgms and homogeneous catalysis for pharmaceutical synthesis.

http://dx.doi.org/10.1595/205651317X693877 *Johnson Matthey Technol. Rev.*, 2017, **61**, (1), 60–62

JOHNSON MATTHEY
TECHNOLOGY REVIEW

www.technology.matthey.com

"Assessing and Measuring Environmental Impacts in Engineering"

Edited by Jiří Jaromír Klemeš (Research Institute of Chemical and Process Engineering, University of Pannonia, Hungary), Butterworth-Heinemann, an imprint of Elsevier, Oxford, UK, 2015, 608 pages, ISBN: 978-0-12-799968-5, £85.00, US$140.00, €100.00

Reviewed by Julia Rowe
Johnson Matthey Plc, 5th Floor, 25 Farringdon Street, London EC4A 4AB, UK

Email: julia.rowe@matthey.com

As the editor describes in the introduction, "This book offers an overview of a project where a number of leading personalities in the research and development of the methodology in sustainability field agreed to join forces in the development of a comprehensive edited publication covering the major aspects and issues of assessing and measuring the environmental impact and sustainability". The subject of sustainability measurement is one that is not often found in published research papers. This book brings together the expertise of 15 groups of respected academics in the field over the last decade, in a collection of self-standing papers.

The book has been structured into four parts allowing the reader to access whichever topic is of most interest, without needing to read all the previous chapters.

- **Chapters 1–3**: Definitions of sustainability and systems approaches to measurement
- **Chapters 4–7**: Sustainability assessment and quantification of environmental footprints
- **Chapters 8–13**: Designing sustainable processes – planning and strategic tools, and supply chain considerations
- **Chapters 14–15**: Policies steering industrial and economic development towards sustainability.

Sustainable Development

Each paper starts with the 1987 definition of sustainability from the Bruntland Commission: "Sustainable development is development that meets the needs of the present without compromising the ability of future generations to meet their own needs" (1) and then sets out to define a way to quantify the sustainability of a chosen system or manufactured product. These systems vary vastly in their complexity, from a range of biofuels in Chapters 4 and 8 to whole brownfield development sites and even cities in Chapters 10 and 15.

The reader comes away with the overwhelming conclusion that the quantification of sustainable development is still in its infancy and that there is no 'one size fits all' methodology for doing so. The authors show that it is possible to define a set of parameters and equations to discriminate between the environmental benefits of a variety of related scenarios in a particular system. At the same time, they also note that the same equations cannot necessarily be extended to

an unrelated system or scenario, where the relative importance of individual environmental parameters likely will need to be ranked differently. In most chapters the overall conclusion appears to be that it is better to report transparently the individual footprints of a system, for example the carbon, water or nitrogen footprints, rather than depend upon a single amalgamated 'environmental footprint' to compare scenarios.

In every paper the authors concentrate on explaining their mathematical methods from first principles, so this book would not suit a reader who shies away from complex mathematical equations. However, the merit of this approach is that it enables the practitioner to really understand the limitations in their chosen method of measuring sustainable development. Thus, I would recommend it as an introductory text book to any postgraduate scientist or engineer interested in working in this field.

What is absent from the book is a discussion of the relative merits of the various software packages currently available for calculating environmental footprints such as SimaPro (2), GaBi (3) and ecoinvent (4). This seems a little short-sighted, since they are often what are cited in academic papers by industrial practitioners in the field of product environmental footprinting, who may have limited understanding of the mathematics and assumptions behind the software they depend upon for evaluating real-life solutions to sustainability dilemmas. Neither could I find any discussion of the application of the publically available International Organization for Standardization (ISO) standards for environmental footprinting 14040:2006 (5). There is also no mention of various government-funded initiatives currently underway to calculate and reduce the environmental footprints of product groups, most significantly the European Commission's Product Environmental Footprinting (PEF) (6, 7) and Circular Economy (8) projects. Perhaps this is because these programmes are still 'active', but as they form a large part of the work being carried out in this field, in Europe at least, over the last five years, their entire omission may seem surprising to readers a few years from now.

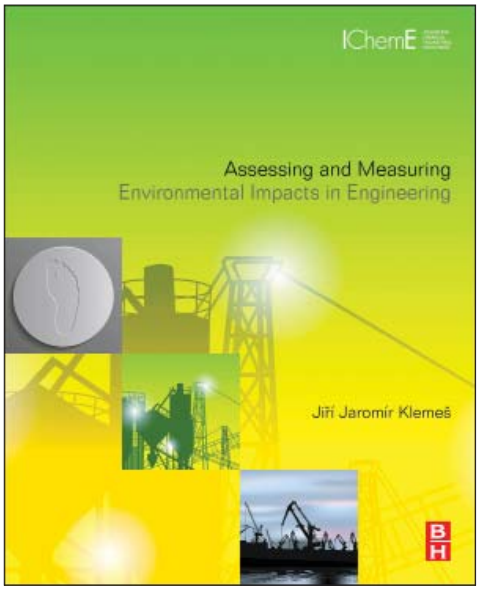

"Assessing and Measuring Environmental Impacts in Engineering"

References

1. 'Our Common Future, Chapter 2: Towards Sustainable Development', from "Our Common Future: Report of the World Commission on Environment and Development", A/42/427, UN Documents, The United Nations, Secretary General, New York, USA, 4th August, 1987
2. SimaPro 8.2.3, PRé Consultants bv, The Netherlands, 31st March, 2016
3. GaBi Version 7.3, thinkstep, Germany, 27th July, 2016
4. ecoinvent 3.3, ecoinvent, Zürich, Switzerland, 15th August, 2016
5. ISO 14040:2006, 'Environmental Management – Life Cycle Assessment – Principles and Framework', International Organization for Standardization, Geneva, Switzerland, 2006
6. Communication from the Commission to the European Parliament and the Council, 'Building the Single Market for Green Products, Facilitating Better Information on the Environmental Performance of Products and Organisations (Text with EEA Relevance)', COM(2013) 196 final, Brussels, Belgium, 9th April, 2013
7. S. Manfredi, K. Allacker, K. Chomkhamsri, N. Pelletier and D. M. de Souza, European Commission Joint Research Centre, Institute for Environment and Sustainability, H08 Sustainability Assessment Unit, 'Product Environmental Footprint (PEF) Guide: Deliverable 2 and 4A of the Administrative Arrangement between DG Environment and the Joint Research Centre No N 070307/2009/552517, including Amendment No 1 from December 2010', Ref. Ares(2012)873782, Ispra, Italy, 17th July, 2012
8. Communication from the Commission to the European Parliament, the Council, the European Economic and Social Committee and the Committee of the Regions, 'Closing the loop – An EU Action Plan for the Circular Economy', COM(2015) 614 final, Brussels, Belgium, 2nd December, 2015

The Reviewer

Julia Rowe has a PhD in Chemistry. She has worked for Johnson Matthey Plc for 20 years, first as a Chemical Engineer and then as Sustainability Practitioner. She takes a particular interest in environmental footprinting of the company's products.

JOHNSON MATTHEY
TECHNOLOGY REVIEW
www.technology.matthey.com

Johnson Matthey Highlights

A selection of recent publications by Johnson Matthey R&D staff and collaborators

EMISSION CONTROL TECHNOLOGIES

DOC Modeling Combining Kinetics and Mass Transfer using Inert Washcoat Layers

B. Lundberg, J. Sjöblom, Å. Johansson, B. Westerberg and D. Creaser, *Appl. Catal. B: Environ.*, 2016, **191**, 116

A kinetic and transport model for DOCs was developed. NO_2 was found to react preferentially with CO rather than C_3H_6. This causes NO oxidation to be inhibited. Experiments were carried out using inert washcoat layers of different thicknesses to resolve transport, kinetic and inhibition effects. The effect of washcoat transport resistance was clearest for the oxidation of C_3H_6 and CO. The kinetic model worked well when O, CO and NO_2 were the only surface species.

Study of Particulate Matter and Gaseous Emissions in Gasoline Direct Injection Engine using On-Board Exhaust Gas Fuel Reforming

M. Bogarra, J. M. Herreros, A. Tsolakis, A. P. E. York and P. J. Millington, *Appl. Energy*, 2016, **180**, 245

A prototype on-board fuel reformer was used in a GDI engine to investigate the effects of reformate combustion in addition to gasoline. The particulate and gaseous emissions were measured. 5%–6% lower fuel consumption and hence CO_2 emissions, was achieved by using the fuel reformer. Reformate could also reduce the engine PM emissions, depending on their nature with soot cores being removed more efficiently than volatile PM. A TWC also reduced the emissions of PM.

The Kinetics of Oxidation of Diesel Soots and a Carbon Black (Printex U) by O_2 with Reference to Changes in Both Size and Internal Structure of the Spherules during Burnout

C. J. Tighe, M. V. Twigg, A. N. Hayhurst and J. S. Dennis, *Carbon*, 2016, **107**, 20

At 450–550ºC the rates of oxidation of two soots produced from burning either ultra low sulfur diesel or biodiesel in an engine, were measured with oxygen concentrations of 2.7–24.4 vol%; Printex U was also investigated. The volatile material from these carbons were removed by initially heating in argon; the resulting particles were found to burn in two steps. 20% of the carbon in a soot particle was consumed in an initial, fast, transient reaction. During the second stage of burnout the rates of oxidation were in line with a model presuming these soots consist of porous spherules which burn throughout their interiors. The overall rates were half-order with respect to O_2 with an apparent activation energy of 145 ± 8 kJ mol^{-1}.

FINE CHEMICALS

Biocatalytic Dynamic Kinetic Resolution for the Synthesis of Atropisomeric Biaryl N-Oxide Lewis Base Catalysts

S. Staniland, R. W. Adams, J. J. W. McDouall, I. Maffucci, A. Contini, D. M. Grainger, N. J. Turner and J. Clayden, *Angew. Chem. Int. Ed.*, 2016, **55**, (36), 10755

Dynamic kinetic resolution (DKR) of rapidly racemising precursors showing free bond rotation was used to enantioselectively synthesise atropisomeric biaryl pyridine and isoquinoline N-oxides. The DKR was attained by ketoreductase (KRED) catalysed reduction of an aldehyde to form a configurationally stable atropisomeric alcohol, with a significant rise in rotational barrier emerging from the loss of a bonding interaction between the N-oxide and the aldehyde. The synthesis of either M or P enantiomer in excellent enantiopurity was possible by using various KRED. The asymmetric allylation of benzaldehyde derivatives with allyltrichlorosilane was catalysed by the enantioenriched biaryl N-oxide compounds.

Chemoselective Transfer Hydrogenation of α,β-unsaturated Carbonyl Compounds using Potassium Formate over Amine-grafted Ru/AlO(OH) Catalysts

Y. Gao, J. Wang, A. Han, S. Jaenicke and G. K. Chuah, *Catal. Sci. Technol.*, 2016, **6**, (11), 3806

An active and highly chemoselective heterogeneous catalyst was prepared by grafting 3-(2-aminoethylamino) propyltrimethoxysilane onto Ru/AlO(OH) and was used for the transfer hydrogenation of α,β-unsaturated carbonyl compounds to the equivalent allylic alcohols. The sustainable hydrogen donor was potassium formate. Various substrates cinnamaldehyde, α-amylcinnamaldehyde, citral, 3-methyl-2-butenal,

trans-2-pentenal and *trans*-hexenal were selectively hydrogenated at the C=O moiety with >96% selectivity. To compare, cinnamaldehyde was hydrogenated at the C=C bond using unmodified 1 wt% Ru/AlO(OH) catalyst and yielded 3-phenylpropanal as the product. 20–25% selectivity to cinnamyl alcohol was demonstrated by the higher loaded samples with 2–10 wt% Ru. Low coordination sites were found to be more selective to hydrogenation of the internal C=C than the terminal C=O bond.

FINE CHEMICALS: API MANUFACTURING

Convergent Synthesis of the Renin Inhibitor Aliskiren Based on C5–C6 Disconnection and CO_2H–NH_2 Equivalence

E. Cini, L. Banfi, G. Barreca, L. Carcone, L. Malpezzi, F. Manetti, G. Marras, M. Rasparini, R. Riva, S. Roseblade, A. Russo, M. Taddei, R. Vitale and A. Zanotti-Gerosa, *Org. Process Res. Dev.*, 2016, **20**, (2), 270

Aliskiren, the renin inhibitor, has been synthesised by a novel route involving a C5 and C6 disconnection for the first time. The C5 carbon acts as a nucleophile while a Curtius rearrangement is used to introduce the amine group. The C4 and C5 stereogenic centres are created simultaneously by an asymmetric hydrogenation step. The method is simple to operate, exhibits step economy and provides a good overall yield. It is considered suitable for scale manufacture.

Development of a Multi Kilogram-Scale, Tandem Cyclopropanation Ring-Expansion Reaction en Route to Hedgehog Antagonist IPI-926

B. C. Austad, A. B. Hague, P. White, S. Peluso, S. J. Nair, K. M. Depew, M. J. Grogan, A. B. Charette, L.-C. Yu, C. D. Lory, L. Grenier, A. Lescarbeau, B. S. Lane, R. Lombardy, M. L. Behnke, N. Koney, J. R. Porter, M. J. Campbell, J. Shaffer, J. Xiong, J. C. Helble, M. A. Foley, J. Adams, A. C. Castro and M. R. Tremblay, *Org. Process Res. Dev.*, 2016, **20**, (4), 786

The semisynthesis of IPI-926 requires formation of a D-homocyclopamine ring system. This is done by chemoselective cyclopropanation followed by a stereoselective acid-catalysed carbocation rearrangement. New iodomethylzinc bis(aryl)phosphate reagents have been developed to achieve this step. They are soluble, prepared under mild conditions and remain stable during the reaction. They may also have favourable energetics compared to other alternatives such as $EtZnCH_2I$. The process optimisation investigations are explained in the present paper.

NEW BUSINESSES: FUEL CELLS

Importance of Mass Transport and Spatially Heterogeneous Flux Processes for *in Situ* Atomic Force Microscopy Measurements of Crystal Growth and Dissolution Kinetics

M. Peruffo, M. M. Mbogoro, M. Adobes-Vidal and P. R. Unwin, *J. Phys. Chem. C*, 2016, **120**, (22), 12100

This paper critically analyses literature data for gypsum dissolution to develop finite element method models to study the coupled mass transport-surface kinetic problem for dissolution processes in AFM. It was found that mass transport must be taken into account when carrying out *in situ* AFM on macroscopic surfaces. This applies even when the high-convection fluid cells are used. Dissolution kinetics of crystals was found to be influenced largely by other processes elsewhere on the surface.

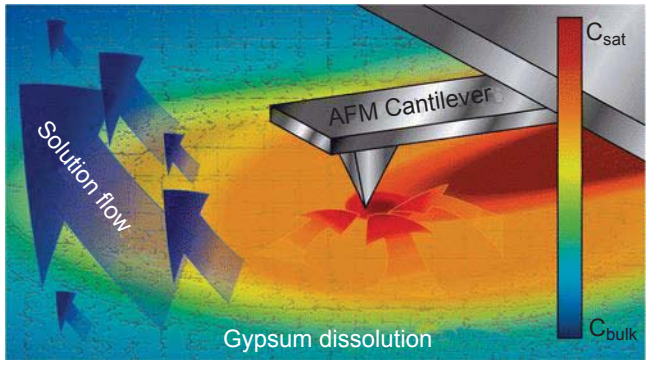

Reprinted with permission from M. Peruffo, M. M. Mbogoro, M. Adobes-Vidal and P. R. Unwin, *J. Phys. Chem. C*, 2016, **120**, (22), 12100. Copyright (2016) American Chemical Society

PRECIOUS METAL PRODUCTS

Characterization of Platinum and Iridium Oxyhydrate Surface Layers from Platinum and Iridium Foils

B. Johnson, C. Ranjan, M. Greiner, R. Arrigo, M. E. Schuster, B. Höpfner, M. Gorgoi, I. Lauermann, M. Willinger, A. Knop-Gericke and R. Schlögl, *ChemSusChem*, 2016, **9**, (13), 1634

Thin platinum and iridium hydrous oxide layers were created by electrochemically oxidising platinum and iridium polycrystalline foils through anodisation, and were examined by photoelectron spectroscopy during heating and time series (temperature-programmed spectroscopy). High-energy photoelectron spectroscopy was used to investigate the films which contain oxygen in the form of bound oxides, water and hydroxides. The Pt films were found to be unstable and started to degrade instantly after removing from the electrolyte to form core-shell structures with a metallic inner core and a hydrous oxide outer shell almost lacking of Pt. It might be possible to manufacture PtO_x phases with increased stability due to the proof for metastable intermediate states of degradation. Accelerated degradation is caused by heating the film to 100ºC and this demonstrates that stoichiometric oxides such as PtO_2 or PtO are not the active species in the electrolyte. The Ir films have increased stability and higher surface Ir content and defect density can be lowered by gentle

heating at low temperatures. Although both layers are based on noble metals, their surface structures are notably dissimilar.

A New Approach to Develop Palladium-modified Ti-based Alloys for Biomedical Applications

C. Qiu, A. Fones, H. G. C. Hamilton, N. J. E. Adkins and M. M. Attallah, *Mater. Des.*, 2016, **109**, 98

Ti-6Al-4V (Ti64) with Pd was modified using a combination of a new powder mixing or coating method and SLM or HIP with the aim of further enhancing its corrosion resistance. Porosity, surface structure, microstructure and composition using optical microscopy, SEM, EDX and EMA were characterised for the modified alloy samples. The mechanical properties were measured *via* tensile tests and electrochemical tests were used to evaluate their corrosion properties. Pd was homogeneously distributed among the base Ti alloy powder particles without impairing their sphericity using a new physical powder mixing method. Pd was mostly situated at grain boundaries after HIPing while during SLM Pd has dissolved into the matrix. Increased laser scanning speed continuously raised both the porosity in the as-SLMed samples and surface roughness. Pd boosted corrosion resistance in 2 M HCl by moving the corrosion potential into the passive region of Ti64 but did not cause substantial improvement in tensile properties.

PRECIOUS METAL PRODUCTS: ADVANCED GLASS TECHNOLOGIES

Liquid Crystals as Optical Amplifiers for Bacterial Detection

C. Zafiu, Z. Hussain, S. Küpcü, A. Masutani, P. Kilickiran and E.-K. Sinner, *Biosens. Bioelectr.*, 2016, **80**, 161

Lipopolysaccharides (LPS) self-assembled into monolayers on top of liquid crystals are a simple model to study the interface between LPS and bacteria. This is potentially useful for detection and screening. The LPS layers' stability depends largely on the choice of saccharides. Both gram-positive and gram-negative bacteria will interact with the LPS layer. The detection limits were a minimum of 500 cells per millilitre of solution while the detection time was less than 15 min.

PROCESS TECHNOLOGIES

Structure-transport Relationships in Disordered Solids using Integrated Rate of Gas Sorption and Mercury Porosimetry

A. Nepryahin, E. M. Holt, R. S. Fletcher and S. P. Rigby, *Chem. Eng. Sci.*, 2016, **152**, 663

New details on structure-transport relationships in disordered porous pellets were delivered by a new experimental method. The relative importance of specific sub-sets of pores to mass transport rates within the network of two disordered porous solids were investigated using integrated rate of adsorption and mercury porosimetry experiments. This was accomplished by assessing the relative rates of low pressure gas uptake into a network, both before and after a known set of pores was filled with frozen, entrapped mercury. The compaction pressure influences the relative contribution to overall mass transport made by the subset of the largest pores for the catalyst pellets which were formed by tableting. The spatial distribution of entrapped mercury was mapped by CXT and this showed that the relative importance of the sub-sets is linked to their level of pervasiveness across the pellet and whether they percolate to the centre of the pellet. The impact of manufacturing process parameters on pellet structure and mass transport properties can be comprehensively revealed using a combination of integrated mercury porosity, gas sorption and CXT.

http://dx.doi.org/10.1595/205651317X694524 *Johnson Matthey Technol. Rev.*, 2017, **61**, (1), 66–76

JOHNSON MATTHEY
TECHNOLOGY REVIEW

www.technology.matthey.com

Nitinol for Medical Applications: A Brief Introduction to the Properties and Processing of Nickel Titanium Shape Memory Alloys and their Use in Stents

Considerations for the manufacture of Nitinol parts for stents and some other medical applications

By Deepak Kapoor
Johnson Matthey Inc, 1070 Commercial St, Suite 110, California 95112, USA

Email: Deepak.Kapoor@jmusa.com

Shape memory alloys are remarkable materials that open up a wide range of uses. Nitinol, an alloy of nickel and titanium, is one of the most important of these materials. Some of its major applications are in medical devices where its unique properties allow minimally invasive surgery and implants to improve quality of life for millions of people. With the growing global population and increasing numbers of people able to access quality healthcare, the availability of advanced materials such as Nitinol is essential to allow continued progress in improving lives across the world. This article will review the discovery, material properties, processing methods and medical applications of Nitinol, with a special focus on stents for the treatment of arterial diseases, which constitute one of Nitinol's major uses.

Introduction

Per the United Nations Department of Economic and Social Affairs, the world population is expected to increase to 8.5 billion by 2030 and 9.7 billion by 2050. Globally, life expectancy at birth is projected to rise to 77 years in 2045–2050 (1). While this increase is projected based on a reduction of the spread of human immunodeficiency virus (HIV) and other infections as well as non-communicable diseases, advances in medicine and better access to healthcare certainly contribute to increased life expectancy. Globalisation has increased living standards in many countries where populations historically may not have had access to good healthcare. A combination of increased living standards and the choices people make has also increased the incidence of lifestyle related illness such as cardiovascular diseases (2). As companies race to develop medical devices to cure challenging physical conditions and diseases, they rely on novel materials for solutions. A variety of metals like stainless steel, titanium and its alloys, platinum and associated platinum group metals (pgms) and cobalt-based alloys are used in medical devices (3, 4). One material that has seen increased use and acceptance within the medical device community is Nitinol (NiTi), a shape memory alloy made of nickel and titanium in almost equal concentrations.

A shape memory alloy has the ability to restore its original shape after deformation. Used in a variety of applications in industries ranging from consumer

appliances to automotive to aerospace and medical, shape memory alloys have gained a strong foothold because they offer designers incredible flexibility compared to conventional materials or systems. In medical devices, Nitinol is popular due to its biocompatibility, superelasticity and fatigue and kink resistance (5). Nitinol is used to manufacture catheter tubes, guidewires, stone retrieval baskets, filters, needles, dental files and archwires and other surgical instruments (6).

A particularly important use of Nitinol is in stents. **Figure 1** shows an illustration of stent application: normal blood flow in an artery (**Figure 1(a)**), decreased blood flow due to plaque (**Figure 1(b)**), and a stent placed to open the artery and restore blood flow (**Figure 1(c)**) (7). Global Data (8) valued the global market for peripheral vascular stents for lower extremities at approximately US$2.2 billion in 2012 and forecast it to reach US$3.6 billion by 2019. The growth is driven by the availability of improved technologies like drug eluting and bio-absorbable stents, patient awareness, physician training and the growing number of cases of peripheral artery disease (PAD) due to diabetes, hypertension, obesity and tobacco use (9). Transparency Market Research (10) predict an US$11 billion market by 2019 for all forms of Nitinol stent devices.

Nitinol was a serendipitous discovery by William Buehler from the US Government Naval Ordnance Laboratory in the 1960s. Buehler and his team were developing fatigue, wear and impact resistant materials for missile cones of US Navy missiles. One such formulation was similar to the Nitinol we know today, an equiatomic alloy of nickel and titanium. Buehler would fold the material into an accordion shape and pry it open multiple times to demonstrate its flexibility and that it would not break. At a meeting one day, a team member lit a pipe lighter under the accordion shape and to everyone's amazement, the sheet of nitinol regained its original flat shape. Buehler named the material 'NITINOL' which stood for Nickel Titanium Naval Ordnance Laboratory (11). Frederick Wang, also from the Naval Ordnance Laboratory, was an expert in crystal physics. He discovered the reason behind the behaviour of the material. It was due to atomic rearrangement or phase changes at different temperatures while the material was still a solid.

Nitinol was used in orthodontic archwires around 1976 and the first military application of Nitinol was hydraulic couplings for the Grumman F-14 Tomcat fighter aircraft in 1978. By the late 1980s, the first commercial Nitinol medical device, the Homer Mammalok®, a breast tumour localisation device, and the first Nitinol based implant, the Mitek® bone anchor, became commercially available (12).

This article will review the properties, processing methods and applications of Nitinol with a focus on stents, their most important current use.

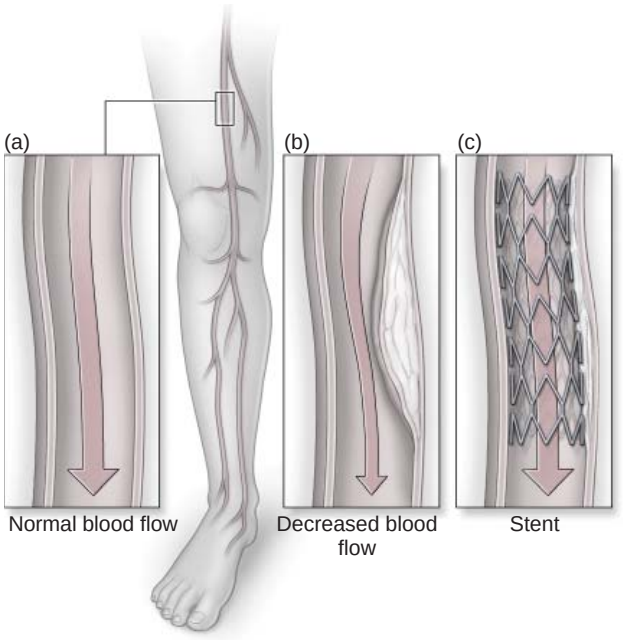

Fig. 1. Schematic of stent used to treat a peripheral artery (7). Art by Scott Leighton, Medicus Media, USA

The Shape Memory Effect

The most common demonstration of the shape memory effect is that a piece of the alloy can be deformed – for example, by winding a piece of straight wire into a tight coil – and then the deformation can be completely removed by heating the metal a small amount, as by dipping it into hot water. As it is heated, the metal instantly 'remembers' its original shape and returns to the form of a straight wire.

The shape memory effect is caused when a material undergoes a change in crystal form as it is cooled or heated through a range of characteristic transformation temperatures. In Nitinol, the change is from an ordered cubic crystal structure (austenite) to a monoclinic crystal phase (martensite) (13). This behaviour is known as the martensitic transformation. The temperatures at which the formation of martensite starts and ends are called M_s and M_f. Austenite formation starts and ends at A_s and A_f, respectively (14, 15).

The majority of commercial applications of Nitinol utilise a useful property which is the exceptional elasticity, commonly referred to as 'superelasticity' (more accurately called pseudoelasticity) when one deforms the alloy at a temperature above the active austenite finish temperature, A_f. Above this temperature, the material is in the high-temperature or austenitic phase. When stress is applied, the deformation causes a stress-induced phase transformation from austenite to deformed martensite. When the applied stress is removed, the material returns to its original shape, and the crystal form returns to the austenite phase (13). The thermomechanical behaviour of materials in the martensitic and austenitic states is well explained in the literature (14, 15).

Conventional materials like stainless steels exhibit different elastic deformation behaviour than structural biological materials in the human body. Elastic deformation of such materials is limited to about 1% and strain is proportional to applied load (16). Hair, tendon and bone can be elastically deformed up to 10% strain in a non-linear way. Superelastic (austenitic) Nitinol behaves in a similar way to those biological materials; when loaded, it accommodates a large strain without increase in stress, and when unloaded, the strain reduces at a lower but constant stress. Nitinol stress-strain behaviour has been shown to be very similar to that of structures in the human body (16, 17).

Superelastic Nitinol alloys take advantage of a stress-induced martensitic transformation to achieve incredible amounts of flexibility and kink resistance. For example, alloys which are intended to be superelastic at room temperature are generally produced with their active A_f temperatures just below room temperature, say in the range of 0–20ºC (18). Such a material will also exhibit good superelastic properties at body temperature (37ºC). Superelastic alloys comprise the largest volume of Nitinol material manufactured today.

Shape memory Nitinol alloys exploit the ability of the materials to recover a trained shape upon heating above their active A_f temperature. Therefore, this is the most critical property to specify (18). The active A_f represents the finish of the transformation from martensite to austenite upon heating, and therefore the temperature at which the shape recovery is complete.

A representation of the shape memory and superelastic effect (19) with specific reference to Nitinol is seen in **Figure 2**. Since the material is equiatomic, one sphere in the crystal structure represents nickel and the other represents titanium. The structure at the top

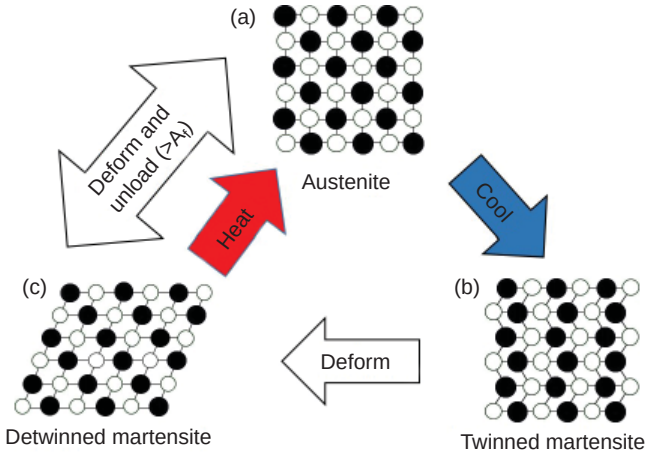

Fig. 2. Schematic illustration of shape memory effect

(**Figure 2(a)**) represents the crystal structure of the material in the stable or austenitic state. This is when the material is above the A_f. When the material is cooled below the martensite start temperature, M_s, it starts transformation into twinned martensite (like a herringbone) shown in the lower right structure, **Figure 2(b)**. Below the martensitic finish (M_f) temperature, the material is completely martensitic. This martensitic transformation is called thermally induced or twinned martensite. When twinned martensite is subject to stress, it transforms into deformed or detwinned martensite, **Figure 2(c)**. The induced strain does not recover upon unloading. Upon heating the material above the A_f, the material returns to austenite exhibiting the shape memory effect. If the material in the austenitic state is deformed, the austenite transforms into stress induced martensite and upon removal of the load, the material returns to austenite as it is the more stable form (19). This phenomenon is the basis for superelasticity.

Material Characterisation

Knowledge of the transformation temperatures (A_s, A_f, M_s and M_f) of the alloy is a key requirement for using Nitinol. There are two commonly used methods of performing transformation temperature testing: differential scanning calorimetry (DSC) and bend and free recovery (BFR).

The DSC method (20) yields a plot such as **Figure 3** by measuring the amount of heat given off or absorbed by a tiny sample of the alloy (<50 mg) as it is cooled and heated through its phase transformations

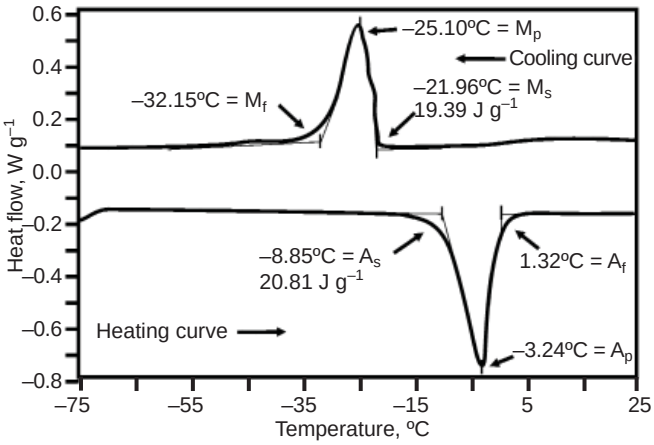

Fig.3. Characteristic curve produced from a differential scanning calorimetry (DSC) test (13)

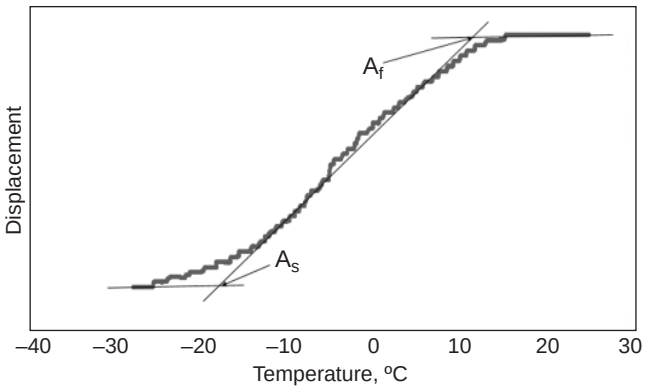

Fig 4. Bend and free recovery (BFR) determination of austenite transformation temperatures A_s and A_f

(21). DSC results obtained in the fully annealed condition, annealed at temperatures of 800–850ºC for 15–60 minutes (20), are often used as the basis for Nitinol raw material selection (ingot) since they effectively characterise the baseline properties of the material prior to cold working and heat treatment. The DSC yields excellent, repeatable results on fully annealed samples. One important drawback to the DSC method is that tests on partially cold worked materials, such as those used to optimise superelasticity, can yield poor, inconclusive results. Active A_f tests are recommended for materials in these conditions (21).

While DSC is used for characterising raw materials, the temperature most frequently specified for the finished product (whether wire, sheet or tube) is the active A_f temperature which is generally determined by a BFR test (22). In this test, one deforms a sample of the material after cooling it into the martensitic region and then records the amount of shape recovery that occurs as it is warmed. A graph, **Figure 4**, of temperature *versus* sample displacement is plotted and used to determine the active A_f temperature where the shape recovery is complete. BFR is a very good functional test that shows distinct shape recovery.

Tensile testing is performed to characterise the strength and ductility of the material (23). In a typical tensile test (23), the sample is pulled to 6% strain, then unloaded and subsequently pulled to failure. In addition to the ultimate tensile strength and elongation that are common to other materials, there are other critical parameters that are measured when testing Nitinol. When the test is conducted above the active A_f of the sample, upper plateau strength, lower plateau strength and the residual elongation (or permanent set) are also recorded. As the material is being loaded, the material transforms from austenite into stress induced martensite, and as the sample is unloaded, the material reverses into austenite. During loading, the material strains at a constant stress (where upper plateau is recorded) and when the material is unloaded, the strain is reduced but at a lower stress level (where lower plateau is recorded). Per the ASTM F2516 standard, the upper plateau is the stress at 3% strain recorded during tensile loading and lower plateau is the stress at 2.5% strain recorded as the sample is unloaded. This stress hysteresis is the basis of stent design and performance (24). Residual elongation is the strain after the load to 6% strain and unload is completed. **Figure 5** depicts these points.

Processing

Nitinol ingots are melted using combinations of vacuum induction melting (VIM) and vacuum arc remelting (VAR) (25). Most Nitinol materials are a simple alloy of nickel and titanium with the ratio of the two constituents at about 50 atomic percent each (about 55 percent by weight of nickel). However, subtle adjustments in the ratio of the two elements can make a large difference in the properties of the NiTi alloy, particularly its transformation temperatures. If there is any excess nickel over the 50:50 ratio, one sees a dramatic decrease in the transformation temperatures and an increase in the austenite yield strength. Increasing the nickel-to-titanium ratio to 51:49 causes the active A_f to drop by over 100ºC (**Figure 6**) (26). This sensitivity of the properties to very small

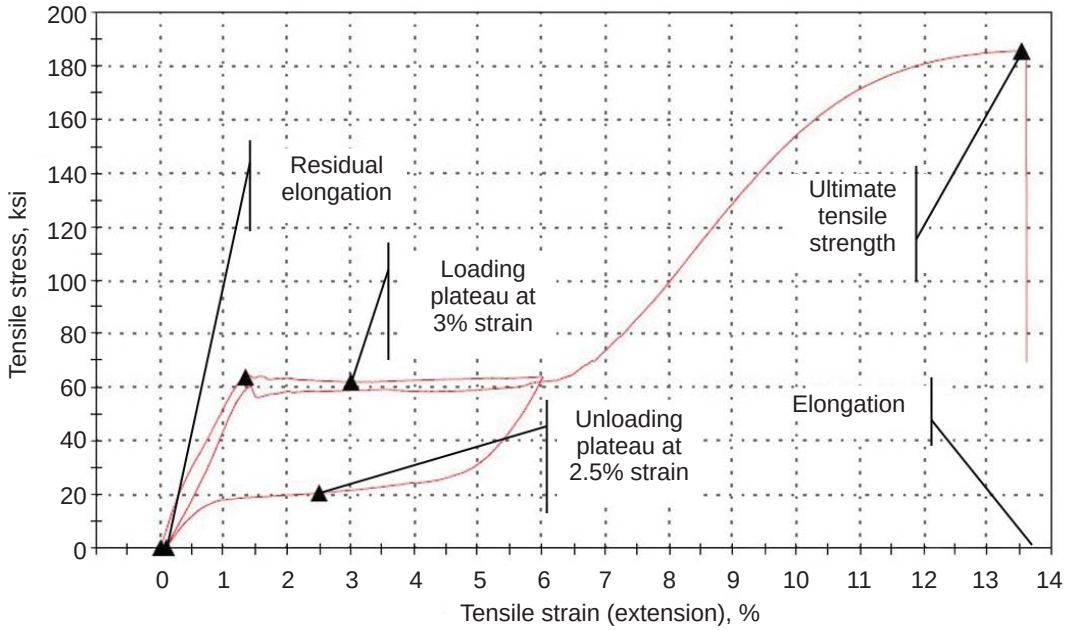

Fig. 5. Typical stress-strain plot of superelastic Nitinol showing measured properties

increases in the percentage of nickel makes it difficult to manufacture Nitinol of uniform and repeatable properties, but at the same time gives manufacturers a powerful method to control properties and to make ingots of the desired transformation temperature. The shaded rectangle in **Figure 6** represents the Ni content of typical binary superelastic alloys (26). The sensitivity of the A_f temperature to alloy composition is so great that chemistry is not recommended as a way to specify the alloy of interest. The transformation temperature, instead, is a much more accurate means to specify the alloy.

The raw material ingot or wrought microstructure is not refined to provide superelastic or shape memory properties and tends to have a low fracture resistance (26). In order to refine the microstructure of the material to make it useful, hot working at 600–800ºC through forging, swaging and hot rolling operations is required (26). The output from this process is intermediate forms like bars, rods and plates, according to specified chemical and metallurgical requirements (27).

Melting methods, type of raw materials and processing techniques result in impurities which lead to the formation of non-metallic inclusions in the ingot (28). It is critical to control the oxygen, nitrogen and carbon content in the melt because of the formation of titanium oxides, nitrides and carbides. These hard inclusions act as discontinuities in the matrix. These have been the subject of numerous studies on device failure and fatigue strength. Studies have shown that both inclusion size and total number of inclusions are important factors in determining fatigue resistance (29). It has been shown that material with smaller

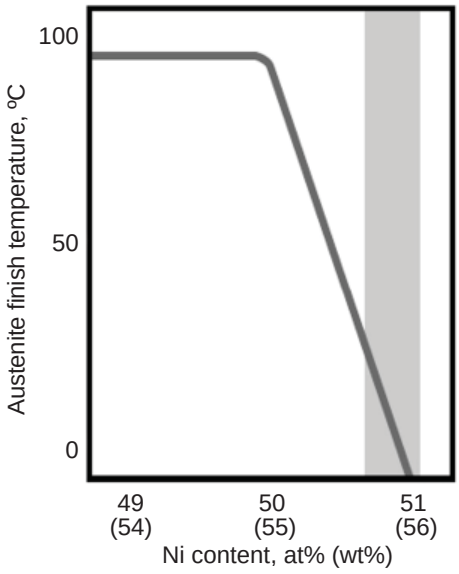

Fig. 6. Schematic of the effect of the Ni content of Nitinol on the active austenite finish temperature, A_f (26)

inclusion sizes overall shows much improved fatigue life when compared to material with larger inclusions (28, 29). Over the past few years, advances in process optimisation and input raw material purity have led to the successful development of Nitinol ingots with fewer or smaller inclusions (29), while Steegmüller *et al.* (30) observed that inclusion size, rather than number of inclusions, plays a dominant role in influencing fatigue life.

The intermediate forms are then further processed through cold working operations to make the final products that possess appropriate tensile strength, transformation temperatures and size. Rods can be drawn through dies to make smaller diameter wires. Plates are rolled down to make thinner sheet. Nitinol sheet is popular because it offers design flexibility not available with other forms, designing products flat and then forming it to make devices.

To make a tube, one starts with bars that are gun-drilled to create a 'tube hollow'. Gun-drilling is a necessary evil; it immediately reduces the effective yield of the process as it removes a considerable amount of material to create a hollow core. The tube hollows are subject to step-by-step cross-sectional area reduction using successively smaller dies to size the outer diameter and successively smaller mandrels to size and support the inner diameter during tube drawing.

A combination of cold working (defined as the percentage reduction in cross-sectional area) and heat treatment (thermomechanical processing) is critical to attaining the desired properties in the material. During cold working fabrication operations such as drawing or rolling, Nitinol alloys work harden very rapidly. If the material is not annealed after a certain amount of cold work, the strength rises to the point where the fracture strength is reached on further deformation and failure occurs.

Heat treatment is used to set the final shape in the Nitinol component. If the Nitinol has a reasonable amount of cold work (of the order of 30–50%), temperatures of 450–550ºC (26) with appropriate dwell times will create a straight, flat or shaped part. The term 'shape setting' is a general term that refers to setting a shape in cold-drawn material. In addition to straight wires and tubes or flat sheet, shaped parts can be created using bespoke fixtures. **Figure 7** shows a simple example of a part shape set from a straight tube. The end of the tube is constrained in hook shape in a fixture. The fixture with the tube is placed in a furnace

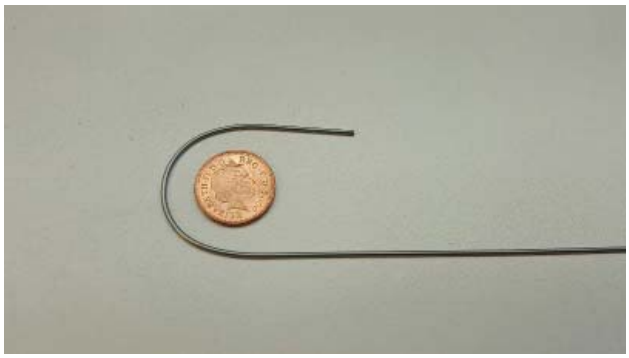

Fig 7. Example of a shape set part

and heated to approximately 500ºC for a few minutes. Upon removal from the furnace, the fixture with the part is quenched in water. The nitinol tube is removed from the fixture and it exhibits the hook shape. In this specific example the tube is superelastic at room temperature. When the legs of the hook are pried apart and the load is released, the legs return to their original hook shape.

Another objective of heat treatment is to establish the final mechanical properties and transformation temperatures in the Nitinol component (31). After the material has been cold worked, the proper heat treatment will establish the best possible shape memory or superelastic properties in the material while retaining enough of the residual cold work effect to resist permanent deformation during cycling. It also helps to set the active A_f of the parts.

Properties that Suit Medical Applications

Numerous references discuss Nitinol properties that make it attractive for use in medical devices (5, 6, 32). The major use for Nitinol is in stents, however there are a number of other applications which will be briefly introduced here. Due to the shape memory effect, Nitinol is quite versatile in applications that use elevated temperature to activate a device (called thermal deployment) like the Simon Nitinol® vena cava filter (6). Superelastic Nitinol also elastically attains a free shape after being released from a constraining device like a cannula (called elastic deployment) in devices like stone retrieval baskets. Nitinol guidewires are used to guide catheters into difficult to reach places of the body. They are favourable because they are kink resistant, unlike stainless steel. The wire is elastic and it can follow a tortuous path in the body without damage. Nitinol will rotate smoothly and impart torque (33). Due to its kink resistance and torquability, Nitinol

tubes are used as catheter shafts or delivery devices for stents, drugs, guidewires or as biopsy needles (34). The superelastic hysteresis of Nitinol, sometimes referred to as the 'flag' of a stress-strain diagram, is beneficial for stent performance.

Nitinol is biocompatible. When Nitinol implants receive appropriate surface treatment through electropolishing and passivation, they develop a passive titanium oxide layer, which forms a barrier that prevents corrosion and release of toxic Ni ions into the bloodstream (35, 36). Nitinol orthodontic archwires rely on the ability of the Nitinol to accommodate a wide strain when loaded, hence enabling the archwire to exert a constant stress as the teeth move (5, 37). This results in less trips to the dentist to change archwires or undergo painful retightening if using conventional materials. The compliance of Nitinol with bone and other structural elements of the body, in contrast with the stiffness of titanium or stainless steel, makes it a good choice for orthopaedic implants like bone staples and plates (5). Superelasticity and high strain accommodation have also been utilised in endoscopic applications. In order to reach difficult access locations in the body, the concept of articulating laser-cut Nitinol shafts for endoscopy has been discussed by Dewaele *et al.* (38) and Michaels (39).

Stents

Stents are 'scaffold' like structures that support or hold open circulatory vessels (see **Figure 1**). One of the best known applications of Nitinol is to make self-expanding stents, especially for peripheral vascular applications. Peripheral arteries in the lower extremity include the iliac, femoral popliteal and infrapopliteal arteries (8). Stents implanted in the peripheral arteries are exposed to high mechanical stress from the surrounding environment, for example bending of the knee, walking or running. Nitinol is able to handle these external forces better than other materials due to its characteristic properties of superelasticity and stress hysteresis. Due to kink resistance, these stents are well suited for the tortuous vessel pathways of peripheral arteries. Bare metal stents, drug eluting stents, covered stents and bioabsorbable stents are the four types of peripheral vascular stents available (8). In the Global Data study (8) 63% of the peripheral stents profiled were made using Nitinol, and in their Nitinol Medical Devices market study, Transparency Market Research (10) estimates that over 50% of the peripheral and coronary stents currently available in the market are made from Nitinol.

Stents can be classified into two types: self-expanding and balloon expandable stents, based on how the stent is deployed. A self-expanding stent is manufactured to a diameter larger than the vessel diameter. It is then crimped into a delivery catheter. When the stent is released from the catheter, it remembers its original shape and expands outward, thus the term self-expanding. Balloon expandable stents are manufactured in a crimped state and a balloon is inflated to expand the stent outwards to the vessel wall. In both cases, upon expansion, the stent contacts and supports the vessel wall (40). Morgan (33) and Stoeckel *et al.* (41) describe the practical use of Nitinol hysteresis and the stress-strain curve in stent assembly into a catheter, deployment during the surgical procedure and behaviour in the body vessel.

Stents can be produced by laser cutting tube or braiding wire. Stent manufacturing starts with laser cutting the tube into a strut pattern. The laser cut pattern is subject to deburring and slag removal using sand or bead blasting. The resulting frame is then expanded or shape-set in a multistep operation using progressively larger mandrels until the stent reaches the required size. The inner surface can be honed to smooth out the inner diameter and remove defects. The stent is then electropolished and passivated. Some stents are produced by laser cutting or photoetching sheet and then forming it into a cylindrical stent. Though use of sheet for stents is not as widespread as tubing, sheets can be rolled into thicknesses as low as 25.4 μm (0.001 inches). It would be considerably difficult to draw tubing to these thin wall thicknesses. Sheet also provides very good thickness tolerance control. It is more difficult to maintain tolerance and concentricity on drawn tubes.

Poncin *et al.* (42) review stent materials and tube requirements to produce a stent. Concentricity (sometimes specified as uniform wall thickness) control and surface finish of the tube inner diameter are critical to good yield when making stents. Uniform wall thickness is critical for laser processing, stent assembly and deployment. Laser cutting machines are programmed and set up to cut tube wall thicknesses defined for a specific job. Per Poncin, a thinner than nominally specified tube wall will result in a larger than required slot cut into the material and potential back-wall damage or burn. Conversely, a thicker than nominal tube wall could result in incomplete

cuts. Inconsistent tube wall thickness can result in non-uniform strut thickness and when the stent is crimped for assembly into a catheter, the stent wall can buckle or collapse due to this non-uniformity causing damage to the stent (43).

Tube manufacturers work on techniques to limit the damage to the inner diameter from defects like draw lines and scratches. Depending upon their depth, such inner diameter defects can continue to manifest in the stent even after deburring and electropolishing. These defects are like notches in the material and during cycling of the stent, these locations act as the points with maximum stress and can cause premature failure. These inner diameter defects can also cause stents to break during the expansion process described earlier. The outer diameter is less susceptible to defects as the outer diameters are shaped and sized by high quality dies creating uniform surfaces. Additionally, for laser cutting, tight tolerance tubes are manufactured by centreless grinding the tube outer diameter. This material removal operation removes defects present on the outer diameter.

A considerable amount of research has been published on the design, metallurgy, manufacture, fatigue and corrosion characterisation of stents. Bonsigniore (44) provides a review of stent history, designs and properties. Stoeckel *et al.* (45) detail various stent designs, materials, types of raw material forms and stent geometries. Gong *et al.* (46) provide a comparison between finite element analysis and experimental evaluations of stent designs. Schuessler *et al.* (47) provide an overview of contemporary and future stent materials and manufacturing technologies. Stoeckel *et al.* (41) describe material and design requirements for self-expanding Nitinol stents. Robertson *et al.* (48) and Pelton *et al.* (49) discuss fatigue life and fracture of Nitinol implants. Mahtabi *et al.* (50) present the state-of-the art on fatigue behaviour of Nitinol and also evaluate effects of material preparation and testing techniques. Corrosion of Nitinol and potential for Ni-ion release is of interest especially for permanent implants. Trépanier *et al.* (51) discuss the improvement in corrosion resistance with passivation and electropolishing. Trépanier *et al.* (52) present improvements in corrosion from processing material to develop a smooth and uniform oxide layer on the material. Sullivan *et al.* (53) discuss the effect of radial compression on Ni release from surfaces with thin and thick oxides.

One drawback of Nitinol is that it is not radiopaque, a requirement for proper placement of a stent or ability to locate the device in the body. As stent designs become smaller or the geometry changes to create fine struts and meshes, the X-ray signature of the stent reduces. Markers are materials with higher radiopacity that are assembled onto stents to improve X-ray visibility (54). Tantalum markers are coined, riveted or welded onto stent ends. Various marking systems made out of precious metals like platinum-iridium or gold are also used to mark stents but due to differences in the galvanic potential between precious metals and Nitinol, design and processing needs careful consideration to prevent galvanic corrosion (41). Cowley *et al.* (55) discuss the use of platinum alloys in marking applications.

Summary

For over thirty years, Nitinol has been used in a wide range of medical devices. This article has focused on stents, but other applications include catheters, biopsy needles, surgical instruments and numerous more. As the use becomes more widespread, the industry is faced with challenging applications that test the capability of the material. Chemical composition is carefully controlled during melting and recent developments in melting have yielded materials with low inclusion sizes, a key to improving the fatigue life of the material. The performance of the product can be optimised by thermomechanical processing and one can tailor properties to meet functional requirements. Superior concentricity and surface uniformity of tube inner diameter help stent producers increase yields. Products with small form factors are being used for physiological conditions that cannot be tackled with conventional materials. The unique properties of the material make it a desirable choice for product designers whose design ambitions would probably be limited without the versatility of such a material.

References

1. ‘World Population Prospects: The 2015 Revision, Key Findings and Advance Tables’, ESA/P/WP.241, United Nations, Department of Economic and Social Affairs, Population Division, New York, USA, 2015, pp. 2–6
2. M. Sharma and P. K. Majumdar, *Indian J. Occup. Environ. Med.*, 2009, **13**, (3), 109
3. T. Hall, ‘Specialty Metals Make Sophisticated Medical Devices Possible’, *Med. Design Briefs*, 1st September, 2013

4. **'**Overview of Biomaterials and Their Use in Medical Devices', in "Handbook of Materials for Medical Devices", ASM International, Ohio, USA, 2003, pp. 1–11
5. T. Duerig, A. Pelton and D. Stöckel, *Mater. Sci. Eng. A*, 1999, **273–275**, 149
6. A. R. Pelton, D. Stöckel and T. W. Duerig, *Mater. Sci. Forum*, 2000, **327–328**, 63
7. 'Peripheral Artery Disease', Harvard Health Publications, Harvard Medical School, USA, April, 2012
8. GlobalData, 'MediPoint: Peripheral Vascular Stents for the Lower Extremity – Global Analysis and Market Forecasts', GlobalData Healthcare, London, UK, April, 2013
9. GlobalData, 'MediPoint: Peripheral Vascular Interventions – Global Analysis and Market Forecasts', GlobalData Healthcare, London, UK, March, 2016
10. Transparency Market Research, 'Nitinol Medical Devices Market - Semi-finished Raw Material (Nitinol Tubes, Wiring and Others) and Final Medical Components (Nitinol Stents, Guidewires and Others) – Global Industry Analysis, Size, Share, Growth, Trends and Forecast, 2013–2019', Transparency Market Research, Albany, New York, USA, May, 2014
11. G. B. Kauffman and I. Mayo, *Chem Matters*, October, 1993, 4
12. T. Duerig and K. Melton, 'The History of Our Industry', NDC Tech Note: The International Conference on Shape Memory and Superelastic Technologies (SMST), Oxfordshire, UK, 18th–22nd May, 2015
13. D. E. Hodgson and J. W. Brown, 'Using Nitinol Alloys', Shape Memory Applications, Inc., San Jose, California, USA, 2000
14. L. G. Machado and M. A. Savi, *Braz. J. Med. Biol. Res*., 2003, **36**, (6), 683
15. D. E. Hodgson, M. H. Wu and R. J. Biermann, 'Shape Memory Alloys', in "ASM Handbook Volume 2: Properties and Selection: Nonferrous Alloys and Special-Purpose Materials", ASM International, Ohio, USA, 1990, pp. 897–902
16. D. Stöckel, 'Nitinol – A Material with Unusual Properties', *Endovascular Update*, 1998, (1), 1
17. S. A. Shabalovskaya, *Bio-Med. Mater. Eng.*, 1996, **6**, (4), 267
18. D. Kapoor, 'An Overview of Nitinol: Superelastic and Shape Memory', *Med. Design Briefs*, October, 2015
19. R. R. Adharapurapu, 'Phase Transformations in Nickel-Rich Nickel-Titanium Alloys: Influence of Strain-Rate, Temperature, Thermomechanical Treatment and Nickel Composition on the Shape Memory and Superelastic Characteristics', PhD Thesis, University of California, San Diego, USA, 2007
20. 'Standard Test Method for Transformation Temperature of Nickel-Titanium Alloys by Thermal Analysis', ASTM F2004-05(2010), ASTM International, West Conshohocken, Pennsylvania, USA
21. Johnson Matthey Medical Components, Measuring Transformation Temperatures in Nitinol Alloys: http://jmmedical.com/resources/211/Measuring-Transformation-Temperatures-in-Nitinol-Alloys.html (Accessed on 4th January 2017)
22. 'Standard Test Method for Determination of Transformation Temperature of Nickel-Titanium Shape Memory Alloys by Bend and Free Recovery', ASTM F2082 / F2082M-16, ASTM International, West Conshohocken, Pennsylvania, USA
23. 'Standard Test Method for Tension Testing of Nickel-Titanium Superelastic Materials', ASTM F2516-14, ASTM International, West Conshohocken, Pennsylvania, USA
24. T. Duerig, D. Stoeckel and D. Johnson, 'SMA – Smart Materials for Medical Applications', European Workshop on Smart Structures in Engineering and Technology, Giens, France, 21st May, 2002, in Proceedings of SPIE, Vol. 4763, ed. Brian Culshaw, 2003, pp. 7–15
25. A. R. Pelton, S. M. Russell and J. DiCello, *J. Met.*, 2003, **55**, (5), 33
26. S. M. Russell, 'Nitinol Melting and Fabrication', in "SMST-2000 Proceedings of the International Conference on Shape Memory and Superelastic Technologies", Pacific Grove, California, USA, 30th April–4th May, 2000, eds. S. M. Russell and A. R. Pelton, ASM International, Ohio, USA, 2000
27. 'Standard Specification for Wrought Nickel-Titanium Shape Memory Alloys for Medical Devices and Surgical Implants', ASTM F2063-12, ASTM International, West Conshohocken, Pennsylvania, USA
28. P. K. Kumar and C. Lasley, *J. Mater. Eng. Perform.*, 2014, **23**, (7), 2457
29. S. W. Robertson, M. Launey, O. Shelley, I. Ong, L. Vien, K. Senthilnathan, P. Saffari, S. Schlegel and A. R. Pelton, *J. Mech. Behav. Biomed. Mater.*, 2015, **51**, 119
30. R. Steegmüller, J. Ulmer, M. Quellmalz, M. Wohlschlögel and A. Schüßler, *J. Mater. Eng. Perform.*,

2014, **23**, (7), 2450

31. Johnson Matthey Medical Components, Nitinol Shape Setting: http://jmmedical.com/resources/251/Nitinol-Shape-Setting.html (Accessed on 4th January 2017)
32. P. P. Poncet, 'Nitinol Medical Device Design Considerations', in "SMST-2000 Proceedings of the International Conference on Shape Memory and Superelastic Technologies", Pacific Grove, California, USA, 30th April–4th May, 2000, eds. S. M. Russell and A. R. Pelton, ASM International, Ohio, USA, 2000
33. N. B. Morgan, *Mater. Sci. Eng. A*, 2004, **378**, (1–2), 16
34. P. P. Poncet, 'Applications of Superelastic Nitinol Tubing', in "SMST-1994 Proceedings of the First International Conference on Shape Memory and Superelastic Technologies", Pacific Grove, California, USA, 7th–10th March, 1994, ASM International, Ohio, USA, 1994
35. S. A. Shabalovskaya, J. Anderegg and J. Van Humbeeck, *Acta Biomater.*, 2008, **4**, (3), 447
36. B. O'Brien, W. M. Carroll and M. J. Kelly, *Biomaterials*, 2002, **23**, (8), 1739
37. D. Stoeckel, *Min. Invas. Therapy Allied Technol.*, 2000, **9**, (2), 81
38. F. Dewaele, A. F. Kalmar, F. De Ryck, N. Lumen, L. Williams, E. Baert, H. Vereecke, J. P. K. Okito, C. Mabilde, B. Blanckaert, V. Keereman, L. Leybaert, Y. Van Nieuwenhove, J. Caemaert and D. Van Roost, *Surg. Innov.*, 2014, **21**, (3), 303
39. B. Michaels, 'Using Nitinol and Lasers to Make Articulated Endoscopic Tool Tips', Medical Product Manufacturing News, Medtech Pulse, UBM Canon, Santa Monica, California, USA, 27th February, 2014
40. T. Duerig and M. Wholey, *Min. Invas. Therapy Allied Technol.*, 2002, **11**, (4), 173
41. D. Stoeckel, A. Pelton and T. Duerig, *Eur. Radiol.*, 2004, **14**, (2), 292
42. P. Poncin and J. Proft, 'Stent Tubing: Understanding the Desired Attributes', in "Medical Device Materials: Proceedings of the Materials & Processes for Medical Devices Conference 2003", 8th–10th September, 2003, Anaheim, California, USA, ed. S. Shrivastava, ASM International, Ohio, USA, 2004, pp. 253–259
43. Dave Mackiewicz, Process Engineer, Johnson Matthey, San Jose, California, USA, Private communication, January, 2016
44. C. Bonsignore, 'A Decade of Evolution in Stent Design', in "SMST-2003: Proceedings of the International Conference on Shape Memory and Superelastic Technologies", Pacific Grove, California, USA, 5th–8th May, 2003, eds. A. R. Pelton and T. Duerig, ASM International, Ohio, USA, 2004, pp. 519–528
45. D. Stoeckel, C. Bonsignore and S. Duda, *Min. Invas. Therapy Allied Technol.*, 2002, **11**, (4), 137
46. X.-Y. Gong, A. R. Pelton, T. W. Duerig, N. Rebelo and K. Perry, 'Finite Element Analysis and Experimental Evaluation of Superelastic Nitinol Stent', in "SMST-2003: Proceedings of the International Conference on Shape Memory and Superelastic Technologies", Pacific Grove, California, USA, 5th–8th May, 2003, eds. A. R. Pelton and T. Duerig, ASM International, Ohio, USA, 2004, pp. 453–462
47. A. Schuessler, U. Bayer, G. Siekmeyer, R. Steegmueller, M. Strobel and A. Schuessler, 'Manufacturing of Stents: Optimize the Stent with New Manufacturing Technologies', in 5th European Symposium of Vascular Biomaterials ESVB, Strasbourg, France, 27th April, 2007
48. S. W. Robertson, A. R. Pelton and R. O. Ritchie, *Int. Mater. Rev.*, 2012, **57**, (1), 1
49. A. R. Pelton, V. Schroeder, M. R. Mitchell, X.-Y. Gong, M. Barney and S. W. Robertson, *J. Mech. Behaviour. Biomed. Mater.*, 2008, **1**, (2), 153
50. M. J. Mahtabi, N. Shamsaei and M. R. Mitchell, *J. Mech. Behaviour. Biomed. Mater.*, 2015, **50**, 228
51. C. Trépanier, R. Venugopalan and A. R. Pelton 'Corrosion Resistance and Biocompatibility of Passivated NiTi', in "Shape Memory Implants", ed. L. Yahia, Springer-Verlag, Berlin, Heidelberg, Germany, 2000, pp. 35–45
52. C. Trépanier, M. Tabrizian, L'H. Yahia, L. Bilodeau and D. L. Piron, *J. Biomed. Mater. Res.: A*, **43**, (4), 1998, 433
53. S. J. L. Sullivan, M. L. Dreher, J. Zheng, L. Chen, D. Madamba, K. Miyashiro, C. Trépanier and S. Nagaraja, *Shape Memory Superelast.*, 2015, **1**, (3), 319
54. R. Steegmüller, M. Strobel, E. Flaxmeier and A. Schüßler, 'Micro-Welding for Improved Radiopacity of Nitinol-Stents', in "SMST-2004: Proceedings of the International Conference on Shape Memory and Superelastic Technologies", Baden-Baden, Germany, 3rd–7th October, 2004, ASM International, Ohio, USA, 2004, pp. 591–595
55. A. Cowley and B. Woodward, *Platinum Metals Rev.*, 2011, **55**, (2), 98

The Author

Deepak Kapoor is Product Manager for Johnson Matthey Noble Metals, based in San Jose, USA, and is responsible for the development and marketing of high precision medical components based on Nitinol.

Johnson Matthey Technology Review is Johnson Matthey's international journal of research exploring science and technology in industrial applications

www.technology.matthey.com

Johnson Matthey Technology Review
Johnson Matthey Plc
Orchard Road
Royston
SG8 5HE
UK
Tel +44 (0)1763 253 000
Email tech.review@matthey.com